สารยับยั้งไทโรซิเนสจากเปลือกต้นละมุดสีดา *Manilkara kauki* (L.) Dubard

นางสาวสิรินดา ศรีสุภาพ

วิทยานิพนธ์นี้เป็นส่วนหนึ่งของการศึกษาตามหลักสูตรปริญญาวิทยาศาสตรมหาบัณฑิต
สาขาวิชาเทคโนโลยีชีวภาพ
คณะวิทยาศาสตร์ จุฬาลงกรณ์มหาวิทยาลัย
ปีการศึกษา 2560

TYROSINASE INHIBITORS FROM BARK OF TALAWRINTA (*Manilkara kauki* (L.) Dubard)

Miss Sirinada Srisupap

A Thesis Submitted in Partial Fulfillment of the Requirements
for the Degree of Master of Science Program in Biotechnology
Faculty of Science
Chulalongkorn University
Academic Year 2017

Thesis Title	TYROSINASE INHIBITORS FROM BARK OF TALAWRINTA (*Manilkara kauki* (L.) Dubard)
By	Miss Sirinada Srisupap
Field of Study	Biotechnology
Thesis Advisor	Assistant Professor Chanya Chaicharoenpong, Ph.D.

Accepted by the Faculty of Science, Chulalongkorn University in Partial Fulfillment of the Requirements for the Master's Degree

.....Dean of the Faculty of Science

(Professor Polkit Sangvanich, Ph.D.)

THESIS COMMITTEE

.....Chairman

(Associate Professor Nattaya Ngamrojanavanich, Ph.D.)

.....Thesis Advisor

(Assistant Professor Chanya Chaicharoenpong, Ph.D.)

.....Examiner

(Associate Professor Preecha Phuwapraisirisan, Ph.D.)

.....External Examiner

(Damrong Sommit, Ph.D.)

สิรินดา ศรีสุภาพ : สารยับยั้งไทโรซิเนสจากเปลือกต้นละมุดสีดา *Manilkara kauki* (L.) Dubard (TYROSINASE INHIBITORS FROM BARK OF TALAWRINTA (*Manilkara kauki* (L.) Dubard)) อ.ที่ปรึกษาวิทยานิพนธ์หลัก: ผศ. ดร.จรรยา ชัยเจริญพงศ์, 128 หน้า.

เมลานินคือสารจำเป็นสำหรับการปกป้องผิวหนังของมนุษย์จากรังสีอัลตราไวโอเลต อย่างไรก็ตามการผลิตเมลานินที่มากเกินไปในชั้นผิวหนังกำพร้านำไปสู่ความผิดปกติของการผลิตเม็ดสีมากเกินไป เช่น ฝ้า กระ และจุดด่างดำ ไทโรซิเนสคือหนึ่งในเอนไซม์หลักของกระบวนการผลิตเม็ดสี ละมุดสีดา (*Manilkara kauki* (L.) Dubard) เป็นหนึ่งในพืชสกุล *Manilkara* ของวงศ์พิกุล การศึกษานี้พยายามที่จะตรวจสอบหาปริมาณฟีนอลิกทั้งหมด ปริมาณฟลาโวนอยด์ทั้งหมด ฤทธิ์ต้านอนุมูลอิสระ และฤทธิ์ต้านไทโรซิเนสในระดับหลอดทดลองของส่วนต่างๆ ของต้นละมุดสีดา และแยกสารต้านไทโรซิเนสจากเปลือกต้นละมุดสีดา ส่วนสกัดหยาบเมทานอล และน้ำของผล ใบ เมล็ด เปลือกไม้ และเนื้อไม้ของละมุดสีดา ถูกนำมาประเมินผลปริมาณฟีนอลิกทั้งหมด ปริมาณฟลาโวนอยด์ทั้งหมด ฤทธิ์ต้านอนุมูลอิสระ และฤทธิ์ต้านไทโรซิเนส เปลือกไม้ของต้นละมุดสีดาแสดงปริมาณฟีนอลิกทั้งหมด ปริมาณฟลาโวนอยด์ทั้งหมดในปริมาณสูง และแสดงฤทธิ์ต้านอนุมูลอิสระสูง ส่วนสกัดหยาบเมทานอลของเปลือกไม้ของต้นละมุดสีดาแสดงฤทธิ์ต้านไทโรซิเนสสูงที่สุด (IC_{50} 0.26 ± 0.05 mg/mL) ดังนั้นเปลือกไม้ของต้นละมุดสีดาถูกนำมาสกัดด้วย นอร์มัล-เฮกเซน เอทิลแอซิเทต เมทานอล และน้ำ ตามลำดับ ทั้งส่วนสกัดหยาบเอทิลแอซิเทต และเมทานอลจากเปลือกไม้แสดงปริมาณสารประกอบฟีนอลิก และฟลาโวนอยด์สูง และฤทธิ์ต้านอนุมูลอิสระสูง นอกจากนี้ส่วนสกัดหยาบเอทิลแอซิเทตของเปลือกไม้แสดงฤทธิ์ต้านไทโรซิเนสสูงกว่าส่วนสกัดหยาบนอร์มัล-เฮกเซน เมทานอล และน้ำด้วยค่า IC_{50} 0.24 ± 0.02 และ 0.28 ± 0.04 mg/mL สำหรับแอล-ไทโรซีน และแอล-โดพา เป็นสารตั้งต้นตามลำดับ ดังนั้นส่วนสกัดหยาบเอทิลแอซิเทตถูกนำมาแยกและทำให้บริสุทธิ์ได้สาร I คือ taraxerol และสาร II คือ dihydrokaempferol สาร I แสดงฤทธิ์ต้านไทโรซิเนสด้วยค่า IC_{50} 2.32 ± 0.06 และ 2.65 ± 0.03 mM สำหรับแอล-ไทโรซีน และแอล-โดพาเป็นสารตั้งต้นตามลำดับ สาร II แสดงฤทธิ์ต้านไทโรซิเนสด้วยค่า IC_{50} 1.15 ± 0.06 และ 1.74 ± 0.05 mM สำหรับแอล-ไทโรซีน และแอล-โดพา เป็นสารตั้งต้นตามลำดับ สาร I และสาร II แสดงฤทธิ์ต้านโทโรซิเนสต่ำกว่ากรดโคจิก แต่สาร I และสาร II แสดงฤทธิ์ต้านโทโรซิเนสสูงกว่าอัลฟา-อาร์บูทิน จากผลการทดลองนี้แนะนำว่าส่วนสกัดหยาบเอทิลแอซิเทตของเปลือกต้นละมุดสีดาควรตรวจสอบฤทธิ์ทางชีวภาพอื่นๆเพิ่มเติม เช่น ฤทธิ์ต้านการแพ้ ความเป็นพิษต่อเซลล์ และฤทธิ์ต้านไทโรซิเนสในสิ่งมีชีวิตเพื่อประเมินผลส่วนสกัดหยาบนี้ก่อนที่จะนำไปใช้เป็นส่วนประกอบที่มีศักยภาพในเครื่องสำอางที่ทำให้ผิวขาว

สาขาวิชา เทคโนโลยีชีวภาพ ลายมือชื่อนิสิต .....

ปีการศึกษา 2560 ลายมือชื่อ อ.ที่ปรึกษาหลัก .....

5772289023 : MAJOR BIOTECHNOLOGY

KEYWORDS: MANILKARA KAUKI (L.) DUBARD / ANTIOXIDANT ACTIVITY / TYROSINASE INHIBITORY ACTIVITY

SIRINADA SRISUPAP: TYROSINASE INHIBITORS FROM BARK OF TALAWRINTA (*Manilkara kauki* (L.) Dubard). ADVISOR: ASST. PROF. CHANYA CHAICHAROENPONG, Ph.D., 128 pp.

Melanin is essential for protecting human skin from ultraviolet radiation. However, its overproduction in the basal epithelial layer leads to hyperpigmentary disorders of the skin such as melasma, blemish and age spots. Tyrosinase is one of key enzymes in melanogenesis. *Manilkara kauki* (L.) Dubard or Talawrinta is one of the plants in genus *Manilkara* of Sapotaceae family. This study attempted to investigate *in vitro* total phenolic and flavonoid contents, antioxidant and tyrosinase inhibitory activities of crude extract of different parts of *M. kauki* and purify tyrosinase inhibitors from stem barks of *M. kauki*. Methanol and aqueous crude extracts of fruits, leaves, seeds, stem barks and woods of *M. kauki* evaluated on their total phenolic and flavonoid contents, antioxidant and tyrosinase inhibitory activities. Stem barks of *M. kauki* showed high amount of total phenolic and flavonoid contents and strong antioxidant activity. Methanol crude extracts of stem barks exhibited the highest tyrosinase inhibitory activity (IC_{50} value of 0.26 ± 0.05 mg/mL). Thus, stem barks of *M. kauki* was extracted with *n*-hexane, ethyl acetate, methanol and water, respectively. Both of ethyl acetate and methanol crude extracts of stem barks exhibited high amount of phenolic compounds and flavonoids and strong antioxidant activity. Furthermore, ethyl acetate crude extract of stem bark exhibited higher tyrosinase inhibitory activity than *n*-hexane, methanol and aqueous crude extracts with IC_{50} values of 0.24 ± 0.02 and 0.28 ± 0.04 mg/mL for *L*-tyrosine and *L*-DOPA as substrates, respectively. Thus, ethyl acetate crude extract was further isolated and purified to afford compound I as taraxerol and compound II as dihydrokaempferol. Compound I exhibited tyrosinase inhibitory activity with IC_{50} values of 2.32 ± 0.06 and 2.65 ± 0.03 mM for *L*-tyrosine and *L*-DOPA as substrates, respectively. Compound II exhibited tyrosinase inhibitory activity with IC_{50} values of 1.15 ± 0.06 and 1.74 ± 0.05 mM for *L*-tyrosine and *L*-DOPA as substrates, respectively. Compounds I and II showed lower tyrosinase inhibitory activity than kojic acid but they were exhibited higher tyrosinase inhibitory activity than *α*-arbutin. These results suggested that ethyl acetate crude extract of stem barks of *M. kauki* should be further investigated for others biological activities including anti-allergic, cytotoxicity and *in vivo* tyrosinase inhibitory activities to evaluate it before using as a potential ingredient in whitening cosmetics.

Field of Study: Biotechnology Student's Signature .....

Academic Year: 2017 Advisor's Signature .....

ACKNOWLEDGEMENTS

I would like to express my gratitude to my thesis advisor, Assistant Professor Dr. Chanya Chaicharoenpong for guidance, valuable suggestions and special support in correcting and criticizing all of this study.

I would like to express my sincere thanks to my examination committees, Associate Professor Dr. Nattaya Ngamrojanavanich, Associate Professor Dr. Preecha Phuwapraisirisan and Dr. Damrong Sommit for their useful advice and careful reviewing of this thesis.

I would like to express my thanks to Graduate School, Chulalongkorn University for financial support.

Furthermore, I would like to thanks Institute of Biotechnology and Genetic Engineering, all members of laboratory room no. 604 and all of my friends. Finally, I would especially like to thank my family for supporting me, always beside me and their love through my thesis work.

CONTENTS

Page
THAI ABSTRACT iv
ENGLISH ABSTRACT v
ACKNOWLEDGEMENTS vi
CONTENTS vii
LIST OF TABLES x
LIST OF FIGURES xiv
LIST OF ABBREVIATIONS xvii
CHAPTER I INTRODUCTION 1
CHAPTER II THEORITICAL 3
2.1 Melanin synthesis 3
2.2 *Manilkara kauki* (L.) Dubard 4
2.3 Literature reviews 5
2.3.1 Biological activities of Sapotaceae family 5
2.3.2 Summary of tyrosinase inhibitors of Sapotaceae family 30
CHAPTER III MATERIALS AND METHODS 36
3.1 Plant materials 36
3.2 Reagents 36
3.3 General techniques and procedures 36
3.3.1 Thin layer chromatography (TLC) 36
3.3.2 Preparative thin layer chromatography (PTLC) 36
3.3.3 Column chromatography (CC) 37
3.3.4 Medium pressure liquid chromatography (MPLC) 37
3.3.5 Hot air oven 37
3.3.6 Vacuum rotary evaporator 37
3.3.7 Melting point apparatus 37
3.3.8 UV-Visible spectrophotometry 37
3.3.9 Nuclear magnetic resonance (NMR) spectroscopy 38
3.3.10 High resolution electrospray ionization mass spectroscopy 38

Page

3.4 Methods 38
3.4.1 Extraction 38
3.4.1.1 Preparation of crude extracts of different parts of *M. kauki* 38
3.4.1.2 Preparation of crude extracts of stem barks of *M. kauki* 39
3.4.2 Phytochemical analysis 40
3.4.2.1 Total phenolic content 40
3.4.2.2 Total flavonoid content 40
3.4.3 Biological activity assays 40
3.4.3.1 Antioxidant activity assays 40
3.4.3.1.1 1,1-diphenyl-2-picrylhydrazyl (DPPH) assay 40
3.4.3.1.2 The ferric reducing antioxidant power (FRAP) assay 41
3.4.3.2 Tyrosinase inhibitory assay 41
3.4.3.3 Determination of IC_{50} for tyrosinase inhibitory activity 42
3.4.4 Separation of ethyl acetate crude extract of stem barks of *M. kauki.* 42
CHAPTER IV RESULTS AND DISCUSSION 57
4.1 Extraction of different parts of *M. kauki* 57
4.2 Phytochemical compositions of different parts of *M. kauki* 57
4.2.1 Total phenolic content 57
4.2.2 Total flavonoid content 58
4.3 Biological activities of different parts of *M. kauki* 59
4.3.1 Antioxidant activities 59
4.3.1.1 DPPH radical scavenging activity 59
4.3.1.2 FRAP activity 60
4.3.2 Tyrosinase inhibitory activity 61
4.4 Extraction of stem barks of *M. kauki* 62
4.5 Phytochemical compositions of crude extracts of stem barks of *M. kauki* 63
4.5.1 Total phenolic content 63
4.5.2 Total flavonoid content 63

Page

4.6 Biological activities of crude extracts of stem barks of *M. kauki* 64
4.6.1 Antioxidant activities 64
4.6.1.1 DPPH radical scavenging activity 64
4.6.1.2 FRAP activity 64
4.6.2 Tyrosinase inhibitory activity 64
4.7 Isolation of ethyl acetate crude extract of stem barks of *M. kauki* 65
4.8 Elucidation of isolated compounds of ethyl acetate crude extract of stem barks of *M. kauki* 84
4.8.1 Compound I 84
4.8.2 Compound II 87
4.9 Tyrosinase inhibitory activity of isolated compounds 90
CHAPTER V CONCLUSION 93
REFERENCES 96
APPENDIX 105
VITA 128

LIST OF TABLES

Page

Table 2.1 The summary of biological activities of Sapotaceae family 6

Table 2.2 The isolated compounds of Sapotaceae family 9

Table 2.3 The summary of tyrosinase inhibitors from Sapotaceae family 31

Table 4.1 Characteristic and percentage yield of methanol crude extracts of different parts of *M. kauki* 57

Table 4.2 Characteristic and percentage yield of aqueous crude extracts of different parts of *M. kauki* 57

Table 4.3 Total phenolic content of methanol and aqueous crude extracts of different parts of *M. kauki* 58

Table 4.4 Total flavonoid contents of methanol and aqueous crude extracts of different parts of *M. kauki* 59

Table 4.5 DPPH radical scavenging activity of methanol and aqueous crude extracts of different parts of *M. kauki* 60

Table 4.6 FRAP activity of methanol and aqueous crude extracts of different parts of *M. kauki* 61

Table 4.7 Tyrosinase inhibitory activity (IC_{50}) of methanol and aqueous crude extracts of different parts of *M. kauki* 62

Table 4.8 Characteristic and percentage yield of crude extracts of stem barks of *M. kauki* 63

Table 4.9 Phytochemical composition of crude extracts of stem barks of *M. kauki* 64

Table 4.10 Antioxidant activities of stem barks of *M. kauki* 64

Table 4.11 Tyrosinase inhibitory activity of stem barks of *M. kauki* 65

Table 4.12 Isolation and tyrosinase inhibitory activity of fraction E 66

Table 4.13 Isolation and tyrosinase inhibitory activity of fraction E1 67

Table 4.14 Isolation and tyrosinase inhibitory activity of fraction E1B 67

Table 4.15 Isolation of fraction E1BC 68

Page

Table 4.16 Isolation of fraction E1BC2 68

Table 4.17 Isolation of fraction E1BC2C 68

Table 4.18 Isolation of fraction E1BC2C2 69

Table 4.19 Isolation of fraction E1C 69

Table 4.20 Isolation of fraction E1CG 69

Table 4.21 Isolation and tyrosinase inhibitory activity of fraction E1D 70

Table 4.22 Isolation of fraction E1DI 70

Table 4.23 Isolation of fraction E1DID 71

Table 4.24 Isolation of fraction E1E 71

Table 4.25 Isolation of fraction E1EE 71

Table 4.26 Isolation of fraction E1EF4 71

Table 4.27 Isolation of fraction E1EF4B 72

Table 4.28 Isolation of fraction E1F 72

Table 4.29 Isolation of fraction E1H 72

Table 4.30 Isolation of fraction E1HA 73

Table 4.31 Isolation of fraction E1HB 73

Table 4.32 Isolation of fraction E1HC 73

Table 4.33 Isolation of fraction E1HC4 74

Table 4.34 Isolation of fraction E1HE 74

Table 4.35 Isolation and tyrosinase inhibitory activity of fraction E1I 74

Table 4.36 Isolation of fraction E1IC 75

Table 4.37 Isolation and tyrosinase inhibitory activity of fraction E2 75

Table 4.38 Isolation of fraction E2A 76

Table 4.39 Isolation of fraction E2AD 76

Table 4.40 Isolation of fraction E2AE 76

Page

Table 4.41 Isolation of fraction E2B 77

Table 4.42 Isolation of fraction E2BD 77

Table 4.43 Isolation of fraction E2BE 77

Table 4.44 Isolation of fraction E2BE1 78

Table 4.45 Isolation of fraction E2C 78

Table 4.46 Isolation of fraction E2CC 78

Table 4.47 Isolation of fraction E2CC4 79

Table 4.48 Isolation of fraction E2CE 79

Table 4.49 Isolation of fraction E2CF 79

Table 4.50 Isolation of fraction E2D 79

Table 4.51 Isolation of fraction E2DC 80

Table 4.52 Isolation of fraction E2DC4 80

Table 4.53 Isolation of fraction E2DC5 80

Table 4.54 Isolation of fraction E2DC5C 81

Table 4.55 Isolation of fraction E2E 81

Table 4.56 Isolation of fraction E2ED 81

Table 4.57 Isolation of fraction E2EE 82

Table 4.58 Isolation of fraction E2EF 82

Table 4.59 Isolation of fraction E2F 82

Table 4.60 Isolation and tyrosinase inhibitory activity of fraction E3 83

Table 4.61 Isolation of fraction E3B 83

Table 4.62 Isolation of fraction E3BB 83

Table 4.63 Comparison of ^{1}H and ^{13}C NMR of compound **I** and taraxerol 86

Page

Table 4.64 Comparison of ^{1}H and ^{13}C NMR of compound **II** and dihydrokaempferol 88

Table 4.65 Tyrosinase inhibitory activity values of isolated compounds of stem barks of *M. kauki* 91

Table A Serial dilutions of gallic acid equivalent 106

Table B Serial dilutions of quercetin equivalent 107

Table C Serial dilutions of trolox equivalent 108

LIST OF FIGURES

Page

Figure 1 The skin structure 3

Figure 2 The Melanin biosynthesis pathway 4

Figure 3 (a) The leaves (b) the fruits and (c) whole plant of *M. kauki* 5

Figure 4 Chemical structure of isolated compounds of Sapotaceae family 11

Figure 5 Chemical structure of tyrosinase inhibitors of Sapotaceae family 32

Figure 6 Extraction procedure of different parts of *M. kauki* 38

Figure 7 Extraction procedure of stem barks of *M. kauki* 39

Figure 8 Isolation procedure of ethyl acetate crude extract (E) 42

Figure 9 Isolation procedure of fraction E1 43

Figure 10 Isolation procedure of fraction E1B 44

Figure 11 Isolation procedure of fraction E1C 45

Figure 12 Isolation procedure of fraction E1D 46

Figure 13 Isolation procedure of fraction E1E 47

Figure 14 Isolation procedure of fraction E1F 47

Figure 15 Isolation procedure of fractions E1H, E1HA and E1HB 48

Figure 16 Isolation procedure of fractions E1HC and E1HE 49

Figure 17 Isolation procedure of fraction E1I 49

Figure 18 Isolation procedure of fraction E2 50

Figure 19 Isolation procedure of fraction E2A 50

Figure 20 Isolation procedure of fraction E2B 51

Figure 21 Isolation procedure of fractions E2C, E2CC and E2CE 52

Figure 22 Isolation procedure of fraction E2CF 53

Figure 23 Isolation procedure of fraction E2D 54

Figure 24 Isolation procedure of fraction E2E 55

Page

Figure 25 Isolation procedure of fraction E2F 55

Figure 26 Isolation procedure of fraction E3 56

Figure 27 The summary of isolation of ethyl acetate crude extract of stem bark of *M. kauki* 84

Figure 28 HMBC correlation of taraxerol (compound **I**) 87

Figure 29 The structure of compound **I** 87

Figure 30 HMBC correlation of dihydrokaempferol (compound **II**) 89

Figure 31 The structure of compound **II** 90

Figure 32 Calibration plots of tyrosinase inhibitory activity of compounds **I** and **II** using *L*-tyrosine as a substrate 92

Figure 33 Calibration plots of tyrosinase inhibitory activity of compounds **I** and **II** using *L*-DOPA as a substrate 92

Figure 34 Standard curve of total phenolic content 109

Figure 35 Standard curve of total flavonoid content 109

Figure 36 Standard curve of DPPH radical scavenging assay 110

Figure 37 Standard curve of FRAP assay 110

Figure 38 ^{1}H-NMR spectrum ($CDCl_3$) of compound **I** 111

Figure 39 ^{13}C-NMR spectrum ($CDCl_3$) of compound **I** 112

Figure 40 DEPT90 spectrum ($CDCl_3$) of compound **I** 113

Figure 41 DEPT135 spectrum ($CDCl_3$) of compound **I** 114

Figure 42 HSQC spectrum ($CDCl_3$) of compound **I** 115

Figure 43 HMBC spectrum ($CDCl_3$) of compound **I** 116

Figure 44 COSY spectrum ($CDCl_3$) of compound **I** 117

Figure 45 NOESY spectrum ($CDCl_3$) of compound **I** 118

Figure 46 HR-ESI-MS spectrum of compound **I** 119

Figure 47 ^{1}H-NMR spectrum (CD_3COCD_3) of compound **II** 120

Page

Figure 48 ^{13}C-NMR spectrum (CD_3COCD_3) of compound **II** 121

Figure 49 DEPT90 spectrum (CD_3COCD_3) of compound **II** 122

Figure 50 DEPT135 spectrum (CD_3COCD_3) of compound **II** 123

Figure 51 HSQC spectrum (CD_3COCD_3) of compound **II** 124

Figure 52 HMBC spectrum (CD_3COCD_3) of compound **II** 125

Figure 53 COSY spectrum (CD_3COCD_3) of compound **II** 126

Figure 54 HR-ESI-MS spectrum of compound **II** 127

LIST OF ABBREVIATIONS

δ	Chemicals shift
ºC	Degree celsius
%	Percentage
µg	Microgram
µL	Microliter
µm	Micrometer
µM	Micromolar
Abs	Absorbance
ABTS	2,2'-Azino-bis (3-ethylbenzthiazoline-6-sulphonic acid)
$CDCl_3$	Deuterated chloroform
CD_3OD	Deuterated methanol
cm	Centimeter
cm^{-1}	Reciprocal centimeter
^{13}C-NMR	Carbon nuclear magnetic resonance spectroscopy
COSY	Homonuclear correlation spectroscopy
CC	Column chromatography
d	Doublet (for NMR spectra)
dd	Doublet of doublet (for NMR spectra)
DEPT	Distrotionless enhancement by polarization transfer
DHI	5,6-dihydroxyindole
DHICA	5,6-dihydroxyindole-2-carboxylic acid
DI	Deionized
DMSO	Dimethyl sulfoxide
DPPH	1,1-Diphenyl-2-picryhydrazyl
e.g.	Exempli gratia
et al.	*et alii*
FRAP	The ferric reducing antioxidant power
g	Gram
h	Hour
HIV	Human Immunodeficiency Virus
^1H NMR	Proton nuclear magnetic resonance spectroscopy
HMBC	Heteronuclear multiple bond correlation
HMQC	Heteronuclear multiple quantum correlation
HPLC	High performance liquid chromatography
HRESIMS	High resolution electrospray ionization mass spectrometry
HSQC	Heteronuclear single quantum correlation
Hz	Hertz
IC_{50}	Half maximal inhibitory concentration

IL-1β	Interleukin-1β
IL-8	Interleukin-8
In	Inch
$Inches^2$	Square of inches
J	Coupling constant
kg	Kilogram
L	Liter
L-DOPA	*L*-3,4-dihydroxyphenylalanine
LD_{50}	Half maximal lethal dose
m	Multiple (for NMR spectra)
M	Molar
m/z	Mass-to-charge ratio
m^2	Square of meter
MCF	Michigan Cancer Foundation
mg	Milligram
mg GAE	Milligram of gallic acid equivalent
mg TE	Milligram of trolox equivalent antioxidant capacity
mg QE	Milligram of quercetin equivalent
min	Minute
mL	Milliliter
mm	Millimeter
mM	Millmolar
MPLC	Medium pressure liquid chromatography
MTCC	Microbial Type Culture Collection
NA	No activity
ND	No detection
nm	Nanometer
nM	Nanomolar
NMR	Nuclear magnetic resonance spectroscopy
NOESY	Nuclear Overhauser Enhancement Spectroscopy
P	Product
pH	A logarithmic measure of hydrogen ion concentration
PTLC	Preparative thin layer chromatography
QE	Quercetin equivalent
ROS	Reactive oxygen
s	Singlet (for NMR spectra)
S	Substrate
SC_{50}	Half maximal scavenging of the DPPH
SD	standard deviation
SPSS	Statistical package for the social sciences
t	Triplet (for NMR spectra)

TE	Trolox equivalent
TLC	Thin layer chromatography
TMS	Tetramethylsilane
TPTZ	2,4,6-tripyridyltriazine
UV	Ultraviolet
v/v	Volume by volume
w	Weight
w/v	Weight by volume
w/w	Weight by weight

CHAPTER I
INTRODUCTION

In recent years, trends in using traditional medicinal plants and herbs have been growing rapidly such as traditional medicines, herbal teas, healthy foods and especially herbal cosmetics. Nowadays, Thai medical herbs and plants are one of the ingredients of whitening products. Melanin is produced by melanocytes. Melanocytes are found in the basal layer of epidermis. Melanin is essential for protecting human skin from ultraviolet radiation. However, its overproduction in the basal epithelial layer leads to hyperpigmentary disorders of the skin such as melasma, blemish and age spots [1]. Tyrosinase is one of key enzymes in melanogenesis. *L*-Tyrosine is hydroxylated to *L*-3,4-dihydroxyphenylalanine (*L*-DOPA) by tyrosinase and followed by the oxidation of *L*-DOPA to DOPAquinone. From DOPAquinone, the melanin synthesis pathways diverge to produce either eumelanin or pheomelanin [2].

The plants of genus *Manilkara* are belonging to the Sapotaceae family. Characters of this genus are evergreen and fruit trees that are valuable and useful. Fruits of *Manilkara zapota* had high hydrophilic oxygen radical absorbance capacity and total phenolic compounds, so they were rich sources of diverse antioxidants [3]. *Manilkara subsericea* (Mart.) Dubard was investigated for biological activities. *n*-Hexane crude extract of fruits and ethanol crude extracts of leaves and stems of *M. subsericea* presented antimicrobial activity against *Staphylococcus aureus* ATCC25923 and they exhibited low cytotoxicity on Vero cells [4]. The ethanol extract of *Manilkara bidentata* consisted of pentacyclic triterpene and the extract was investigated the action on collagen and fibronectin synthesis. This extract decreased interleukin-1β (IL-1β) and interleukin-8 (IL-8) pro-inflammatory cytokines. Therefore, this extract showed potential as an anti-inflammatory and anti-aging ingredients for pharmaceutical and cosmetic industries [5]. Furthermore, Sapotaceae was reported to possess pharmacological activities such as antioxidant, antimicrobial, anticancer, antidiabetic, antiulcer, immunomodulatory and tyrosinase inhibitory activities [6].

Manilkara kauki (L.) *Dubard* or Talawrinta is one of the plants in Sapotaceae family. It is a tropical forest plant that found in Thailand, Myanmar, Vietnam, Malaysia and Northern Queensland of Australia [7]. Previous researches, tyrosinase inhibitors were isolated from plants in Sapotaceae family such as leaves of *M. zapota*, barks of *Sideroxylon inerme*, stems of *Synsepalum dulcificum*, barks of *Glycoxylon huber* and flowers of *Mimosops elengi* [6]. This study attempted to investigate total phenolic and flavonoid contents, *in vitro* antioxidant and inhibitory activities of crude extracts of stem barks of *M. kauki* against tyrosinase. In addition, this study had compared the effects of crude extract with that of kojic acid and *α*-arbutin. Furthermore, crude extracts were isolated and elucidated the structure of isolated compounds of stem barks of *M. kauki.*

Objectives

1. To study tyrosinase inhibitory activity of crude extracts and isolated compounds of stem barks of *M. kauki* L. Dubard.

2. To elucidate the structure of isolated compounds of stem barks of *M. kauki.*

CHAPTER II
THEORITICAL

2.1 Melanin synthesis

The skin is the largest organ of the body. It protects us from microbes and the element. The skin helps regulate body temperature and permits the sensation of touch, heat and cold. There are three main layers of skin as epidermis, dermis and hypodermis. The skin structure is shown in Figure 1. Epidermis is the outer layer of skin. It consists of three types of cell; keratinocytes, melanocytes and langerhans cells. Melanocytes are a unique organelle that produce the pigmented biopolymers [8]. Melanin is a pigment that occurs in fungi [9], plants and humans [10]. It is effective for color of skin, hair and eye in humans. There are two types of melanin pigments that were produced by melanocytes cell: eumelanin and pheomelanin. Eumelanin is black to brown shades pigment and while pheomelanin is red to yellow shades pigment [11].

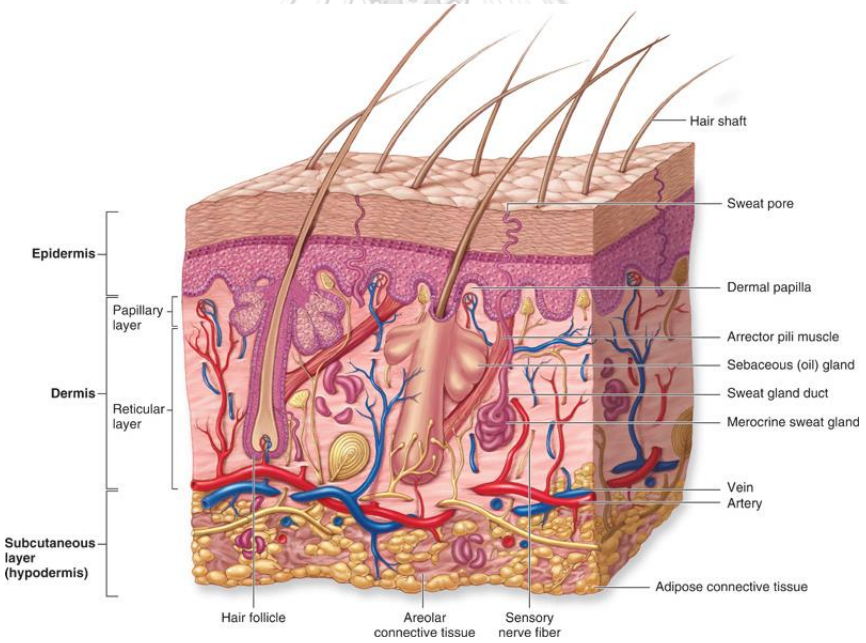

Figure 1 The skin structure

Melanogenesis is occurred by the activation of key enzyme of melanogenesis, tyrosinase. Tyrosinase (E.C.1.14.18.1) is a copper containing enzyme that locates in the membrane of melanosome [12]. Tyrosinase catalyzes the first two steps of melanogenesis. Firstly, the hydroxylation of *L*-tyrosine to *L*-DOPA and secondly, the oxidation of *L*-DOPA to DOPAquinone [13]. Following the formation of DOPAquinone, the melanogenesis splits into synthesis of eumelanin and pheomelanin [14]. For eumelanin pathway, DOPAquinone form will be converted to DOPAchrome

and it is spontaneously converted to 5,6-dihydroxyindole (DHI). Then, DHI is oxidized to indole-5,6-quinone and it is polymerized to eumelanin. Another way, DOPAchrome is converted to 5,6-dyhydroxyindole-2-carboxylic acid (DHICA) via enzymatic conversion by dopachrome tautomerase (DCT) and then, it is oxidized to indole-5,6-quinone carboxylic acid and polymerized to eumelanin. In pheomelanin pathway, cysteine reacts with DOPAquinone to form cysteinylDOPA. Then, It is converted to 1,4-benzothiazonylalanine and polymerized to form pheomelanin. The melanogenesis is presented in Figure 2.

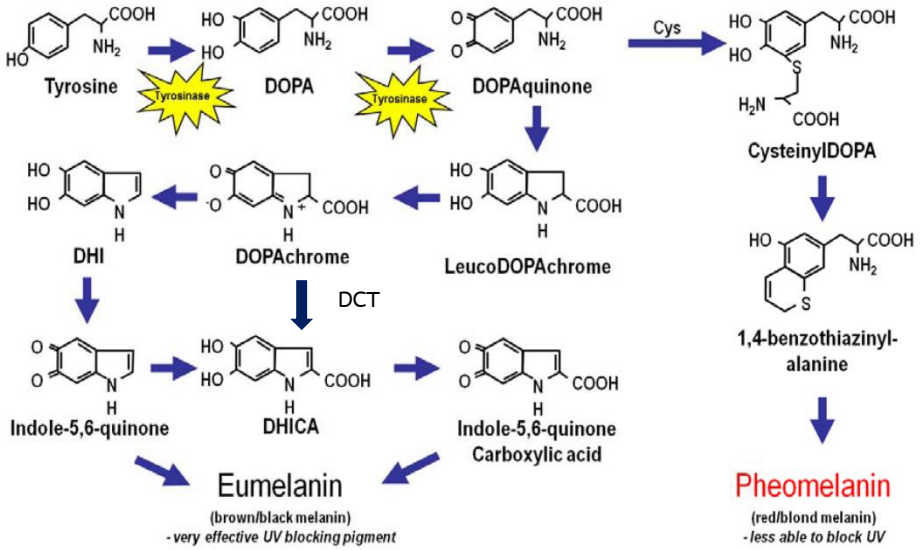

Figure 2 The Melanin biosynthesis pathway

2.2 *Manilkara kauki* (L.) Dubard

Manilkara kauki (L.) Dubard or Talawrinta is one of tropical plants in Sapotaceae family. It grows up to 25-30 meters. Branches are whitish grey or brownish and glabrous. Leaves are broadly ovate, apex rounded, upper surface glabrous and lower surface silvery sericeous. Fruits are oval in shape and have sweet flavor. Barks are grey-brown and deeply fissured. Flowers are yellowish-white [7]. Leaves, fruits and whole plant of *M. kauki* are shown in Figure 3. *M. kauki* was reported to have several kinds of pharmacological activities. The fresh ripe fruits are contains many nutrients such as proteins, fats, minerals and niacin. It has high iron contents which is essential element for blood production. It is useful to help blood system to produce red blood cell for avoid anemia. In addition, the fruits contain a lot of vitamin A which is good for eye health. Furthermore, it can treat diarrhea and inflammation of the mouth [15]. In India, seeds are used as febrifuge and anthelmintic, fruits and barks of *M. kauki* are used as astringent [16] and folk medicine [17].

Figure 3 (a) The leaves (b) the fruits and (c) whole plant of *M. kauki*

2.3 Literature reviews

Several tropical plants exhibited tyrosinase inhibitory activity. Woods of *Cudrania javanensis* Trec. exhibited tyrosinase inhibitory activity with percent inhibition of 77.86 ± 2.41% at concentration of 200 µg/ml[18]. Woods, root barks and roots of *Artocarpin integer* (Thumb.) Merr. showed strong tyrosinase inhibitory activity with percent inhibition of 80.02 ± 3.22%, 82.60 ± 0.76% and 90.57 ± 2.93% at concentration of 200 µg/ml, respectively. Artocarpanone was isolated from ethanol crude extract of roots of *A. integer* (Thumb.) Merr. and exhibited tyrosinase inhibitory activity with IC_{50} value of 44.56 µg/mL [18]. In addition, aqueous crude extract of hearthwood of *Artocaropin lakoocha* Roxb. exhibited tyrosinase inhibitory activity with IC_{50} value of 0.76 µg/mL. Oxyresveratrol which was isolated from aqueous crude extract of heartwood of *A. lakoocha* Roxb. showed tyrosinase inhibitory activity with IC_{50} value of 0.83 µg/mL [19]. The ethyl acetate crude extract of *Phyllanthus emblica* Linn. exhibited tyrosinase inhibitory activity with IC_{50} value of 0.151 ± 0.072 mg/mL [20]. Methanol crude extract of roots of *Carissa opaca* showed tyrosinase inhibitory activity with IC_{50} value of 34.76 µg/mL [21].

2.3.1 Biological activities of Sapotaceae family

Sapotaceae family has shown several kinds of biological activities such as anticancer, antidiabetic, antiulcer, immunomodulatory antioxidant and tyrosinase inhibitory activities. The summary of biological activities of Sapotaceae family is shown in Table 2.1. The isolated compounds except tyrosinase inhibitors of Sapotaceae family are shown in Table 2.2 and chemical constituent of isolated compounds of Sapotaceae family are shown in Figure 4.

Table 2.1 The summary of biological activities of Sapotaceae family

Botanical name	Plant part	Extract	Biological activity	Reference
Achras sapota	Leaves	Methanol	Mosquitocidal activity against a common malarial vector, *Anopheles stephensi* Liston	[22]
Chrysophyllum albidum	Leaves	Petroleum ether	DPPH radical scavenging activity (4,057.50 ± 809.60 g/kg)	[23]
		Ethyl ether	DPPH radical scavenging activity (414.40 ± 92.00 g/kg)	
Madhuca longifolia	Leaves	Petroleum ether	Antimicrobial activity against *Escherichia coli* and *Staphylococcus aureus.*	[24]
	Leaves	Ethanol	Wound healing activity (17.86 ± 0.19%)	[25]
Manilkara hexandra	Seeds	Acetone	Antibacterial activity against *Streptococcus mutans*	[26]
Manilkara huberi	Barks	CH_2Cl_2	Antifungal activity against *Candida albicans, Candida glabrata* and *Candida parapsilosis.*	[27]
Manilkara subsericea	Aerial parts	Ethyl acetate	Molluscicidal activity (LD_{50} = 23.41 ± 1.15 µg/mL)	[28]
Manilkara zapota	Flowers	Ethanol	Anticancer activity against MCF-7 cell line (IC_{50} = 12.5 µg/ml)	[29]
	Leaves	Ethanol	DPPH radical scavenging activity (IC_{50} = of 68.27 µg/mL)	[30]
	Leaves	Petroleum ether	Antifungal activity against *Mucor hiemalis* (MTCC No.157), *Fusarium eumartii* (MTCC No.399) and *Candida albicans* (MTCC No.183)	[31]
	Leaves	Methanol	Antimicrobial activity	[32]
	Seeds	Methanol	DPPH radical scavenging activity (IC_{50} = 8.50 ± 0.55 µg/mL	[33]

Table 2.1 The summary of biological activities of Sapotaceae family (continue)

Botanical name	Plant part	Extract	Biological activity	Reference
M. zapota (continue)	Seeds	Ethanol	Anti-inflammation (87.28% at concentration 500 µg/mL)	[34]
	Seeds	Aqueous	Invertase inhibitory activity (98.7% at concentration 10 mg/mL)	[35]
Mimosops elengi	Barks	Methanol	Antimicrobial activity against *Streptococcus mutans*, *Enterococcus faecalis* and *staphylococcus aureus.*	[36]
	Barks	Ethanol	Diuretic activity	[37]
	Flowers	Methanol	Antibacterial activity against *Bacillus cereus* (MTCC-1305), *Enterobacter faecalis* (MTCC-5112), *Salmonella paratyphi* (MTCC-735), *Staphylococcus aureus* (MTCC-96), *Escherichia coli* (MTCC-729), *Proteus vulgaris* MTCC-426, *Klebsiella pneumoniae* (MTCC-109), *Pseudomonas aeruginosa* (MTCC-647) and *Serratia marcescens* (MTCC-86)	[38]
	Leaves	Ethanol	Anti HIV-1 integrase activity	[39]
	Leaves	Methanol	DPPH radical scavenging activity (74.96 ± 5.18%)	[40]
	Leaves	Methanol	Anti-urease activity (IC_{50} = 62.1±1.20 µg/mL)	[41]
	Stem barks	Ethyl acetate	*Bacillus subtilis*, *Bacillus licheniformis* and *Proteus mirabilis*	[42]

Table 2.1 The summary of biological activities of Sapotaceae family (continue)

Botanical name	Plant part	Extract	Biological activity	Reference
Monoteheca buxifolia	Leaves	Aqueous	Antifungal activity against grain moulds	[43]
	Stems	Ethyl acetate	Antibacterial activity against *Escherichia coli*, *Pseudomonas aeruginosa*, *Erwinia carotovora*, *Salmonella typhi*, *Klebsiella pneumoniae* and *Staphylococcus aureus*	
	Stems	Ethyl acetate	DPPH radical scavenging activity (IC_{50} = 194.24 ± 7.36 µg/mL)	[43]
Pouteria cambodiana	Stem barks	Aqueous	Immunomodulatory activity	[44]
Pouteria ramiflora	Leaves	*n*-Hexane	*α*-Amylase inhibitory activity	[45]
Pouteria sapota	Fruits	*n*-Hexane :CH_2Cl_2 (1:1)	Total soluble phenols activity (28.51 ± 0.61 mg Gallic acid equivalent (GAE) /100 g fresh weight) Total carotenoid activity (1127.94 ± 5.30 µg β-carotene/100 g fresh weight) δ-Tocopherol activity (0.36 ± 0.03 mg/100 g dry weight)	[46]
Synsepalum dulcificum	Seeds	Methanol	Total phenolic content (306.7 ± 44.1 GAE/100 g fresh weight) Total flavonoid content (3.8 mg (Quercetin equivalent (QE)/100 g fresh weight) DPPH radical scavenging activity (96.30% of fresh weight) ABTS radical scavenging activity (32.50% of fresh weight)	[47]

Table 2.1 The summary of biological activities of Sapotaceae family (continue)

Botanical name	Plant part	Extract	Biological activity	Reference
Sideroxylon inerme	Barks	Acetone	Tyrosinase inhibitory activity (IC_{50} = 63.00 ± 2.10 µg/mL)	[48]
		Methanol	Tyrosinase inhibitory activity (IC_{50} = 82.10 ± 2.70 µg/mL)	
		CH_2Cl_2	Tyrosinase inhibitory activity (IC_{50} > 400 µg/mL)	
Tridesmostemon omphalocar Poides	Stem barks	Methanol	Antimicrobial activity against *Escherichia coli*, *Shigella dysenteriae*, *Staphylococcus aureus*, *Proteus vulgaris*, *Klebsiella pneumoniae*, *Streptococcus faecalis*, *Salmonella typhi*, *Candida albicans* and *Candida krusei*	[49]

Table 2.2 The isolated compounds of Sapotaceae family

Botanical name	Plant part	Compound	Reference
Argania spinosa	Seeds	Naringenin-7-*O*-glucoside (**1**) Hesperidin (**2**) (+)-Catechin (**3**) (-)-*epi*-Catechin (**4**) Caffeic acid (**5**) Ferulic acid (**6**) Syringic acid (**7**) Veratric acid (**8**)	[6]
Chrysophyllum cainito	Fruits	Cyanidin-3-*O*-*β*-glucopyranoside (**9**)	[50]
Madhuca latifolia	Fruits	3',4'-Dihydroxy-5,2'-dimenthoxy-6,7-methylen dioxy isoflavone (**10**)	[6]
Manilkara bidentata	Resin	3*β*-*O*-Acetyl-*α*-amyrin (**11**) 3*β*-*O*-*trans* Cinnamyl-*α*-amyrin (**12**) 3*β*-*O*-*trans* Cinnamyl lupeol (**13**)	[5]

Table 2.2 The isolated compounds of Sapotaceae family (continue)

Botanical name	Plant part	Compound	Reference
Manilkara zapota	Fruits	Apigenin-7-*O*-*α*-*L*-rhamnoside (**14**) Dihydromyricetin (**15**) (+)-Gallocatechin (**16**) Leucodelphinidine (**17**) Leucocyanidine (**18**) Leucoperalgonidine (**19**) Methylchlorogenate (**20**)	[6]
	Seeds	*D*-Quercitol (**21**)	
Mimusops hexandra	Barks	Taraxeryl acetate (**22**) Cinnamic acid (**23**)	[51]
Mimusops manilkara	Fruits	*β*-Sitosterol (**24**) *β*-Amyrin acetate (**25**)	[52]
Pouteria campechiana	Leaves	(+)-Catechin-*O*-gallate (**26**) Taxifolin-3-*O*-*α*-*L*-rhamnopyranoside (**27**) (+)-Catechin-*O*-gallate (**28**) *trans*-Taxifolin-3-*O*-*α*-*L*-arabinopyranoside (**29**) Taxifolin-3-*O*-*α*-*L*-arabinofuranoside (**30**)	[6]
Pouteria caimito	Leaves	Spinasterol (**31**)	[53]
Pouteria obovata	Fruits	2*R*,3*R*-4'-*O*-Methyldihydrokaempferol 7-*O*-[3"-*O*-acetyl]-*β*-*D*-glucopyranoside (**32**)	[6]
Pouteria ramiflora	Leaves	Friedelin (**33**) *epi*-Friedelanol (**34**)	[45]
Pouteria sapota	Fruits	Gallocatechin-3-*O*-gallate (**35**)	[6]
Pouteria splendens	Leaves	*trans*-*α*-Farnesol (**36**) *trans*-Nerolidol (**37**) *cis*-*β*-Elemene (**38**) Germacrene D (**39**) *β*-Selinene (**40**) Eremophilene (**41**) *δ*-Cadinene (**42**) 10-*epi*-*α*-Cadinol (**43**) 10-*epi*-*α*-Muurolol (**44**) *epi*-Globulol (**45**) Globulol (**46**) Ledene (**47**) Palustrol (**48**)	[54]

Table 2.2 The isolated compounds of Sapotaceae family (continue)

Botanical name	Plant part	Compound	Reference
P. splendens (continue)	Leaves	Isophytol (**49**) *trans*-Phytol (**50**)	[54]
Pouteria torta torta	Leaves	Lupeol acetate (**51**) Myricetin (**52**) Mericetin-3-*O*-*β*-*D*-galactopyranoside (**53**) Mericetin-3-*O*-*α*-*L*-arabinopyranoside (**54**)	[55] [56]
Tridesmostemon omphalocarpoides	Stem wood	Lichexanthone (**55**)	[6]
Vitellaria paradoxa	Kernels	3-*O*-*β*-*D*-Glucuronopyranosyl 16*α*-hydroxyprotobassic acid (**56**) 3-*O*-*β*-*D*-Glucopyranosyl 16*α*-hydroxyprotobassic acid (**57**) 3-*O*-*β*-*D*-Glucuronopyranosyl protobassic acid (**58**) Mi-Glycoside l (**59**) Protobassic acid (**60**) Bassic acid (**61**) Spinasterol 3-*O*-*β*-*D*-glucopyranoside (**62**) Isotachioside (**63**) Gallic acid (**64**)	[57]

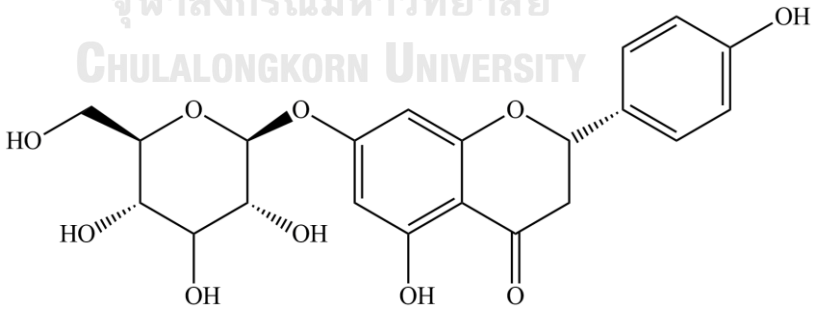

Naringenin-7-*O*-glucoside (**1**)

Figure 4 Chemical structure of isolated compounds of Sapotaceae family

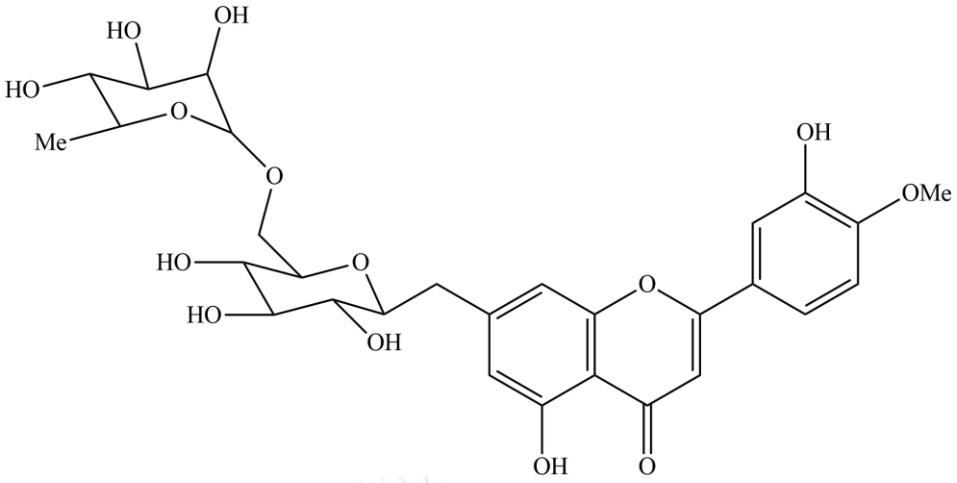

Hesperidin (2)

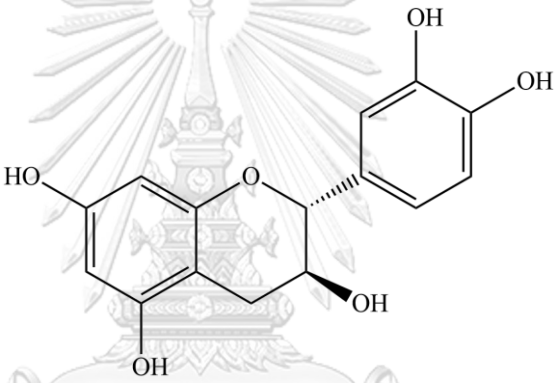

(+)-Catechin (**3**)

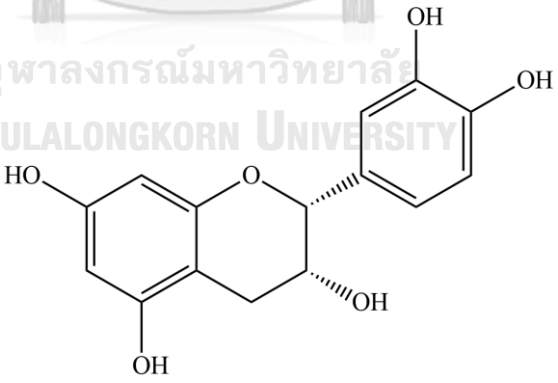

(-)-*epi*-Catechin (**4**)

Figure 4 Chemical structure of isolated compounds of Sapotaceae family (continue)

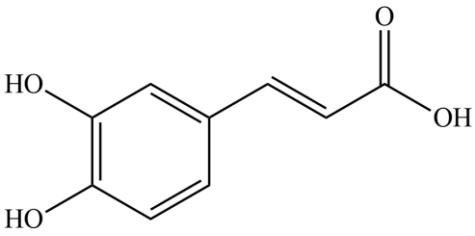

Caffeic acid (**5**)

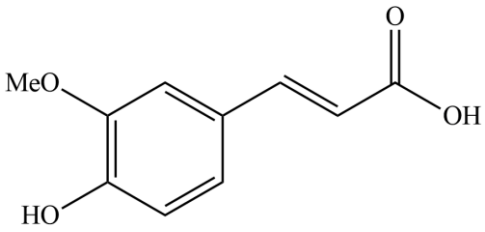

Ferulic acid (**6**)

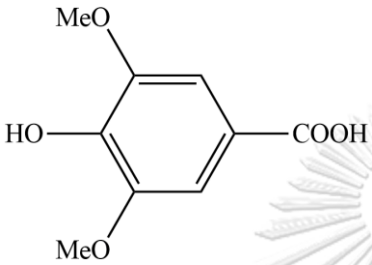

Syringic acid (**7**)

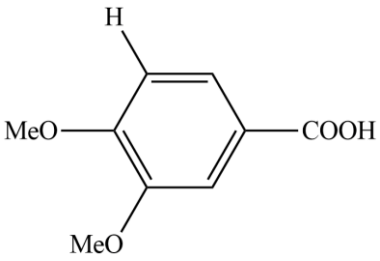

Veratric acid (**8**)

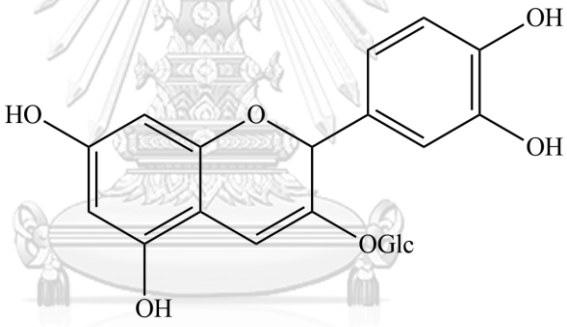

Cyanidin-3-*O*-*β*-glucopyranoside (**9**)

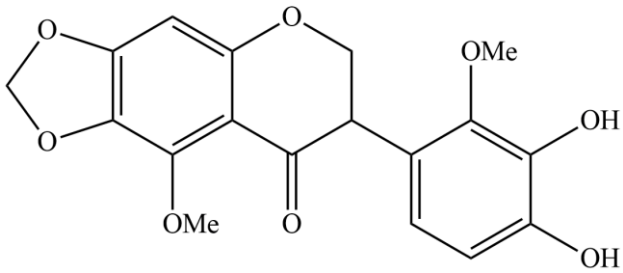

3',4'-dihydroxy-5,2'-dimenthoxy-6,7-methylen dioxy isoflavone (**10**)

Figure 4 Chemical structure of isolated compounds of Sapotaceae family (continue)

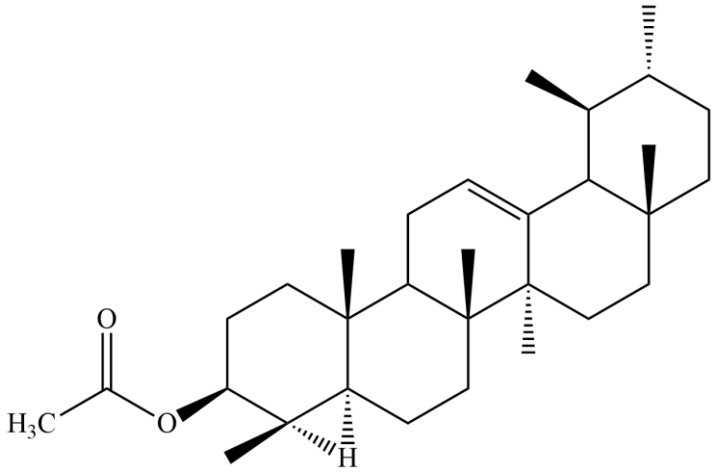

3*β*-*O*-Acetyl-*α*-amyrin (**11**)

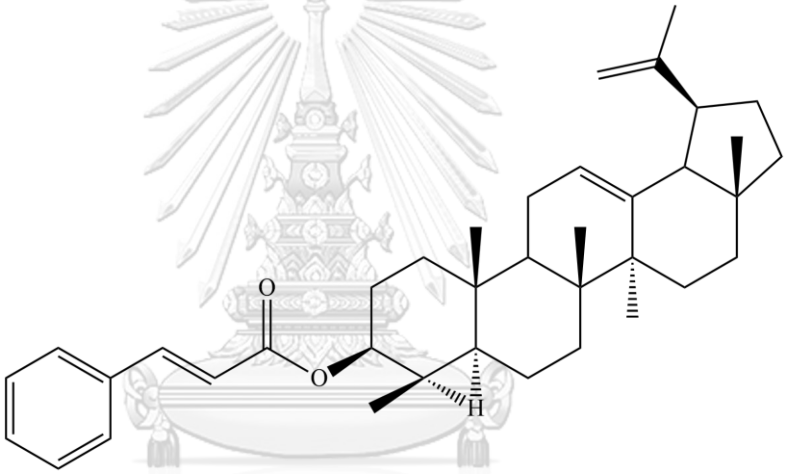

3*β*-*O*-*trans* Cinnamyl-*α*-amyrin (**12**)

Figure 4 Chemical structure of isolated compounds of Sapotaceae family (continue)

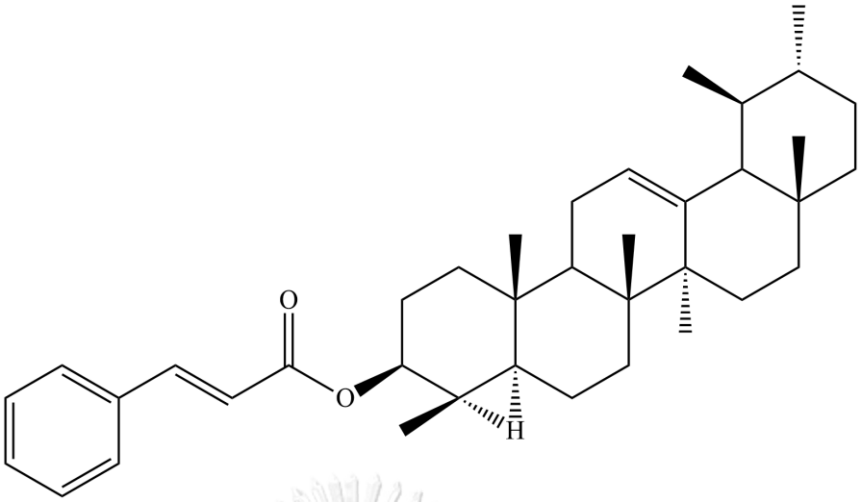

3*β*-*O*-*trans* Cinnamyl lupeol (**13**)

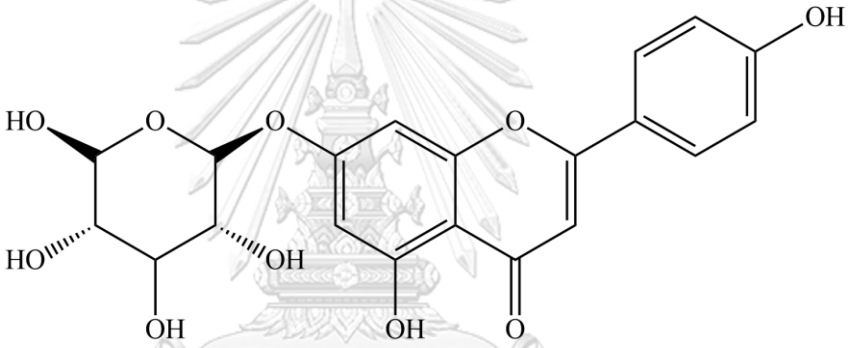

Apingenin-7-*O*-*α*-*L*-rhamnoside (**14**)

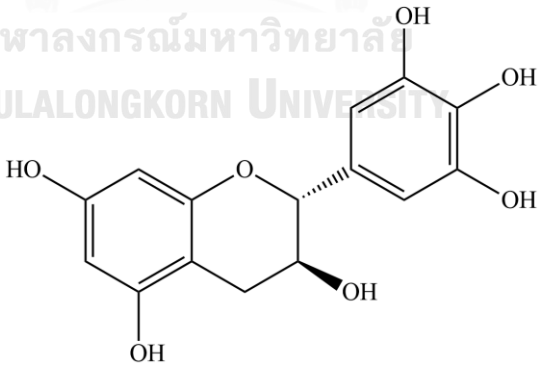

Dihydromyricetin (**15**)

Figure 4 Chemical structure of isolated compounds of Sapotaceae family (continue)

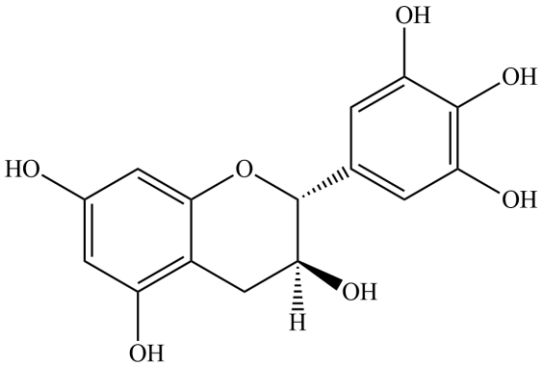

(+)-Gallocatechin (**16**)

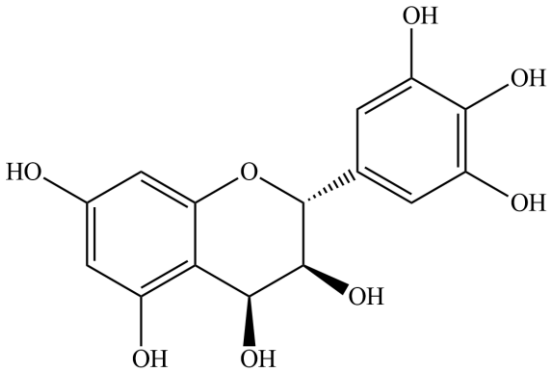

Leucodelphinidine (**17**)

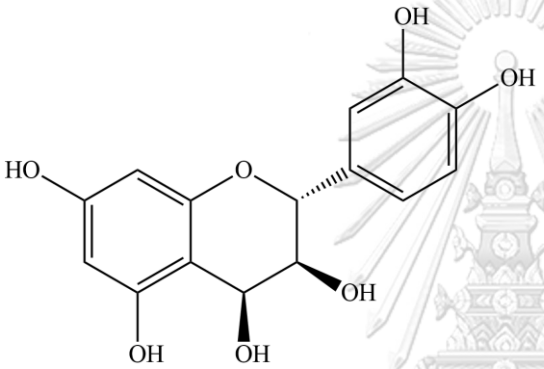

Leucocyanidine (**18**)

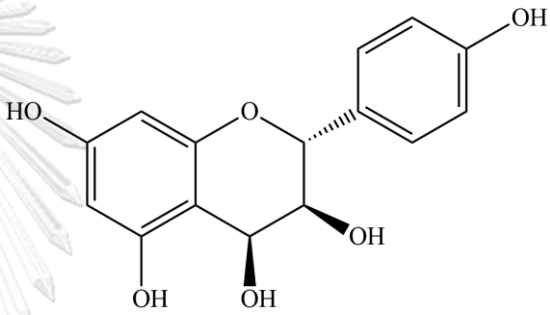

Leucoperalgonidine (**19**)

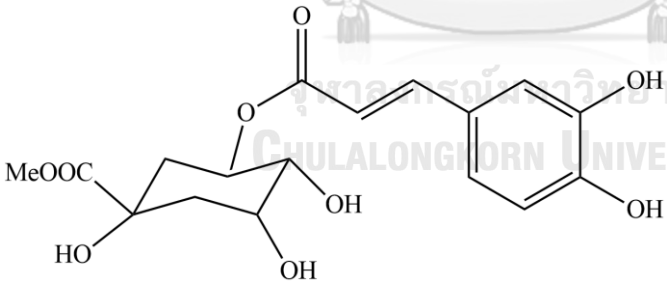

Methylchlorogenate (**20**)

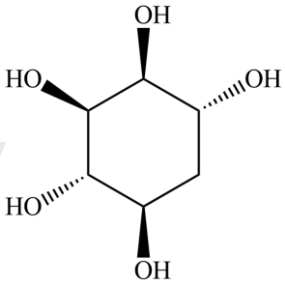

D-Quercitol (**21**)

Figure 4 Chemical structure of isolated compounds of Sapotaceae family (continue)

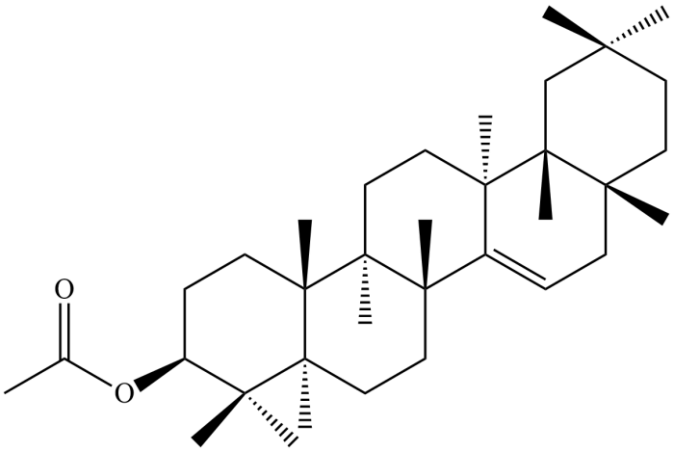

Taraxeryl acetate (**22**)

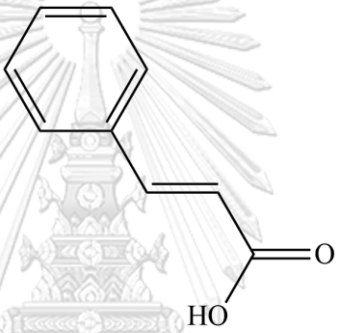

Cinnamic acid (**23**)

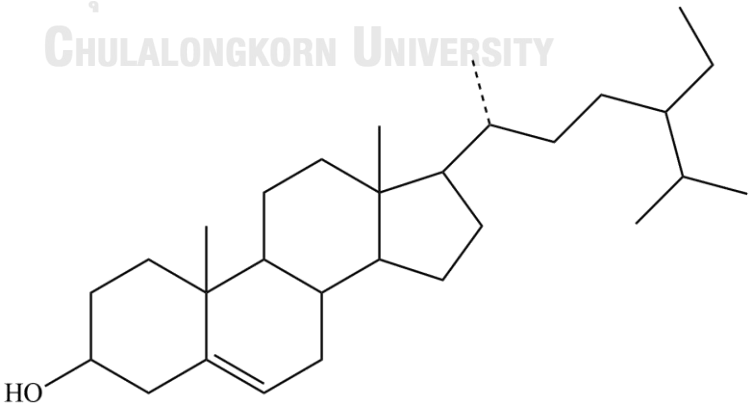

β-Sitosterol (**24**)

Figure 4 Chemical structure of isolated compounds of Sapotaceae family (continue)

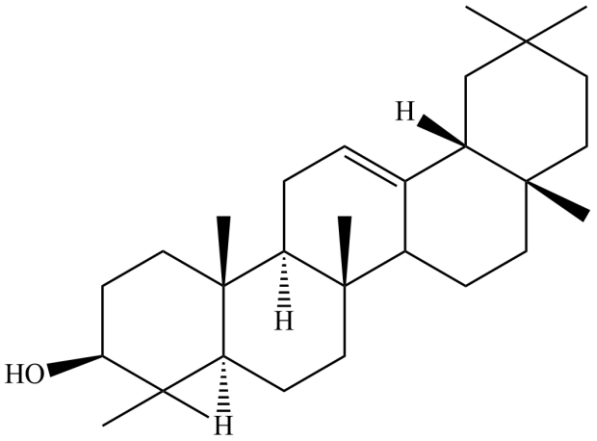

β-Amyrin acetate (**25**)

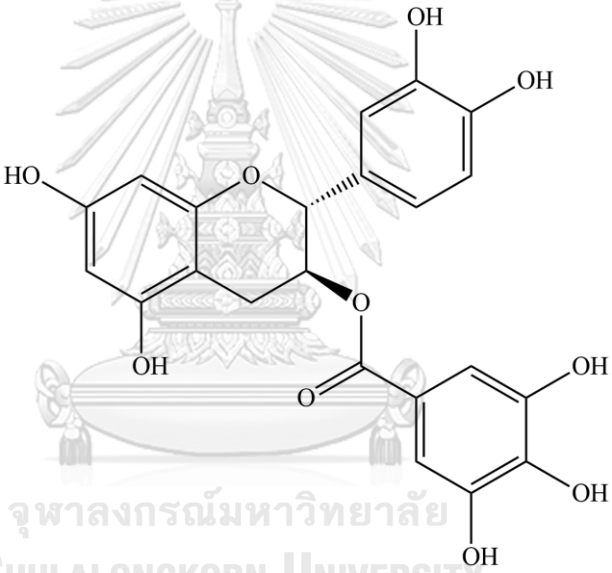

(+)-Catechin-*O*-gallate (**26**)

Figure 4 Chemical structure of isolated compounds of Sapotaceae family (continue)

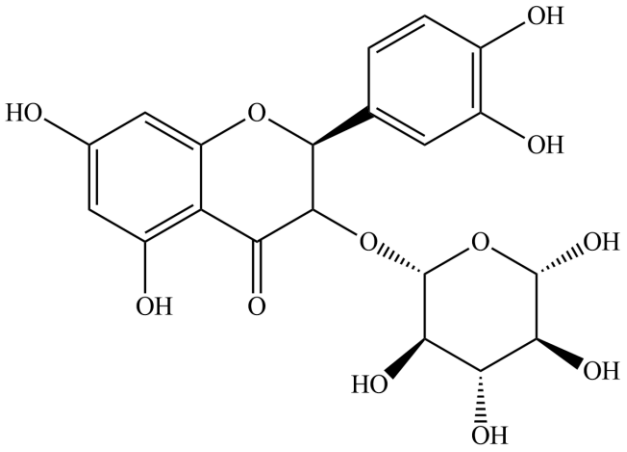

Taxifolin-3-*O*-*α*-*L*-rhamnopyranoside (**27**)

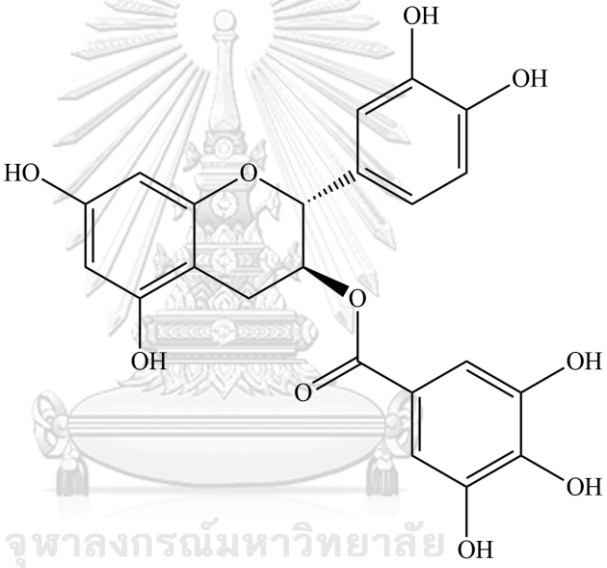

(+)-Catechin-*O*-gallate (**28**)

Figure 4 Chemical structure of isolated compounds of Sapotaceae family (continue)

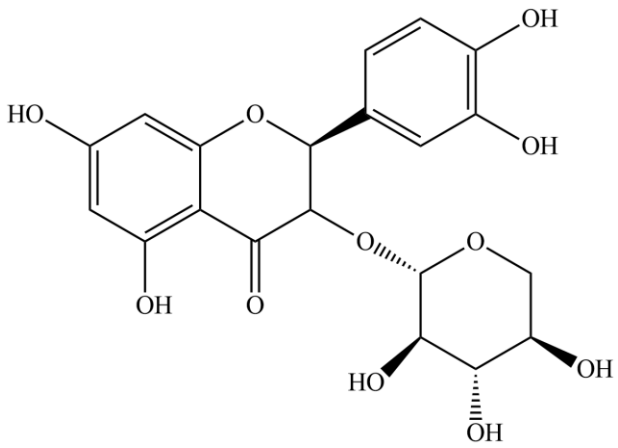

trans-Taxifolin-3-*O*-*α*-*L*-arabinopyranoside (**29**)

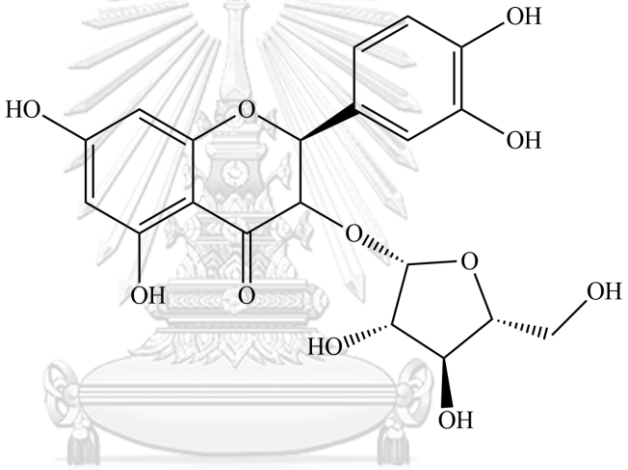

Taxifolin-3-*O*-*α*-*L*-arabinofuranoside (**30**)

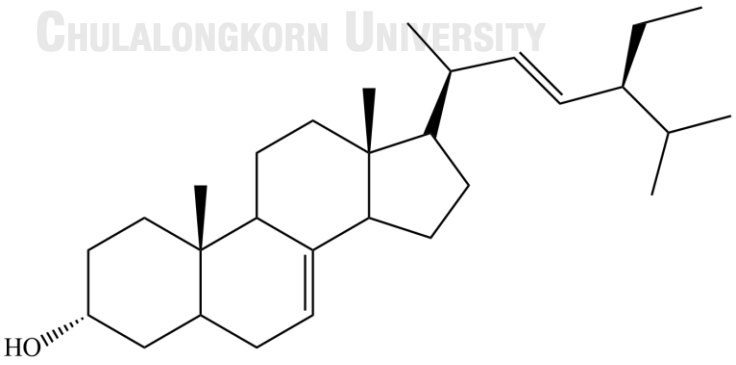

Spinasterol (**31**)

Figure 4 Chemical structure of isolated compounds of Sapotaceae family (continue)

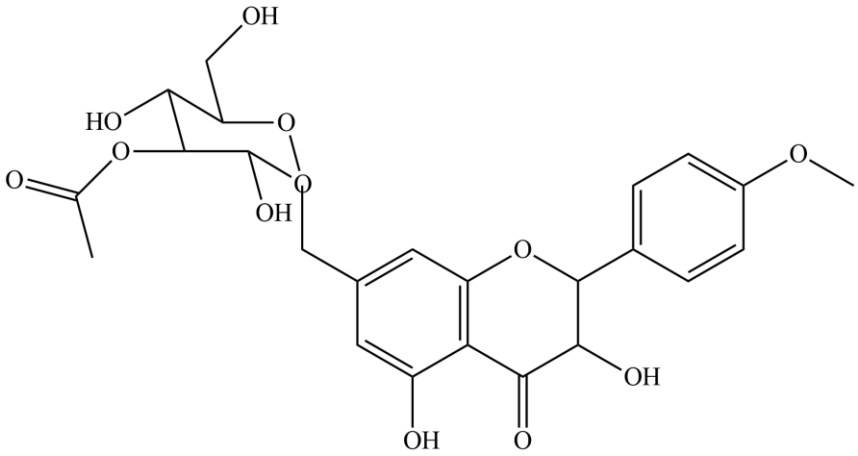

2*R*,3*R*-4'-*O*-Methyldihydrokaempferol 7-*O*-[3"-*O*-acetyl]-*β*-*D*-glucopyranoside (**32**)

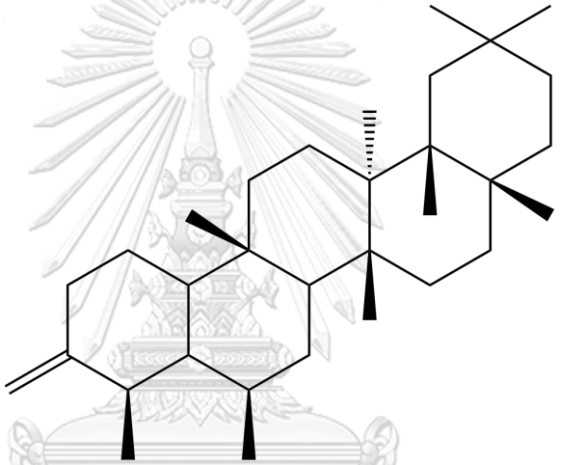

Friedelin (**33**)

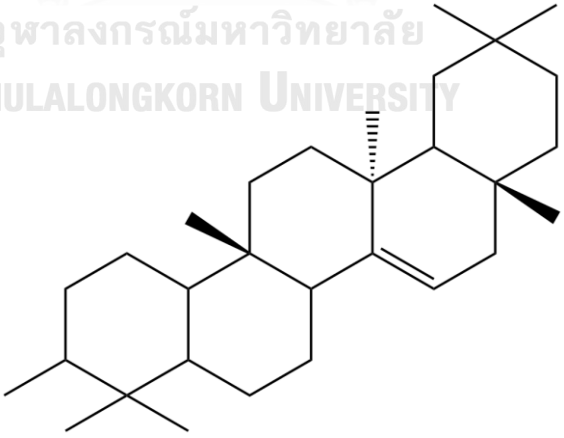

epi-Friedelanol (**34**)

Figure 4 Chemical structure of isolated compounds of Sapotaceae family (continue)

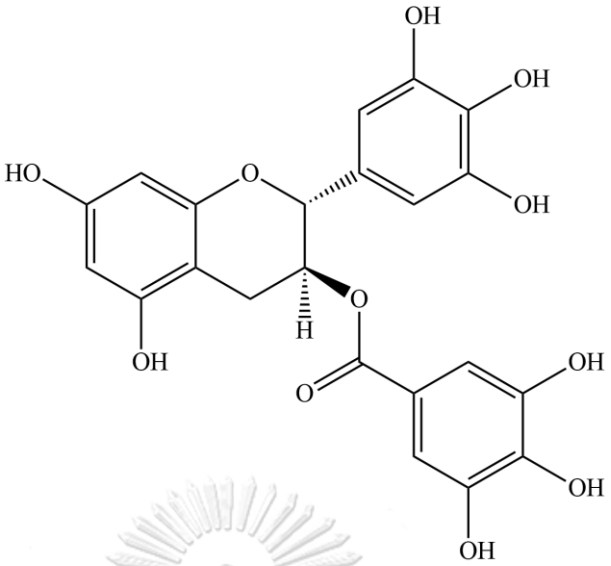

Gallocatechin-3-*O*-gallate (**35**)

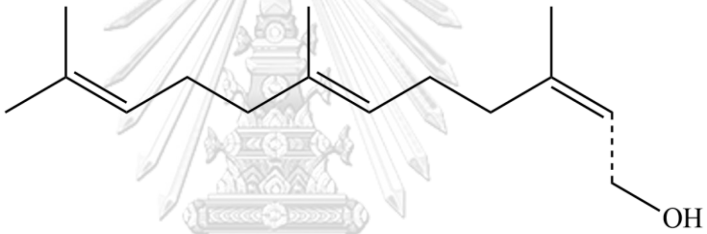

trans-α-Farnesol (**36**)

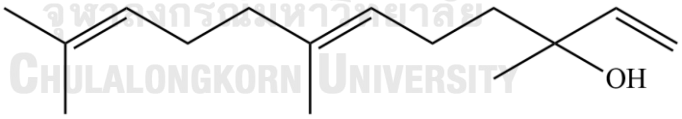

trans-Nerolidol (**37**)

Figure 4 Chemical structure of isolated compounds of Sapotaceae family (continue)

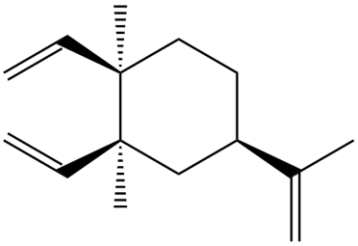

cis-*β*-Elemene (**38**)

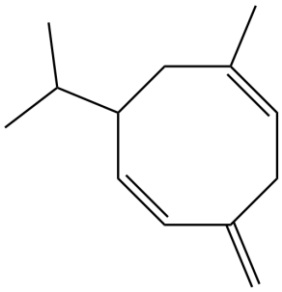

Germacrene D (**39**)

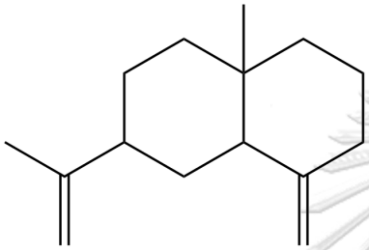

β-Selinene (**40**)

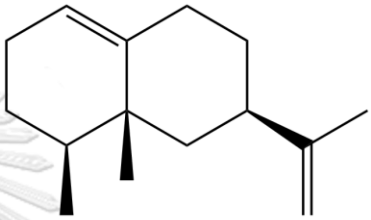

Eremophilene (**41**)

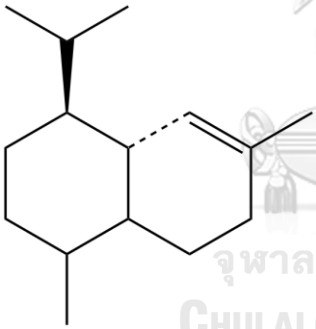

δ-Cadinene (**42**)

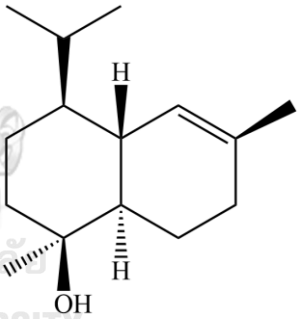

10-*epi*-*α*-Cadinol (**43**)

Figure 4 Chemical structure of isolated compounds of Sapotaceae family (continue)

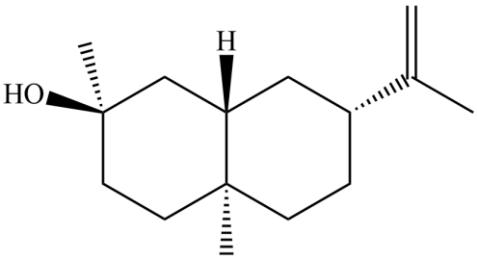

10-*epi*-*α*-Muurolol (**44**)

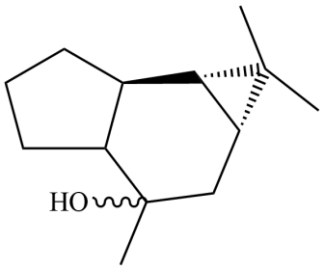

epi-Globulol (**45**)

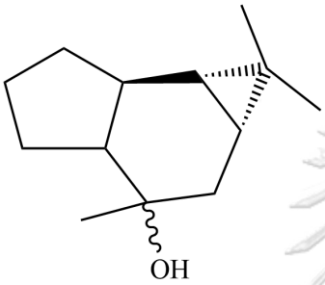

Globulol (**46**)

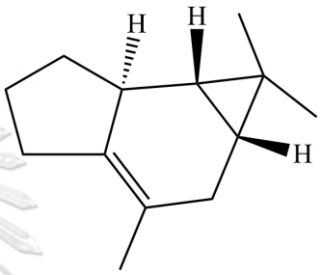

Ledene (**47**)

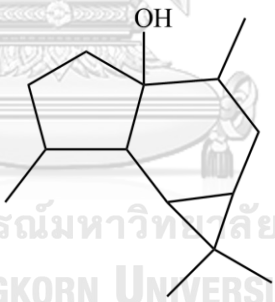

Palustrol (**48**)

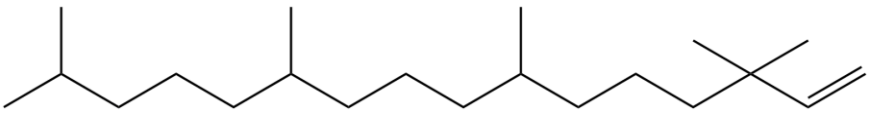

Isophytol (**49**)

Figure 4 Chemical structure of isolated compounds of Sapotaceae family (continue)

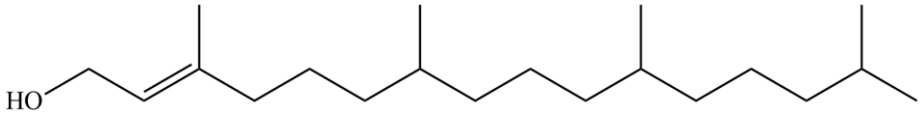

trans-Phytol (**50**)

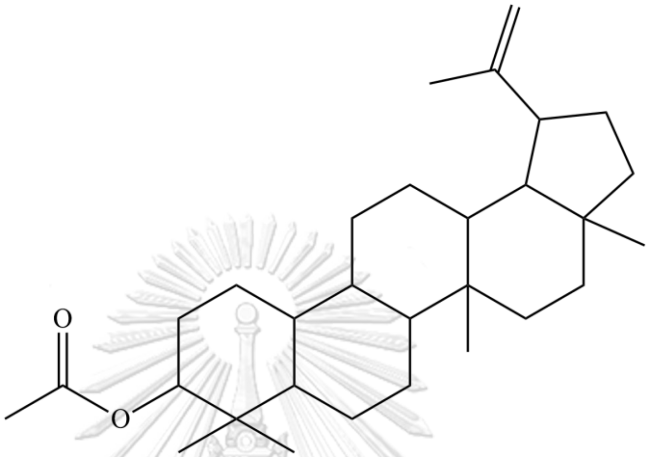

Lepeol acetate (**51**)

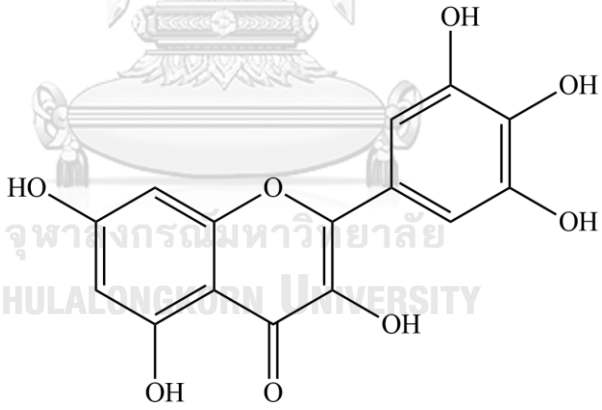

Myricetin (**52**)

Figure 4 Chemical structure of isolated compounds of Sapotaceae family (continue)

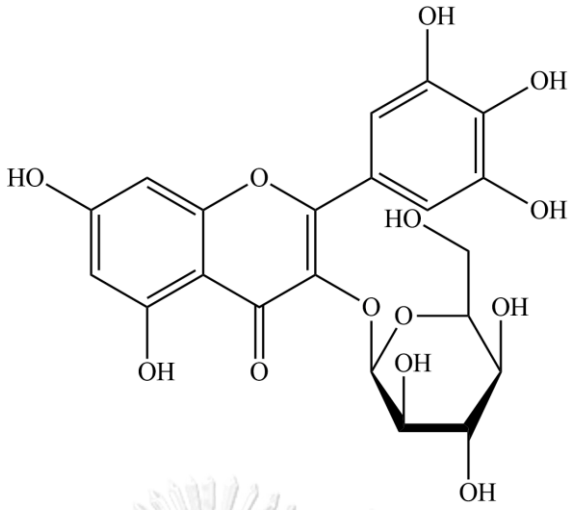

Mericetin-3-*O*-*β*-*D*-galactopyranoside (**53**)

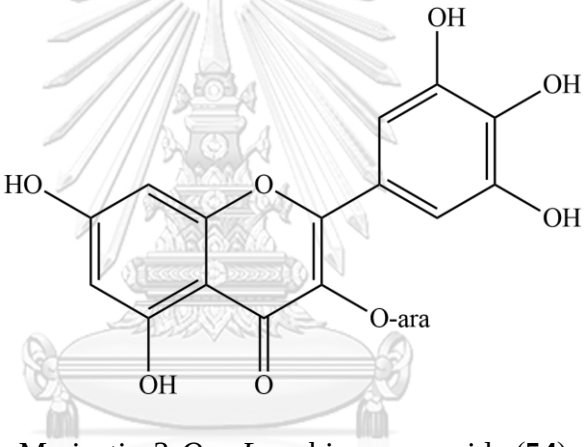

Mericetin-3-*O*-*α*-*L*-arabinopyranoside (**54**)

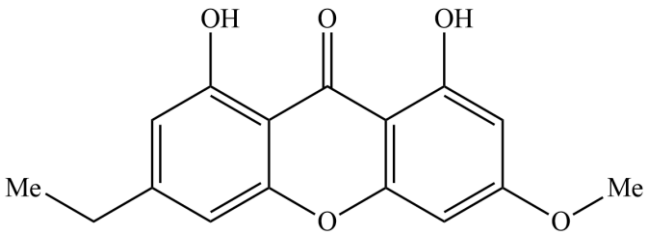

Lichexanthone (**55**)

Figure 4 Chemical structure of isolated compounds of Sapotaceae family (continue)

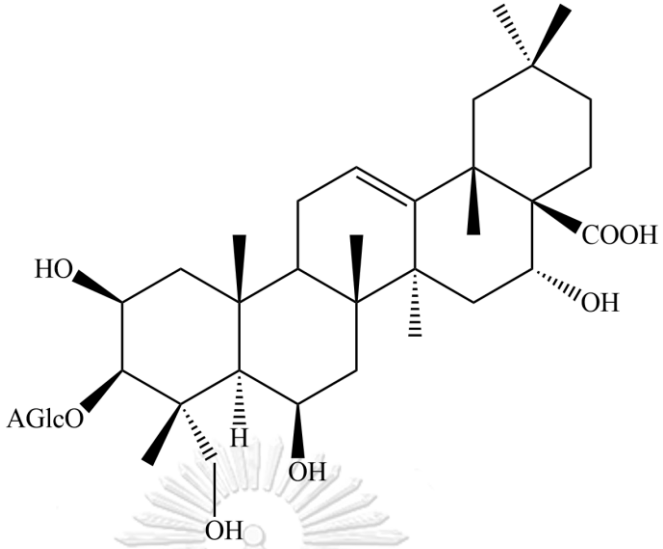

3-*O*-*β*-*D*-Glucuronopyranosyl 16*α*-hydroxyprotobassic acid (**56**)

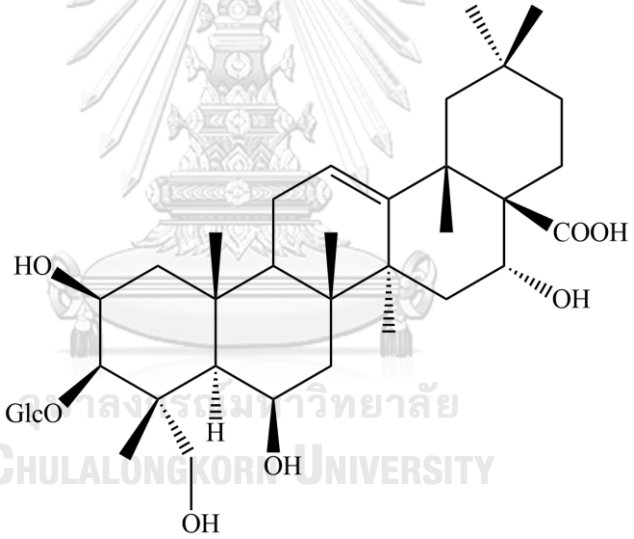

3-*O*-*β*-*D*-Glucopyranosyl 16*α*-hydroxyprotobassic acid (**57**)

Figure 4 Chemical structure of isolated compounds of Sapotaceae family (continue)

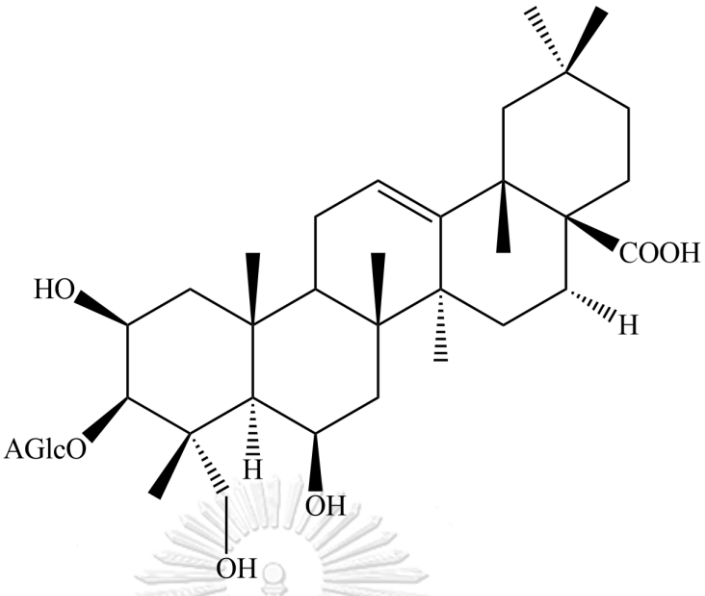

3-*O*-*β*-*D*-Glucuronopyranosyl protobassic acid (**58**)

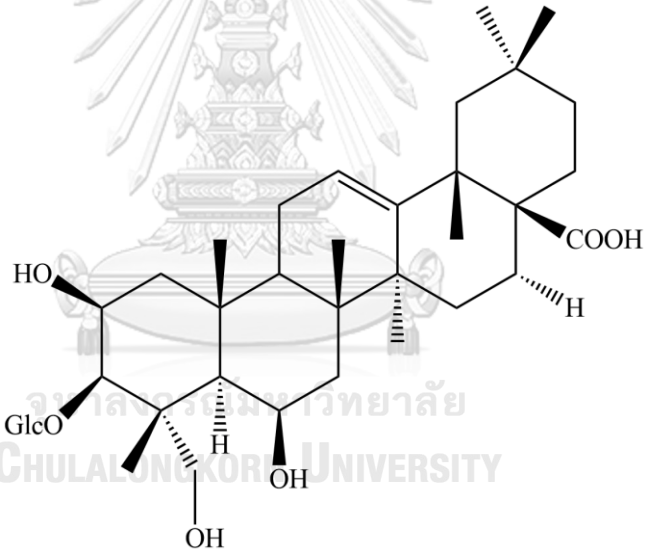

Mi-Glycoside l (**59**)

Figure 4 Chemical structure of isolated compounds of Sapotaceae family (continue)

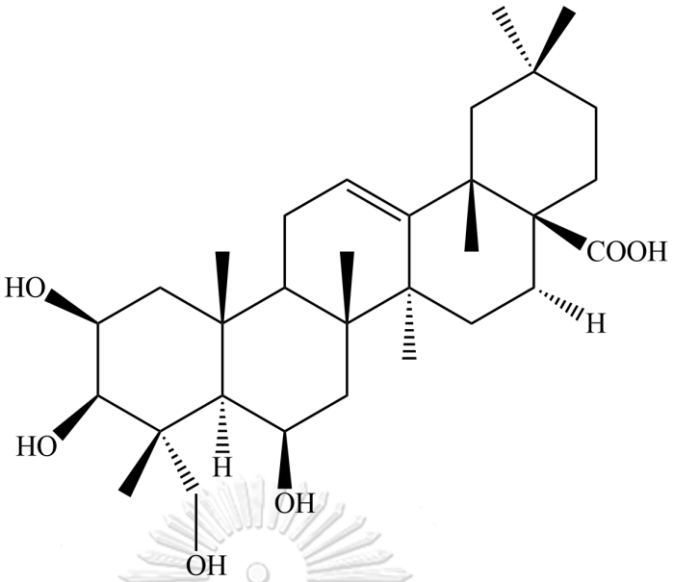

Protobassic acid (**60**)

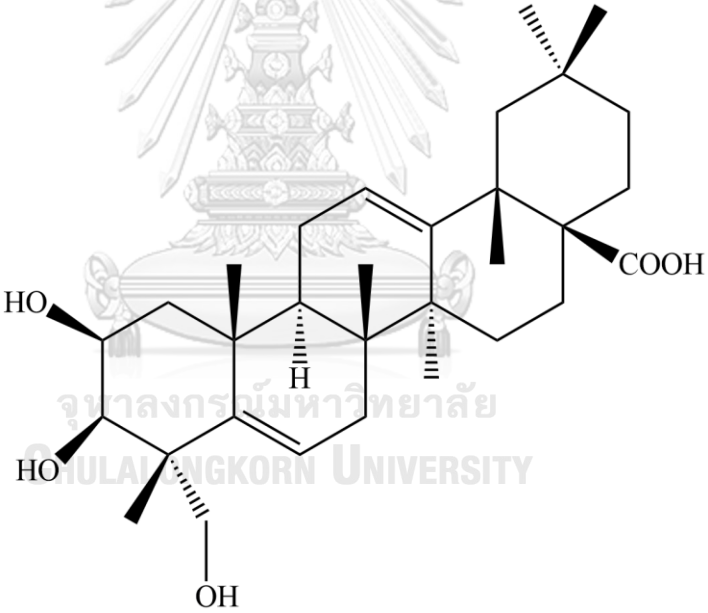

Bassic acid (**61**)

Figure 4 Chemical structure of isolated compounds of Sapotaceae family (continue)

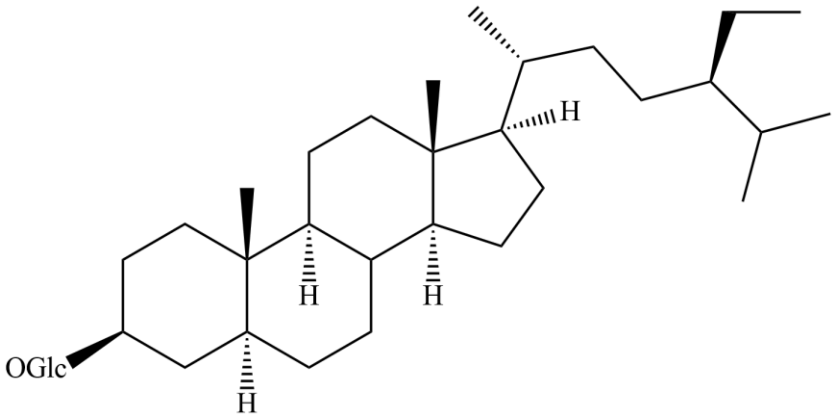

Spinasterol 3-*O*-*β*-*D*-glucopyranoside (**62**)

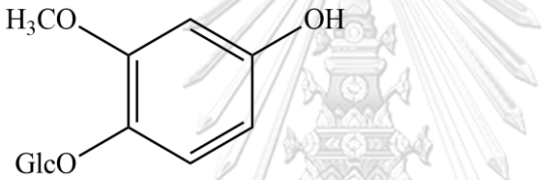

Isotachioside (**63**)

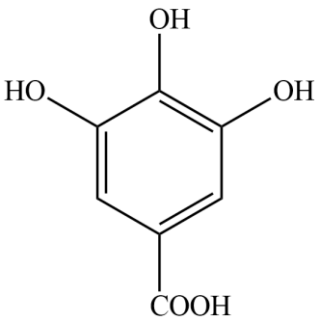

Gallic acid (**64**)

Figure 4 Chemical structure of isolated compounds of Sapotaceae family (continue)

2.3.2 Summary of tyrosinase inhibitors of Sapotaceae family

Sapotaceae was reported to possess pharmacological activities such as antioxidant, antimicrobial, anticancer, antidiabetic, antiulcer, immunomodulatory and tyrosinase inhibitory activities [6]. Tyrosinase inhibitors have been found from natural sources and some of them were developed as cosmetic agents. Tyrosinase inhibitors of Sapotaceae family are shown in Table 2.3. The chemical structure of tyrosinase inhibitors of Sapotaceae family is shown in Figure 5.

Table 2.3 The summary of tyrosinase inhibitors from Sapotaceae family

Botanical name	Plant part	Tyrosinase inhibitor	Reference
Manilkara zapota	Leaves	Myricetin-3-*O*-*α*-*L*-rhamnoside (**65**) (30% inhibition at concentration 100 µg/mL)	[58]
	Barks	Taraxerol methyl ether (**66**) (IC_{50} = 106.53 ± 0.34 and 283.33 ± 0.59 µM for *L*-tyrosine and *L*-DOPA, respectively)	[59]
	Barks	6-Hydroxyflavanone (**67**) (IC_{50} = 41.76 ± 0.20 and 63.10 ± 0.73 µM for *L*-tyrosine and *L*-DOPA, respectively) (+)-Dihydrokaempferol (**68**) (IC_{50} = 32.17 ± 0.32 and 31.60 ± 0.73 µM for *L*-tyrosine and *L*-DOPA, respectively) 3,4-Dihydroxybenzoic acid (**69**) (IC_{50} = 55.21 ± 0.70 and 43.91 ± 0.21 µM for *L*-tyrosine and *L*-DOPA, respectively) Taraxerol (**70**) (IC_{50} = 103.37 ± 0.22 and 272.10 ± 0.16 µM for *L*-tyrosine and *L*-DOPA, respectively) Taraxerone (**71**) (IC_{50} = 70.63 ± 0.36 and 90.60 ± 0.26 µM for *L*-tyrosine and *L*-DOPA, respectively)	[59]
Sideroxylon inerme	Barks	Epigallocatechin gallate (**72**) (IC_{50} = 30.00 ± 1.90 µM) Procyanidin B1 (**73**) (IC_{50} = 200.00 ± 2.20 µM)	[48]
Synsepalum dulcificum	Stems	(+)-*epi*-Syringaresinol (**74**) (IC_{50} = 200.50 µM) 4-Acetonyl-3,5-dimethoxy-*p*-quinol (**75**) (IC_{50} = 208.10 µM) *cis*-*p*-Coumaric acid (**76**) (IC_{50} = 197.90 µM) *trans*-*p*-Coumaric acid (**77**) (IC_{50} = 168.70 µM) *p*-Hydroxybenzoic acid (**78**) (IC_{50} = 358.60 µM)	[60]

Table 2.3 Summary of tyrosinase inhibitors from Sapotaceae family (continue)

Botanical name	Plant part	Tyrosinase inhibitor	Reference
S. dulcificum (continue)	Stems	Vanillic acid (**79**) (IC_{50} = 174.40 µM) *N-cis*-Caffeoyltyramine (**80**) (IC_{50} = 215.50 µM)	[60]

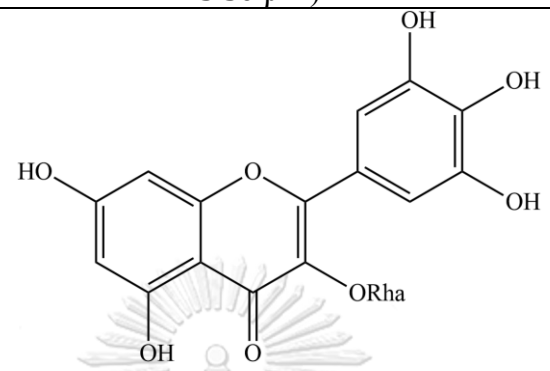

Myricetin-3-*O*-*α*-*L*-rhamnoside (**65**)

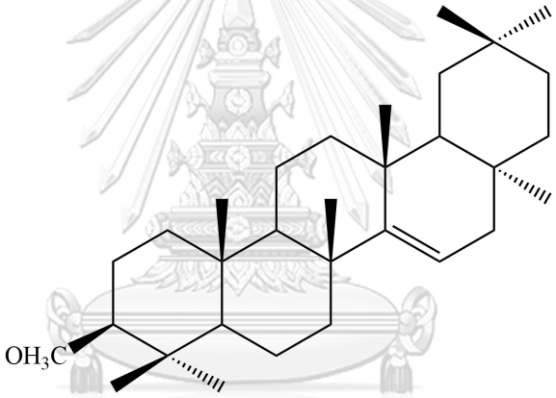

Taraxerol methyl ether (**66**)

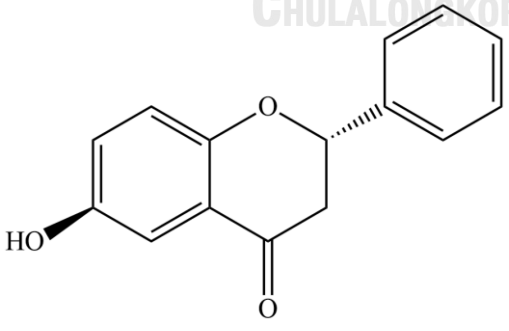

6-Hydroxyflavanone (**67**)

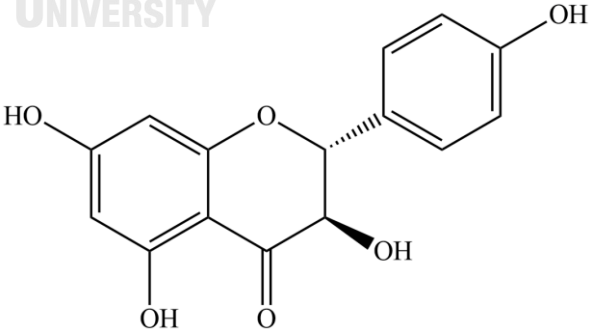

(+)-Dihydrokaempferol (**68**)

Figure 5 Chemical structure of tyrosinase inhibitors of Sapotaceae family

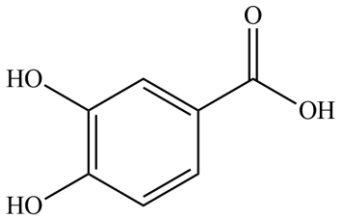

3,4-Dihydroxybenzoic acid (**69**)

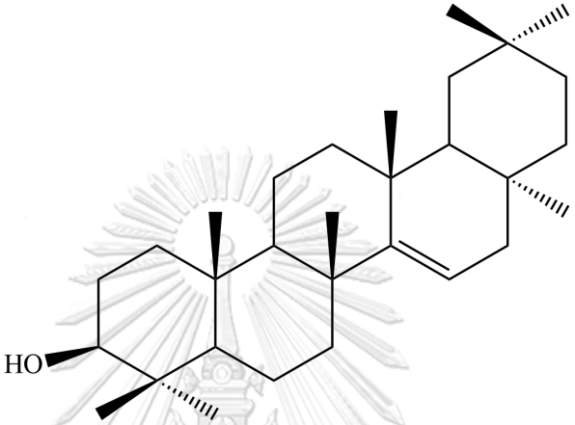

Taraxerol (**70**)

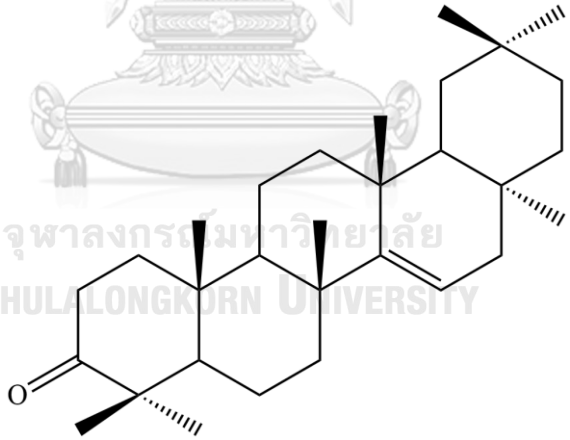

Taraxerone (**71**)

Figure 5 Chemical structure of tyrosinase inhibitors of Sapotaceae family (continue)

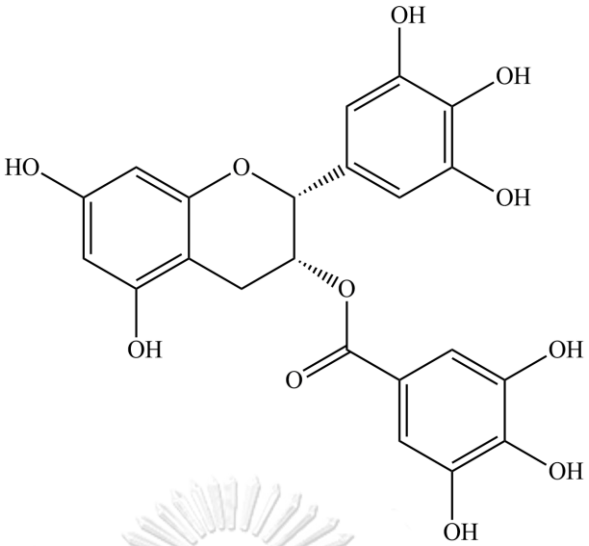

Epigallocatechin gallate (**72**)

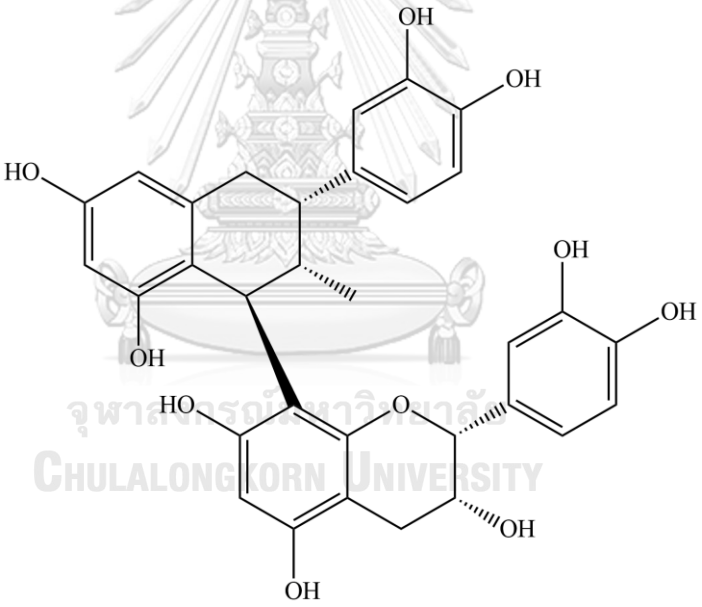

Procyanidin B1 (**73**)

Figure 5 Chemical structure of tyrosinase inhibitors of Sapotaceae family (continue)

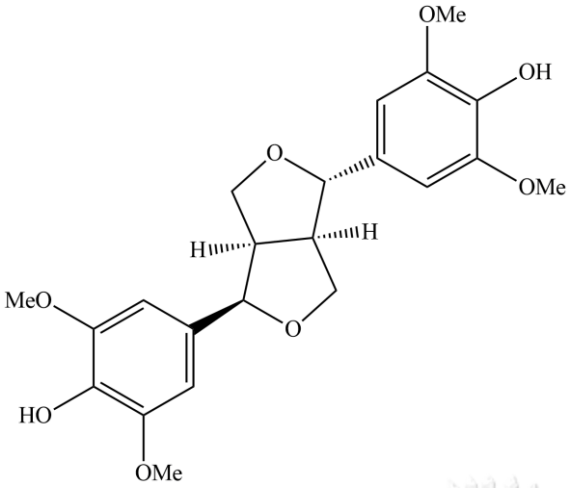

(+)-*epi*-Syringaresinol (**74**)

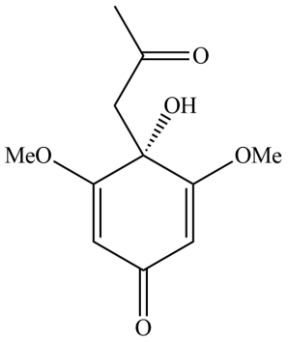

4-Acetonyl-3,5-dimethoxy-*p*-quinol (**75**)

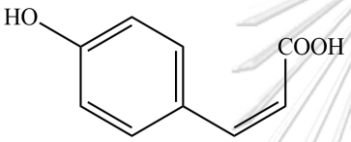

cis-*p*-Coumaric acid (**76**)

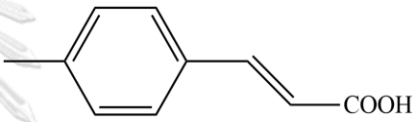

trans-*p*-Coumaric acid (**77**)

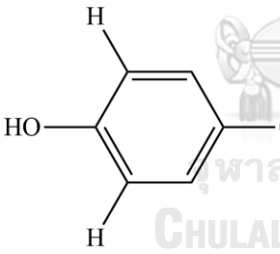

p-Hydroxybenzoic acid (**78**)

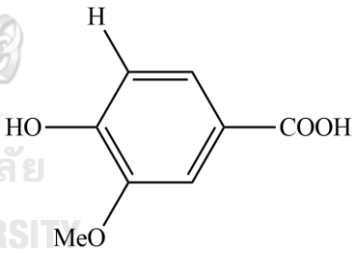

Vanillic acid (**79**)

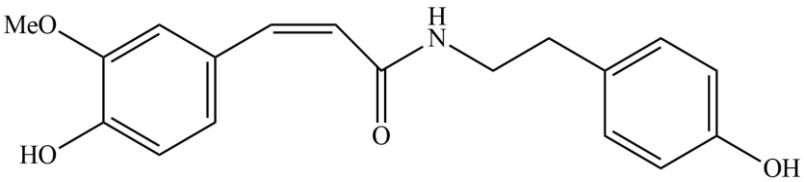

N-*cis*-Caffeoyltyramine (**80**)

Figure 5 Chemical structure of tyrosinase inhibitors of Sapotaceae family (continue)

CHAPTER III
MATERIALS AND METHODS

3.1 Plant materials

The fresh fruits, leaves, seeds, stem barks and woods of *M. kauki* were collected from Jaransanitwong garden, Bangkok, Thailand in December 2015. The plant was identified by a botanist of Department of Botany, Faculty of Science, Chulalongkorn University, Bangkok, Thailand. The voucher specimen (BCU No. A015371) was deposited at Professor Kasin Suvatabhandhu Herbarium, Chulalongkorn University, Bangkok, Thailand.

3.2 Reagents

3.2.1 All commercial grade organic solvents were distilled prior to use such as *n*-hexane, dichloromethane, ethyl acetate, acetone and methanol.

3.2.2 All analytical grade chemicals; sodium dihydrogen phosphate monohydrate, disodium dihydrogen phosphate monohydrate, dimethyl sulfoxide (DMSO), absolute ethanol, sulfuric acid, *L*-tyrosine, *L*-DOPA, kojic acid, *α*-arbutin, chloroform-*d* and acetone-d_6 were purchased from Merck (Germany). Mushroom tyrosinase was purchased from Sigma-Aldrich (USA).

3.3 General techniques and procedures

3.3.1 Thin layer chromatography (TLC)

Techniques:	One dimension
Stationary phase:	Silica gel 60 F_{254} (Merck, Germany) pre-coated plate
Layer thickness:	0.2 mm
Distance of mobile phase:	4 cm
Mobile phase:	Various solvent systems
Detection:	a. UV light at 254 nm b. dipping in 10% sulfuric acid in aqueous ethanol and heating on hot plate

3.3.2 Preparative thin layer chromatography (PTLC)

Techniques:	One dimension
Stationary phase:	Silica gel 60 F_{254} (Merck, Germany) glass-coated plate
Layer thickness:	1 mm

Distance of mobile phase:	18 cm
Mobile phase:	Various solvent systems
Detection:	a. UV light at 254 nm b. dipping in 10% sulfuric acid in aqueous ethanol and heating on hot plate

3.3.3 Column chromatography (CC)

Stationary phase:	Silica gel 60, 70-230 mesh (Merck, Germany), Diaion HP-20, 250-280 mesh (Mistsubishi, Japan) and Sephadex LH-20, 8-11 µm (Bioscience, USA)
Mobile phase:	Various solvent systems
Packing method:	Wet packing
Detection:	Eluted fraction were monitored by TLC

3.3.4 Medium pressure liquid chromatography (MPLC)

(Isolera ISO-1SV, Sweden)

Stationary phase:	Silica gel 50 µm with a surface area of 500 m^2/g (Biotage® SNAP KP-Sil, Sweden)
Mobile phase:	Various solvent systems
Detection	UV-Visible spectrophotometer, range of wavelength was 200-800 nm

3.3.5 Hot air oven

The WiseVen hot air oven (Witeg, Germany) was used for drying plant materials at 60 °C.

3.3.6 Vacuum rotary evaporator

The rotary evaporator model EYELA rotary evaporator N-1000(EYELA, Japan) was used for evaporation solvents under vacuum.

3.3.7 Melting point apparatus

Thermo Scientific 1202D Manual melting point apparatus (Thermo Fisher Scientific, USA) was used for determination melting points.

3.3.8 UV-Visible spectrophotometry

UV spectra were recorded with a Microplate reader Multiscan GO (Thermo Fisher Scientific, USA).

3.3.9 Nuclear magnetic resonance (NMR) spectroscopy

The ^{1}H and ^{13}C NMR spectra were determined at 300 and 75.5 MHz, respectively on Bruker model Fourier Spectrometer (Bruker, USA). Tetramethylsilane (TMS) was used as an internal standard.

3.3.10 High resolution electrospray ionization mass spectroscopy

High resolution mass spectra were determined on Bruker model MICROTOF (Bruker Daltons Inc, Breman, Germany). The coupled mass spectrometer was operated in electrospray ionization (ESI) mode. Scan range were 35-3000 m/z.

3.4 Methods

3.4.1 Extraction

3.4.1.1 Preparation of crude extracts of different parts of *M. kauki*

The fresh plants of fruits (62.40 g), leaves (892.29 g), seeds (26.27 g), stem barks (103.18 g) and woods (146.79 g) of *M. kauki* were dried in hot air oven at 60 °C and then powdered. The dried powder of fruits (22.31 g), leaves (376.93 g), seeds (18.56 g), stem barks (66.65 g) and woods (49.23 g) of *M. kauki* were extracted with methanol at room temperature (30 ± 2 °C) for 72 hours and water at 60 °C for 20 minutes. This process was repeated for 3 times. After filtration, each extract was evaporated under reduced pressure to obtain methanol and aqueous crude extracts. The extraction procedure of different parts of *M. kauki* is shown in Figure 6.

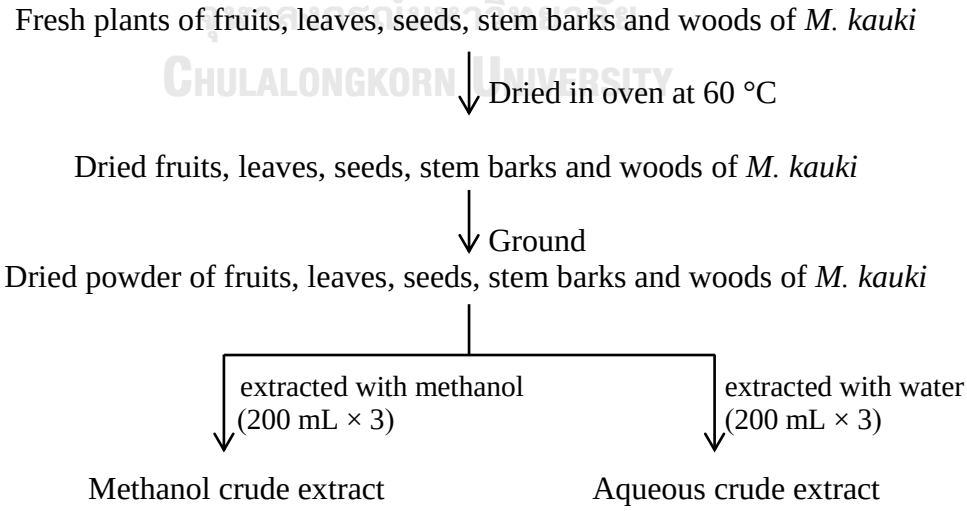

Figure 6 Extraction procedure of different parts of *M. kauki*

3.4.1.2 Preparation of crude extracts of stem barks of *M. kauki*

The fresh plants of stem barks of *M. kauki* were dried in hot air oven at 60 °C and then powdered. The dried powders of stem barks were extracted with *n*-hexane (10 L × 3), ethyl acetate (10 L × 3) and methanol (10 L × 3) at room temperature (30 ± 2 °C) for 72 hours and water (1 L × 3) at 60 °C for 20 minutes, respectively. This process was repeated for 3 times. After filtration, each extract was evaporated under reduced pressure to obtain *n*-hexane (H), ethyl acetate (E), methanol (M) and aqueous (A) crude extracts. The extraction procedure of stem barks of *M. kauki* is shown in Figure 7.

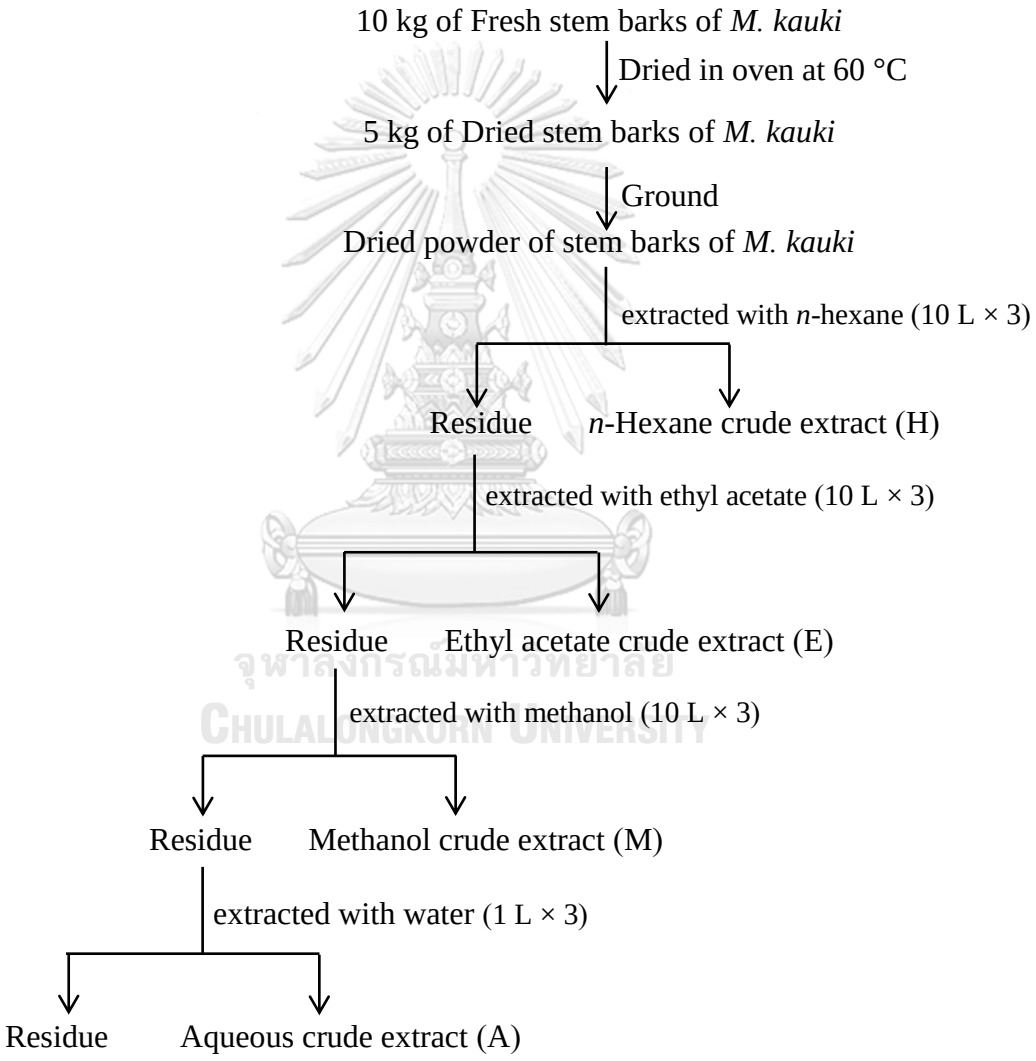

Figure 7 Extraction procedure of stem barks of *M. kauki*

3.4.2 Phytochemical analysis

3.4.2.1 Total phenolic content

Total phenolic content was determined by the Folin-Ciocalteu reagent method [61] with some modification. The 18 µL of sample or standard solution was added into 36 µL of 10% Folin-Ciocalteu reagent and followed by 146 µL of 350 mM Na_2CO_3 solution. The solution was incubated at room temperature (30 ± 2 °C) for 1 hour. The absorbance was measured at 765 nm using spectrophotometer. Gallic acid was used as a standard phenolic compound for calculation. A serial dilution of gallic acid was performed at concentration ranging of 100-1000 µM. The total phenolic content of sample was calculated and expressed as mg of gallic acid equivalent (GAE)/g of dry weight. All samples were analyzed in triplicated.

3.4.2.2 Total flavonoid content

Total flavonoid content was determined by the aluminum chloride colorimetric assay [62]. The sample was dissolved in methanol at concentration of 1.0 mg/mL. The reaction mixture of sample and standard solution contained 125 µL of sample or standard solution and 75 µL of 5% $NaNO_2$ solution. After incubation at room temperature (30 ± 2 °C) for 6 min, the solution was added by 150 µL of 10% $AlCl_3$ solution and incubated at room temperature (30 ± 2 °C) for 5 min. Then, 750 µL of 1 M NaOH and 900 µL of distilled water were added to the reaction solution. After incubation at room temperature (30 ± 2 °C) for 15 min, the absorbance was measured at 510 nm. The total flavonoid content was expressed as mg quercetin equivalent (QE)/g of dry weight. All samples were analyzed in triplicated.

3.4.3 Biological activity assays

3.4.3.1 Antioxidant activity assays

3.4.3.1.1 1,1-diphenyl-2-picrylhydrazyl (DPPH) assay

DPPH assay was determined using spectrophotometric method [63] with some modifications. The sample was dissolved in 95% methanol at concentration of 1.0 mg/mL. The stock solution of 0.6 mM DPPH was prepared by dissolution of 0.6 mM DPPH with 50 mL of methanol and stored at -20 °C until use. The DPPH working solution was mixed with 10 mL of DPPH stock solution and 45 mL of methanol:water (1:19 v/v) in the dark. The reaction mixture of sample or standard solution contained 10 µL of sample or standard and 190 µL of DPPH working solution. The reaction mixture of blank contained 10 µL of 95% methanol and 190 µL of DPPH working solution. After incubation at room temperature (30 ± 2 °C) for 30 min in the dark, the absorbance was measured at 515 nm. The results were expressed in mg of trolox equivalent (TE)/g of crude extract. Calibration curve ranges were 25-1,000 µg/mL.

All samples were analyzed in triplicated. Percentage of DPPH radical scavenging activity was analyzed according to this equation.

$$\text{DPPH radical scavenging activity } (\%) = \frac{A - B}{A} \times 100$$

By A is an absorbance of reaction mixture of blank, B is an absorbance of reaction sample or standard.

3.4.3.1.2 The ferric reducing antioxidant power (FRAP) assay

The FRAP assay was done according to previous study [64] with some modification. The sample was dissolved in 95% methanol at concentration of 1.0 mg/mL. The FRAP working solution contained 10 mL of 300 mM acetate buffer (pH 3.6), 1 mL of 20 mM $FeCl_3 \cdot 6H_2O$ and 1 mL of 10 mM 2,4,6-tripyridyltriazine (TPTZ) in 40 mM HCl and then warmed at 37 °C before using. The reaction mixture of sample and standard solution contained 10 µL of sample or standard solution and 190 µL of FRAP working solution. After incubation at room temperature (30 ± 2 °C) for 30 min in the dark, the absorbance was measured at 593 nm. The results were expressed in mg of trolox equivalent (TE)/g of crude extract. Calibration curve ranges were 25-1,000 µg/mL. All samples were analyzed in triplicated.

3.4.3.2 Tyrosinase inhibitory assay

The tyrosinase inhibitory activity was preformed according to the method of Ishiahra *et al*. with slightly modification [65]. Kojic acid and *α*-arbutin were used as positive controls at concentration of 0.1 mg/mL and 1.0 mg/mL, respectively in phosphate buffer pH 6.5. *L*-tyrosine and *L*-DOPA were used as substrates. The sample was dissolved in 20% DMSO in ethanol at concentration of 1.0 mg/mL. The reaction mixture of control without test sample (A) contained 133 µL of 0.1 M sodium phosphate buffer (pH 6.5), 47 µL of 2.5 mM substrate, 8 µL of DMSO:absolute ethanol (1:4 v/v) and 12 µL of tyrosinase solution (14.7 Units/mg, 1.2 mg/mL of 0.1 M sodium phosphate buffer, pH 6.5). The reaction mixture of blank of control (B) contained 133 µL of 0.1 M sodium phosphate buffer, 47 µL of 2.5 mM substrate and 8 µL of DMSO:absolute ethanol (1:4 v/v). The reaction mixture of sample and positive control (C) contained 133 µL of 0.1 M sodium phosphate buffer (pH 6.5), 47 µL of 2.5 mM substrate, 12 µL of tyrosinase solution and 8 µL of sample solution. The reaction mixture of blank of sample and positive control (D) contained 133 µL of 0.1 M sodium phosphate buffer (pH 6.5), 47 µL of 2.5 mM substrate and 8 µL of sample solution. After incubation at room temperature (30 ± 2 °C) for 20 min, reaction mixture was measured at 475 nm. The assay for each sample was performed in triplicate. The results were then averaged and expressed with standard deviations. Tyrosinase inhibitory activity was analyzed according to the equation below.

$$\%\text{Inhibition} = \frac{(\text{A-B})-(\text{C-D})}{(\text{A-B})} \times 100$$

By A is an absorbance without inhibitor, B is an absorbance of control without inhibitor, C is an absorbance with inhibitor and D is an absorbance of control with inhibitor.

3.4.3.3 Determination of IC_{50} for tyrosinase inhibitory activity

The half maximal inhibitory concentration (IC_{50}) is a concentration of sample reduced by half of inhibition on *in vitro* tyrosinase inhibitory activity. Samples were evaluated by dissolving in 20% DMSO in ethanol and were tested on tyrosinase inhibitory activity assay. Kojic acid and α-arbutin were used as reference compounds.

3.4.4 Separation of ethyl acetate crude extract of stem barks of *M. kauki.*

The ethyl acetate crude extract (E) (70 g) was separated by quick column chromatography with silica gel (280 g). The quick column chromatography was eluted with *n*-hexane:ethyl acetate (1:1 v/v 10 L), ethyl acetate (10 L), ethyl acetate:methanol (9:1 v/v 10 L) and ethyl acetate:methanol: (4:1 v/v 11 L), respectively. The separation was given three fractions as E1-E3. Each fraction was tested on tyrosinase inhibitory activity. The isolation procedure of ethyl acetate crude extract is shown in Figure 8.

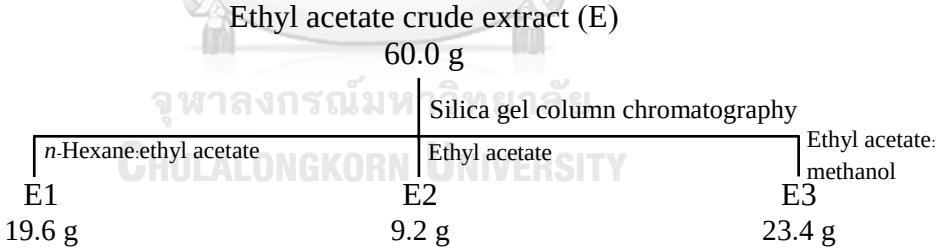

Figure 8 Isolation procedure of ethyl acetate crude extract (E)

The fraction E1 (19.6 g) was separated by silica gel column chromatography, using *n*-hexane, *n*-hexane:dichloromethane (4:1, 3:2 and 1:4 v/v; 15.0, 7.5, and 11.0 L, respectively) and ethyl acetate (4 L) as eluents to get ten fractions (E1A-E1J). Each fraction was tested on tyrosinase inhibitory activity. The isolation procedure of fraction E1 is shown in Figure 9.

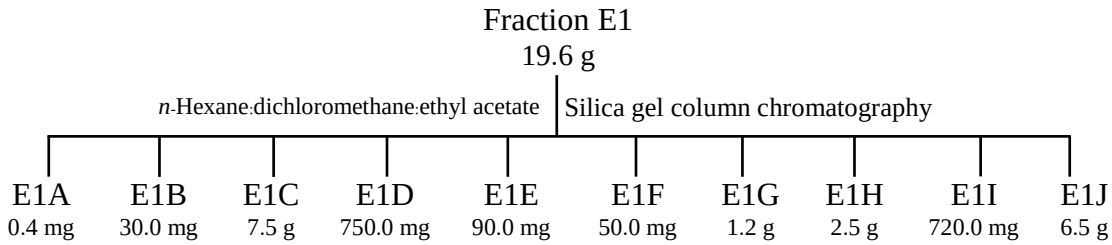

Figure 9 Isolation procedure of fraction E1

The fraction E1B (30.0 mg) was further isolated by column chromatography with *n*-hexane (0.2 L) and *n*-hexane:dichloromethane (49:1, 24.1, 19.1 and 9.1 v/v; 0.7, 1.0, 1.0 and 0.2 L, respectively) as eluents to get six fractions (E1BA-E1BF). The fraction E1BC (24.8 mg) was separated by silica gel column chromatography and eluted with *n*-hexane (0.3 L), *n*-hexane:dichloromethane (99:1, 97:3, 19:1 and 9:1 v/v; 0.3, 1.3, 0.1 and 0.2 L) and dichloromethane (0.2 L) to obtain five fractions (E1BC1-E1BC5). The fraction E1BC2 (22.5 mg) was separated by MPLC using gradient system of *n*-hexane (A) and ethyl acetate (B) as eluent with flow rate 10 mL/min (100% A at 0-11 min, 0-5% B for 12-50 min, 5% B at 51-56 min, 5%-10% B at 57-73 min and 10%-50% at 74-80 min, respectively) to afford six fractions (E1BC2A-E1BC2F). The fraction E1BC2C (19.2 mg) was separated by MPLC, using gradient system of *n*-hexane (A) and ethyl acetate (B) as eluent with flow rate 10 mL/min (100% A at 0-9 min, 0-3% at 10-23 min, 3% B at 24-32 min, 3-5% at 33-39 min and 5-40% at 40-50 min, respectively) to get three fractions (E1BC2C1-E1BC2C3). The fraction E1BC2C2 (6.8 mg) was separated by PTLC using *n*-hexane:acetone (19:1 v/v) as developing solvent to get three fractions (E1BC2C2A-E1BC2C2C). The isolation procedure of fraction E1B is shown in Figure 10.

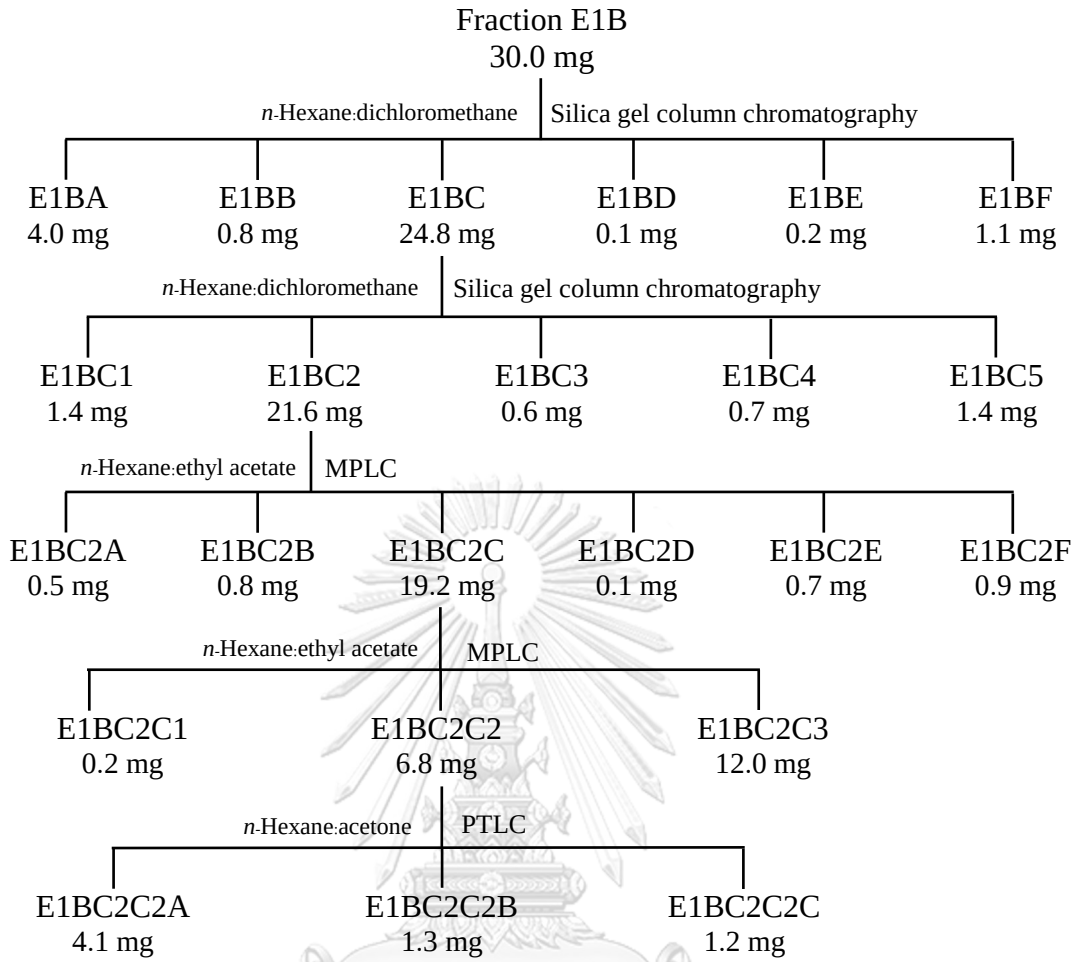

Figure 10 Isolation procedure of fraction E1B

The fraction E1C (7.0 g) showed moderate tyrosinase inhibitory activity. The fraction E1C was separated by MPLC using gradient system of *n*-hexane (A) and dichloromethane (B) with flow rate 10 mL/min (100% A at 0-40 min, 10% B at 41-70 min, 30% B at 71-109 min and 30-50% B at 110-172 min, respectively) to get ten fractions (E1CA-E1CJ). The fraction E1CG (20.0 mg) was separated by PTLC using petroleum ether:dichloromethane (4:1 v/v) as developing solvent to get three fractions (E1CG1-E1CG3). The isolation procedure of fraction E1C is shown in Figure 11.

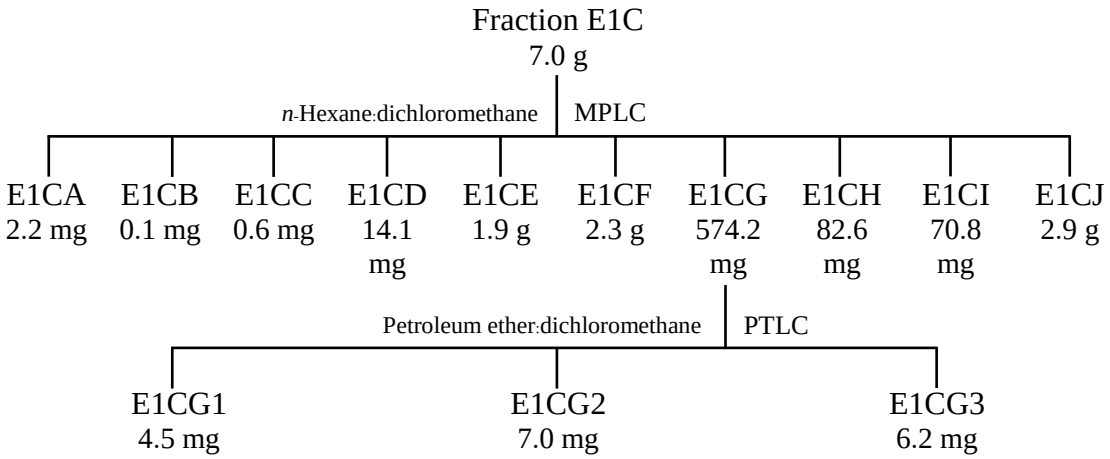

Figure 11 Isolation procedure of fraction E1C

The fraction E1D (730 mg) showed strong tyrosinase inhibitory activity. The fraction E1D was separated by silica gel column chromatography with *n*-hexane (0.7 L) and *n*-hexane:dichloromethane (9:1, 4:1 and 7:3 v/v; 1.1, 1.0 and 2.5 L, respectively) as eluents to afford ten fractions (E1DA-E1DJ). Fraction E1DI (479.8 mg) was further separated by silica gel column chromatography with *n*-hexane:dichloromethane (9:1, 17:3, 4:1 and 7:3 v/v; 0.3, 0.4, 0.3 and 1.2 L, respectively) as eluents to get six fractions (E1DIA-E1DIF). Then, Fraction E1DID (339.0 mg) was separated by silica gel column chromatography with *n*-hexane (0.2 L) and *n*-hexane:acetone (49:1 v/v; 0.9 L) as eluents to obtain four fractions (E1DID1-E1DID4). Fraction E1DID3 was obtained as white solid (319.2 mg, compound **I**). The isolation procedure of fraction E1D is shown in Figure 12.

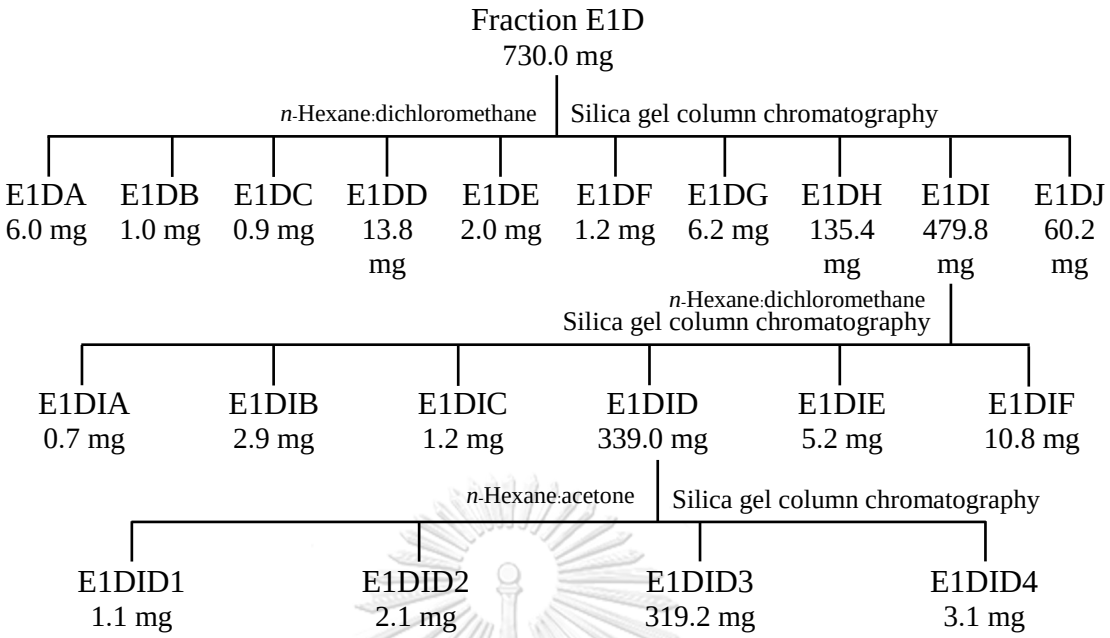

Figure 12 Isolation procedure of fraction E1D

The fraction E1E showed strong tyrosinase inhibitory activity. The fraction E1E (90.4 mg) was separated by silica gel column chromatography with *n*-hexane (0.6 L) and *n*-hexane:dichloromethane (9:1, 4:1, 7:3 and 3:2 v/v; 1.2, 1.0, 0.4 and 1.5 L, respectively) as eluents to afford eight fractions (E1EA-E1EH). The fraction E1EF (74.2 mg) was separated by silica gel column chromatography with *n*-hexane:dichloromethane (9:1, 17:3, 4:1, 7:3 and 3:2 v/v; 0.3, 0.3, 0.8, 0.3 and 0.2 L, respectively) as eluents to obtain five fractions (E1EF1-E1EF5). The fraction E1EF4 (68.5 mg) was separated by silica gel column chromatography with *n*-hexane (0.5 L) and *n*-hexane:acetone (19:1, 9:1 and 17:3 v/v; 0.6, 0.3 and 0.6 L, respectively) as eluents to get five fractions (E1EF4A-E1EF4E). Then, the fraction E1EF4B (55.5 mg) was separated by silica gel column chromatography with *n*-hexane (0.2 L) and *n*-hexane:acetone (99:1, 49:1 and 3:2 v/v; 0.2, 0.4 and 0.2 L) as eluents to get three fractions (E1EF4B1-E1EF4B3). Fraction E1EF4B2 was obtained as white solid (54.9 mg, compound **I**). The isolation procedure of fraction E1E is shown in Figure 13.

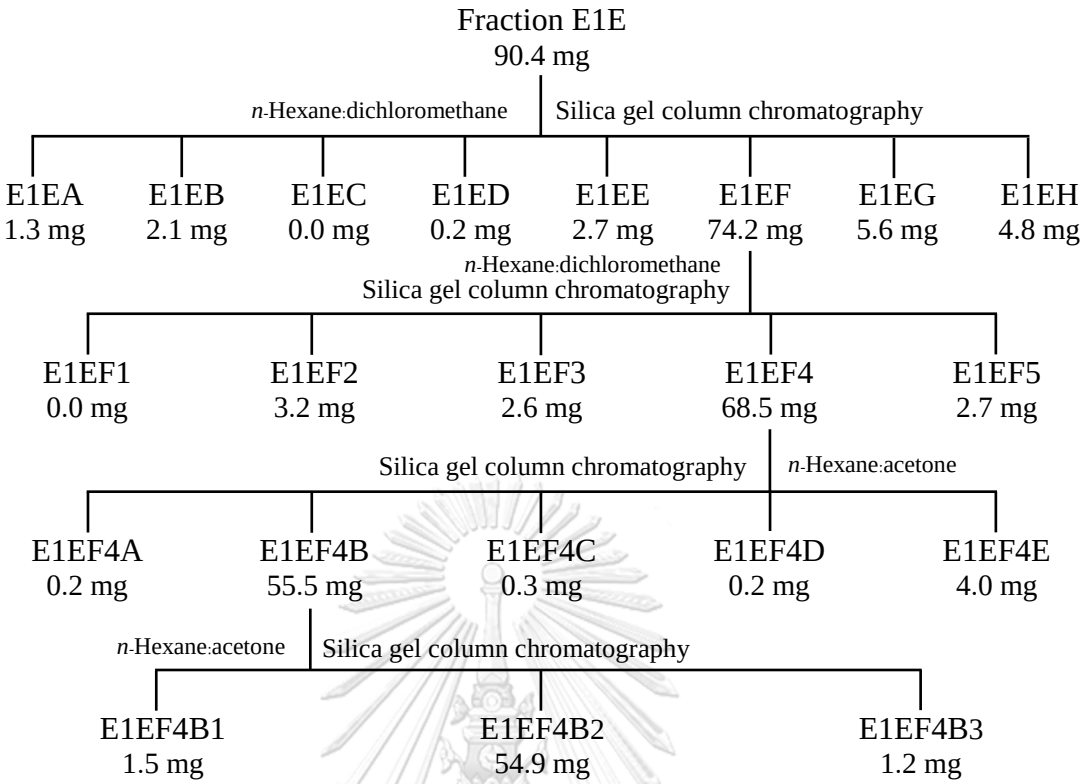

Figure 13 Isolation procedure of fraction E1E

The fraction E1F (50.0 mg) was separated by PTLC using *n*-hexane:dichloromethane (9:1 v/v) as developing solvent to afford four fractions (E1FA-E1FD). Fraction E1FB was obtained as white solid (9.2 mg, compound **I**). The isolation procedure of fraction E1F is shown in Figure 14.

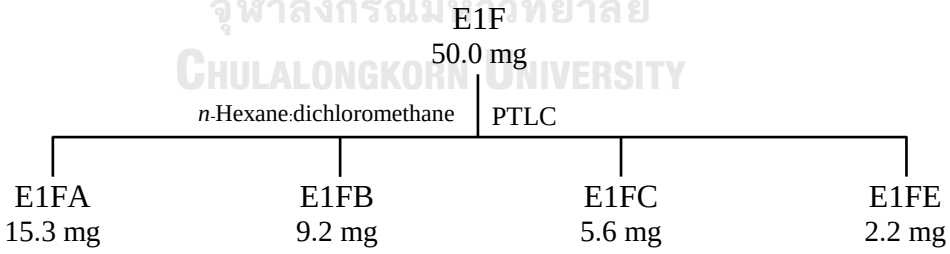

Figure 14 Isolation procedure of fraction E1F

The fraction E1H (0.6 g) was separated by column chromatography with *n*-hexane:ethyl acetate (9:1, 17:3, 4:1 and 2:3 v/v; 1.0, 0.3, 0.4 and 0.2 L , respectively) as eluents to give six fractions (E1HA-E1HF). The isolation procedure of fraction E1H is shown in Figure 15. The fraction E1HA was separated by PTLC using *n*-hexane:dichloromethane (3:2 v/v) as developing solvent to get two fractions (E1HA1-E1HA2). The fraction E1HB (37.0 mg) was separated by MPLC using gradient of *n*-hexane (A) and ethyl acetate (B) as eluent with flow rate 1 mL/min (100% A at 0-75

min, 3% B at 76-135 min, 5% B at 136-196 min, 8% B at 197-257 min and 10% B at 258-322 min, respectively) to obtain nine fractions (E1HB1-E1HB9). The extraction procedure of fraction E1HB is shown in Figure 15. The fraction E1HC (70.0 mg) was separated by silica gel column chromatography with *n*-hexane (0.2 L), *n*-hexane:ethyl acetate (19:1, 47:3 and 93:7 v/v; 0.8, 0.2 and 1.3 L, respectively) and ethyl acetate (0.2 L) to get five fractions (E1HC1-E1HC5). The fraction E1HC4 (33.6 mg) was separated by PTLC using petroleum ether:ethyl acetate (27:3 v/v) as developing solvent to afford five fractions (E1HC4A-E1HC4E). The isolation procedure of fraction E1HC is shown in Figure 16. The fraction E1HE (22.1 mg) was separated by column chromatography with dichloromethane (0.3 L), dichloromethane:acetone (99:1, 24:1 and 47:3 v/v; 0.3, 0.3 and 0.7, respectively) as eluents to obtain four fractions (E1HE1-E1HE4). The isolation procedure of fraction E1HE is shown in Figure 16.

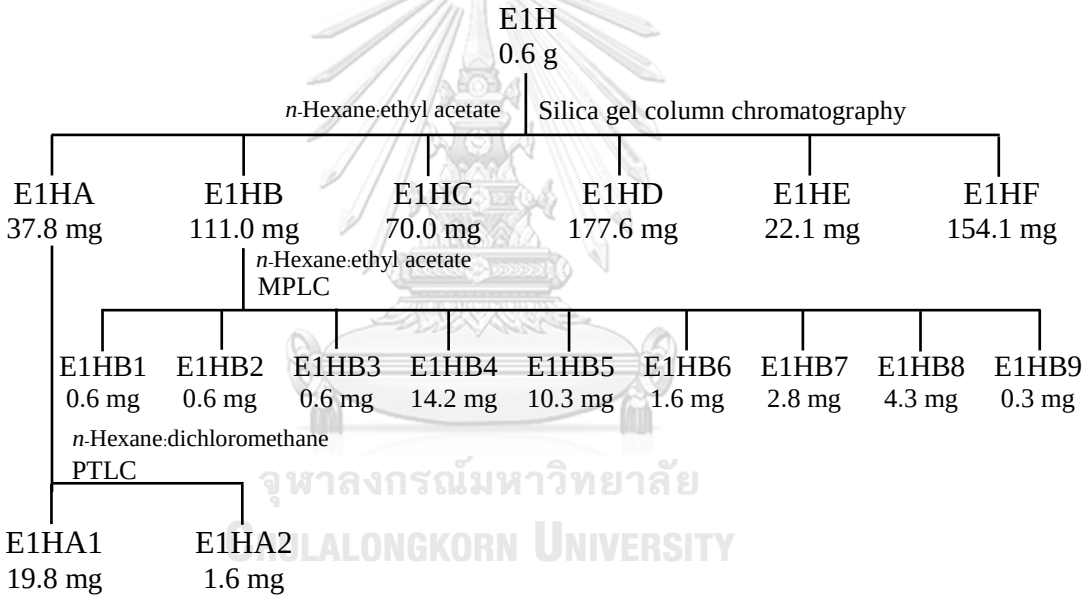

Figure 15 Isolation procedure of fractions E1H, E1HA and E1HB

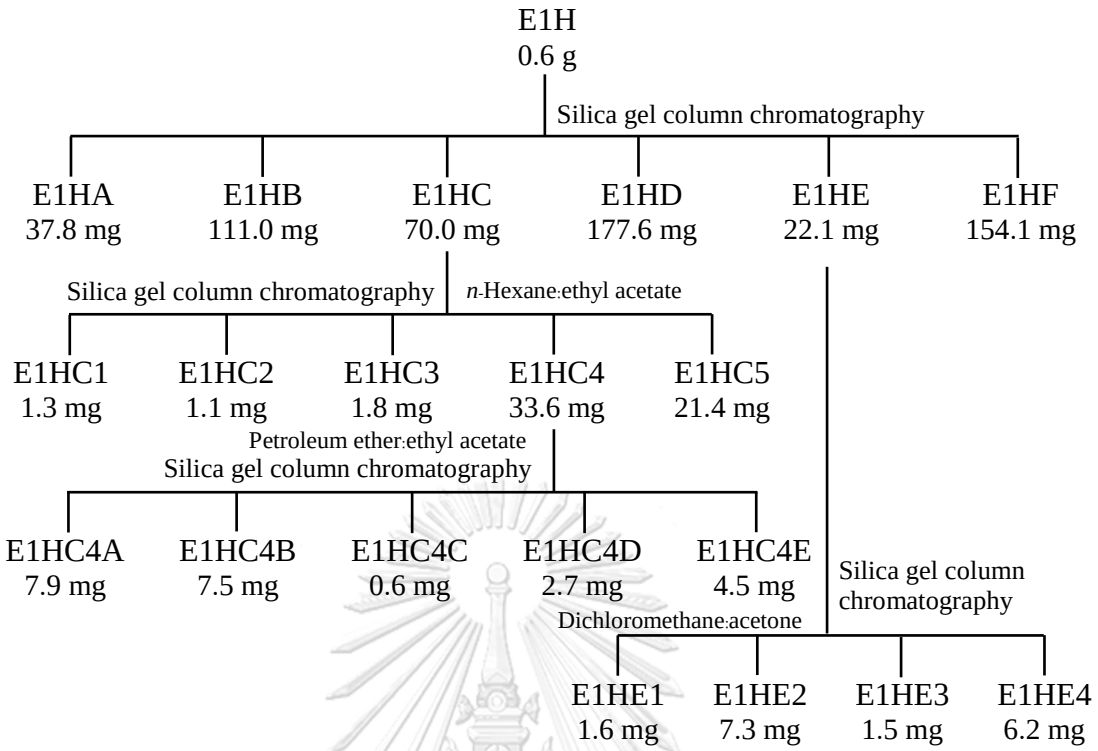

Figure 16 Isolation procedure of fractions E1HC and E1HE

The fraction E1I showed strong tyrosinase inhibitory activity. The Fraction E1I (0.6 g) was separated by silica gel column chromatography with *n*-hexane:ethyl acetate (4:1, 7:3 and 3:2 v/v; 0.2, 0.9 and 0.5 L, respectively) to get six fractions (E1IA-E1IF). Then, fraction E1IC (55.3 mg) was separated by PTLC using *n*-hexane:acetone (3:2 v/v) as developing solvent to get five fractions (E1IC1-E1IC5). Fraction E1IC5 was afforded as yellow solid (7.8 mg, compound **II)**. The isolation procedure of fraction E1I is shown in Figure 17.

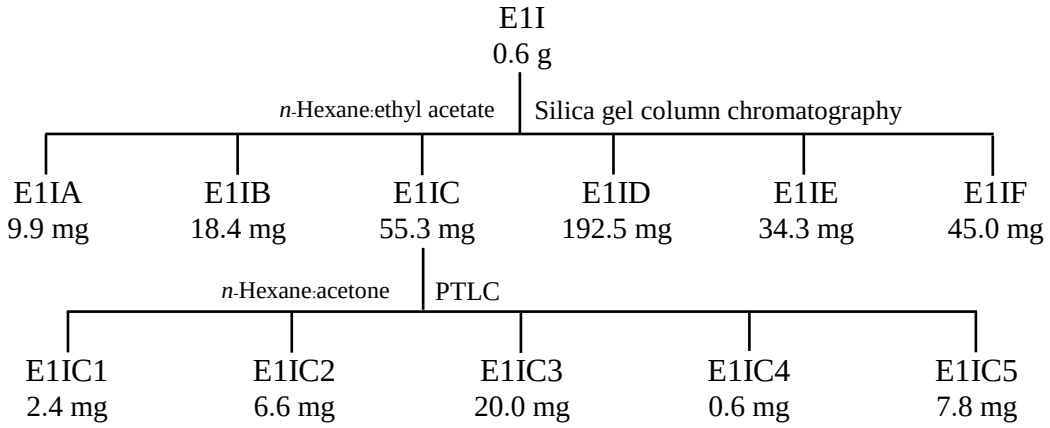

Figure 17 Isolation procedure of fraction E1I

The fraction E2 showed moderate tyrosinase inhibitory activity. The fraction E2 (7.5 g) was separated by MPLC using gradient system of *n*-hexane (A) and acetone (B) as eluent with flow rate 36 mL/min (100% A at 0-3 min, 0-50% B at 4-25 min, 50-95% B at 26-43 min and 95-100% B at 44-56 min, respectively) to obtain six fractions (E2A-E2F). The isolation procedure of fraction E2 is shown in Figure 18.

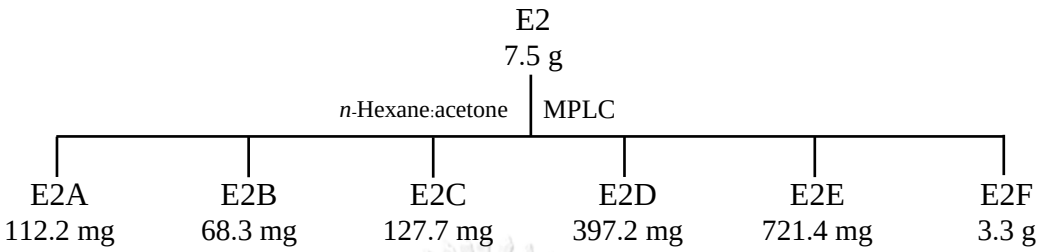

Figure 18 Isolation procedure of fraction E2

The fraction E2A (112.2 mg) was separated by MPLC using gradient system of *n*-hexane (A) and dichloromethane (B) as eluent with flow rate 10 mL/min (100% A at 0-15 min, 0-100% B at 16-89 min and 100% B 90-96 min, respectively) to obtain seven fractions (E2AA-E2AG). The fraction E2AD (13.5 mg) was separated by PTLC using *n*-hexane:dichloromethane (1:1 v/v) as developing solvent to get three fractions (E2AD1-E2AD3). The fraction E2AE (6.9 mg) was separated by PTLC using *n*-hexane:dichloromethane (1:1 v/v) as developing solvent to obtain three fractions (E2AE1-E2AE3). The isolation procedure of fraction E2A is shown in Figure 19.

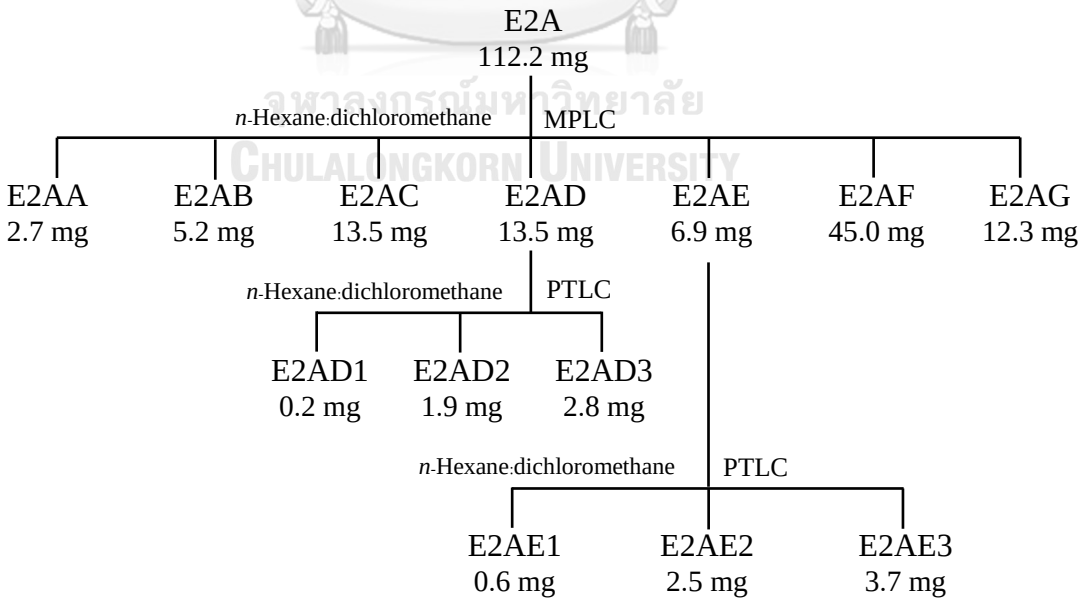

Figure 19 Isolation procedure of fraction E2A

The fraction E2B (60.0 mg) showed strong tyrosinase inhibitory activity. The fraction E2B was separated by MPLC using gradient system of *n*-hexane (A) and acetone (B) as eluent with flow rate 10 mL/min (100% A at 0-6 min, 0-5% B at 6-7 min, 5% B at 8-13 min, 5-10% B at 14-15 min, 10% B at 16-21 min, 10-15% B at 22-23 min, 15% B at 24-29 min, 15-20% B at 30-31 min, 20% B at 32-37 min, 20-30% B at 38-40 min, 30% B at 41-49 min and 30-65% B at 50-60 min, respectively) to get seven fractions (E2BA-E2BG). The fraction E2BD (9.9 mg) was separated by PTLC using *n*-hexane:acetone (4:1 v/v) as developing solvent to obtain two fractions (E2BD1-E2BD2). The fraction E2BE (18.9 mg) was separated by MPLC using gradient system of dichloromethane (A) and ethyl acetate (B) as eluent with flow rate 10 mL/min (100% A at 0-5 min, 0-2% B at 6-10 min, 2% B at 11-14 min, 2-5% B at 15-20 min and 5-10% B at 21-30 min, respectively) to afford three fractions (E2BE1-E2BE3). The fraction E2BE1 (9.6 mg) was further separated by PTLC using dichloromethane:ethyl acetate (49:1 v/v) as developing solvent to afford three fractions (E2BE1A-E2BE1C). The isolation procedure of fraction E2B is shown in Figure 20.

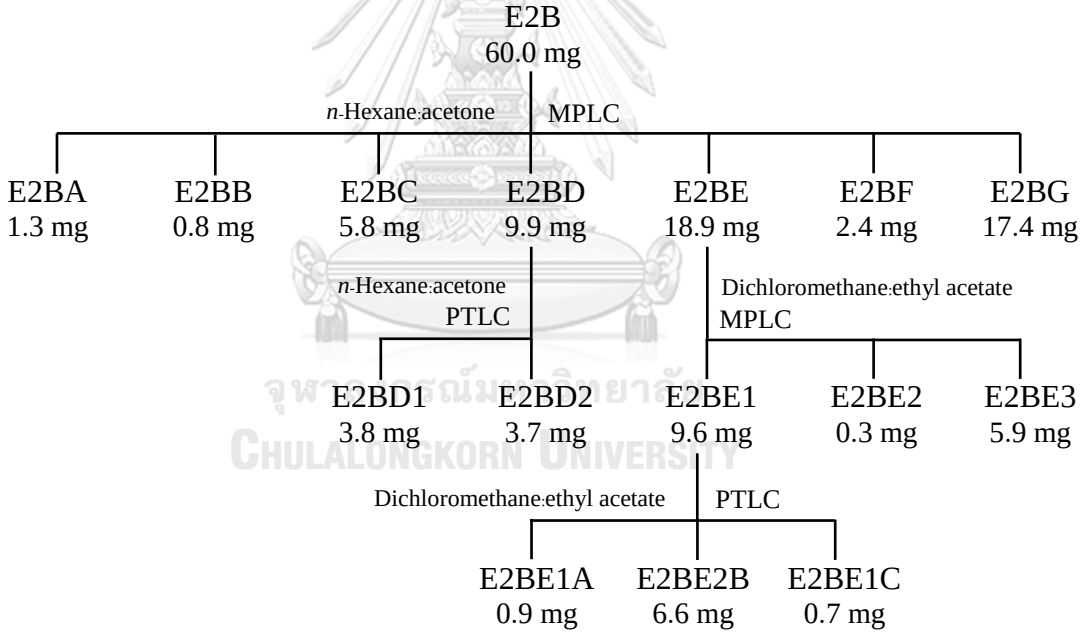

Figure 20 Isolation procedure of fraction E2B

The fraction E2C (127.7 mg) was separated by MPLC using gradient system of *n*-hexane (A) and acetone (B) as eluent with flow rate 10 mL/min (5% B at 0-12 min, 5-10% B at 13-15 min, 10% B at 16-21 min, 10-15% B at 22-23 min, 15% B at 24-29 min, 15-20% B at 30-31 min, 20% B 32-37 min, 20-30% B at 38-39 min, 30% B at 40-45 min, 30-40% B at 46-47 min, 40% B at 48-54 min and 75% B at 55-78 min, respectively) to get eight fractions (E2CA-E2CH). The extraction procedure of fraction E2C is shown in Figure 21. The fraction E2CC (8.9 mg) was separated by

MPLC using gradient system of *n*-hexane (A) and acetone (B) as eluent with flow rate 5 mL/min (100% A at 0-15 min and 0-20% B at 16-81 min, respectively) to obtain four fractions (E2CC1-E2CC4). The fraction E2CC4 (7.0 mg) was separated by PTLC using *n*-hexane:acetone (1:9 v/v) as developing solvent to give four fractions (E2CC4A-E2CC4D). The isolation procedure of fraction E2CC4 is shown in Figure 21. The fraction E2CE (15.0 mg) was separated by PTLC using *n*-hexane:acetone (4:1 v/v) as developing solvent to obtain three fractions (E2CE1-E2CE3). The extraction procedure of fraction E2CE is shown in Figure 21. The fraction E2CF (62.0 mg) was separated by MPLC using gradient system of dichloromethane (A) and ethyl acetate (B) as eluent with flow rate 5 mL/min (100% A at 0-15 min, 0-20% B at 16-86 min ant 20% B at 87-93 min, respectively) to get three fractions (E2CF1-E2CF3). The isolation procedure of fraction E2CF is shown in Figure 22.

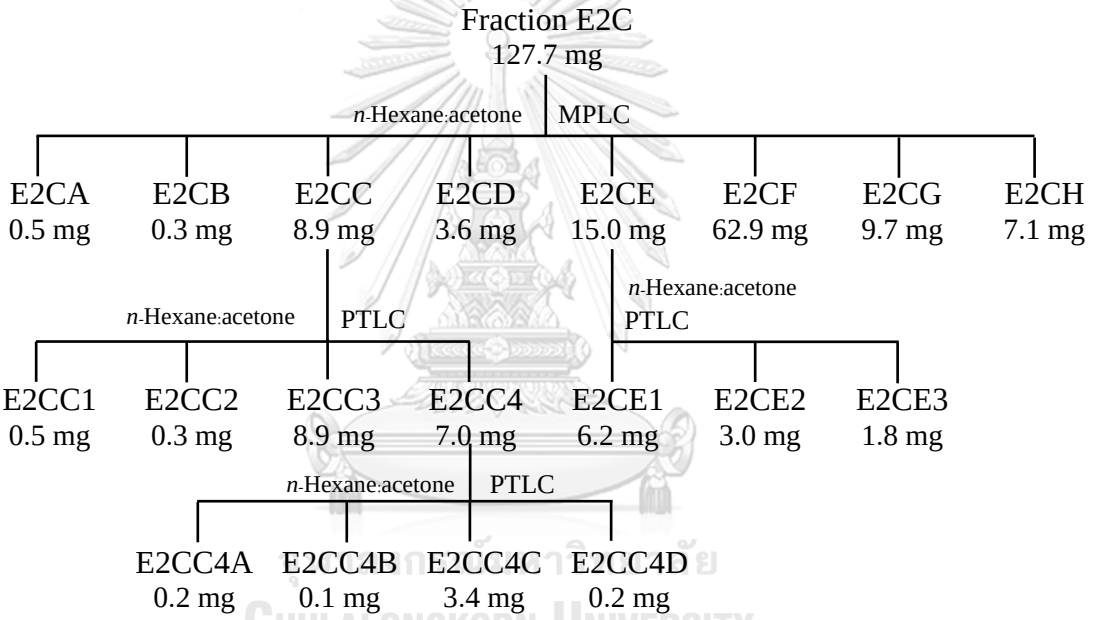

Figure 21 Isolation procedure of fractions E2C, E2CC and E2CE

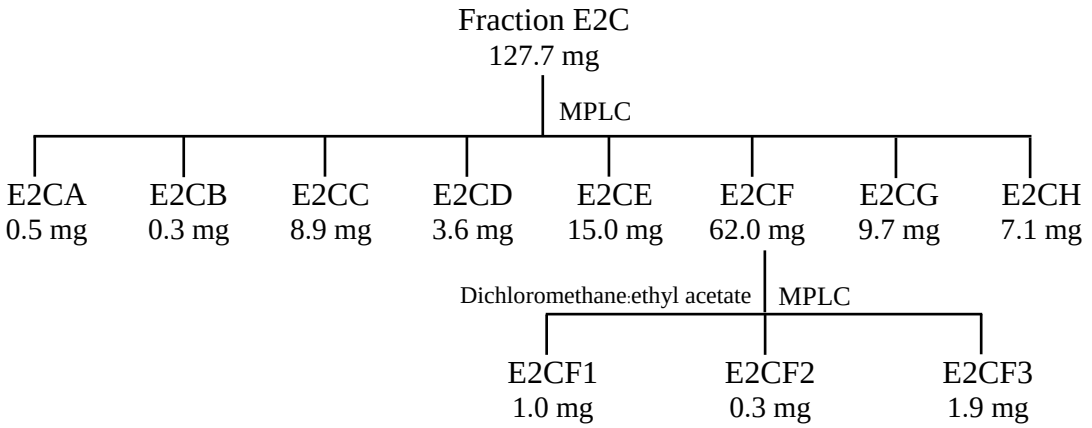

Figure 22 Isolation procedure of fraction E2CF

The fraction E2D (255.0 mg) was separated by MPLC using gradient system of *n*-hexane (A) and ethyl acetate (B) with flow rate 10 mL/min (0-99% B at 0-72 min) to obtain three fractions (E2DA-E2DC). The fraction E2DC (206.9 mg) was separated by MPLC using gradient system of dichloromethane (A) and ethyl acetate (B) as eluent with flow rate 10 mL/min (5% B at 0-10 min, 10% B at 11-16 min, 20% B at 17-22 min, 30% B at 23-28 min, 50% B at 29-35 min and 80% B at 36-46 min, respectively) to get six fractions (E2DC1-E2DC6). The fraction E2DC4 (39.6 mg) was separated by MPLC using gradient system of *n*-hexane (A) and acetone (B) as eluent with flow rate 2 mL/min (10% B at 0-38 min, 10-40% at 39-141 min, 40-42% B at 142-147 min, 42-45% B at 148-158 min and 45% B at 159-165 min, respectively) to afford five fractions (E2DC4A-E2DC4E). The fraction E2DC5 (65.6 mg) was separated by MPLC using gradient system of *n*-hexane (A) and ethyl acetate (B) as eluent with flow rate 2 mL/min (10-30% B at 0-37 min, 30% at 38-63 min, 40% B at 64-89 min, 50% B at 90-114 min, 60% B at 115-135 min and 70% B at 136-161 min, respectively) to obtain three fractions (E2DC5A-E2DC5C). The fraction E2DC5C (45.2 mg) was separated by PTLC using petroleum ether:ethyl acetate (1:9 v/v) as developing solvent to afford two fractions (E2DC5CA-E2DC5CB). The isolation procedure of fraction E2D is shown in Figure 23.

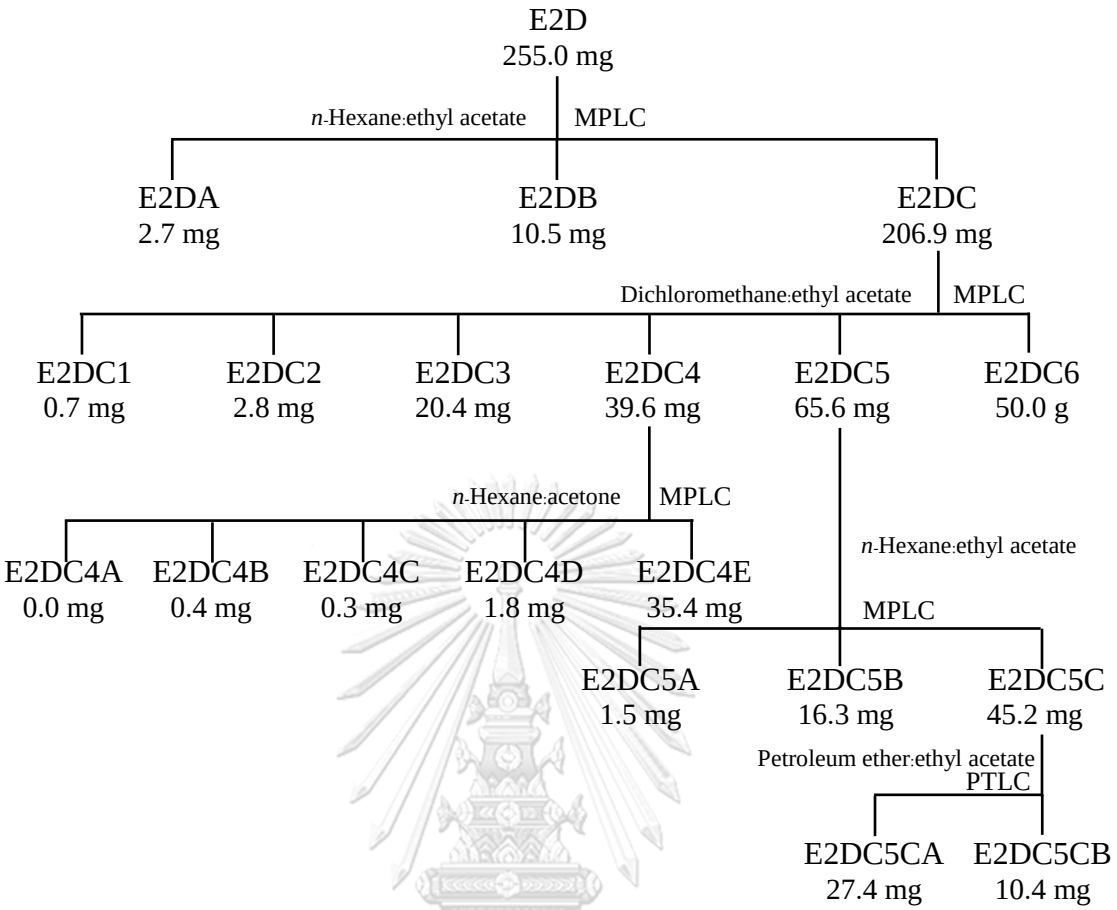

Figure 23 Isolation procedure of fraction E2D

The fraction E2E (100.0 mg) was separated by MPLC using gradient system of *n*-hexane (A) and ethyl acetate (B) as eluent with flow rate 10 mL/min (100% A at 0-10 min, 0-10% B at 11-14 min, 10% B at 15-20 min, 10-20% B at 21-26 min, 20% B at 21-31 min, 30-50% B at 32-37 min, 50% B at 38-52 min and 50-100% B at 53-76 min, respectively) to get seven fractions (E2EA-E2EG). The fraction E2ED (12.7 mg) was separated by PTLC using *n*-hexane:acetone (3:2 v/v) as developing solvent to afford four fractions (E2ED1-E2ED4). The fraction E2EE (25.8 mg) was separated by MPLC using gradient system of dichloromethane (A) and acetone (B) as eluent with flow rate 10 mL/min (100% A at 0-8 min, 0-8% B at 9-39 min, 8-10% B at 40-45 min, 10-15% B at 46-62 min and 15% B at 63-76 min, respectively) to get three fractions (E2EE1-E2EE3). The fraction E2EF (28.6 mg) was separated by MPLC using gradient system of *n*-hexane (A) and acetone (B) as eluent with flow rate 2mL/min (10-50% B at 0-40 min and 50-90% B at 41-121 min, respectively) to obtain six fractions (E2EFA-E2EFF). The isolation procedure of fraction E2E is shown in Figure 24.

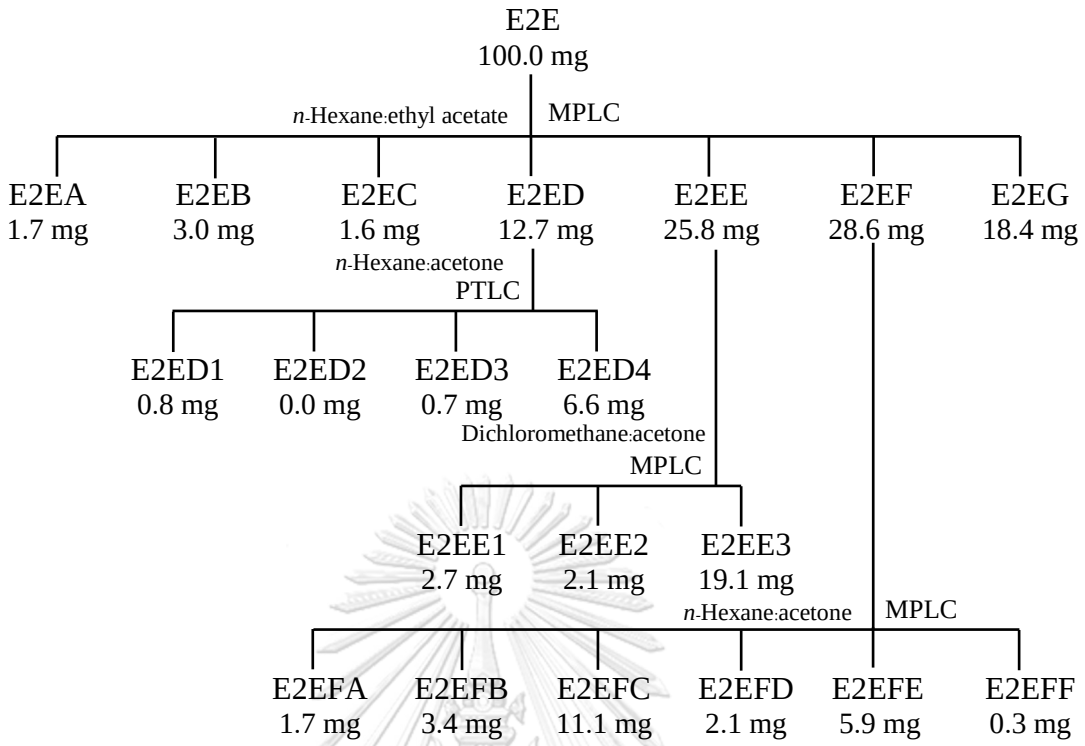

Figure 24 Isolation procedure of fraction E2E crude extract

The fraction E2F (150 mg) was separated by MPLC using gradient system of *n*-hexane (A) and ethyl acetate (B) as eluent with flow rate 5 mL/min (10% B at 0-54 min, 20% B at 55-95 min, 30% B at 96-136 min, 50% B at 137-177 min, 70% B at 178-242 min, respectively) to get eleven fractions (E2FA-E2FJ). The isolation procedure of fraction E2F is shown in Figure 25.

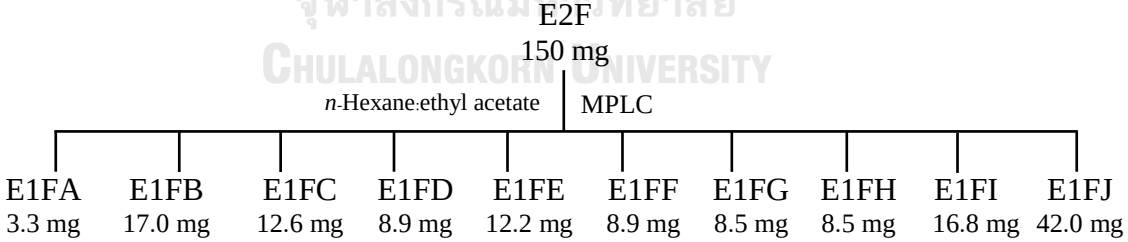

Figure 25 Isolation procedure of fraction E2F

The fraction E3 (2.3 g) was separated by MPLC using isocratic of methanol (A) with flow rate 10 mL/min (100% A at 0-141 min) to get three fractions (E3A-E3C). The fraction E3B (140.0 mg) was separated diaion column chromatography with ethyl acetate and ethyl acetate:methanol (19:1 v/v) to obtain three fractions (E3BA-E3BC). The fraction E3BB (140.0 mg) was separated by diaion column chromatography with water, methanol:water (1:9, 1:4, 3:7, 2:3 and 1:1 v/v; 0.2, 0.2, 0.3, 0.2 and 0.3 L, respectively) and methanol (0.5 L), respectively as eluents to

afford six fractions (E3BB1-E3BB6). The isolation procedure of fraction E3 is shown in Figure 26.

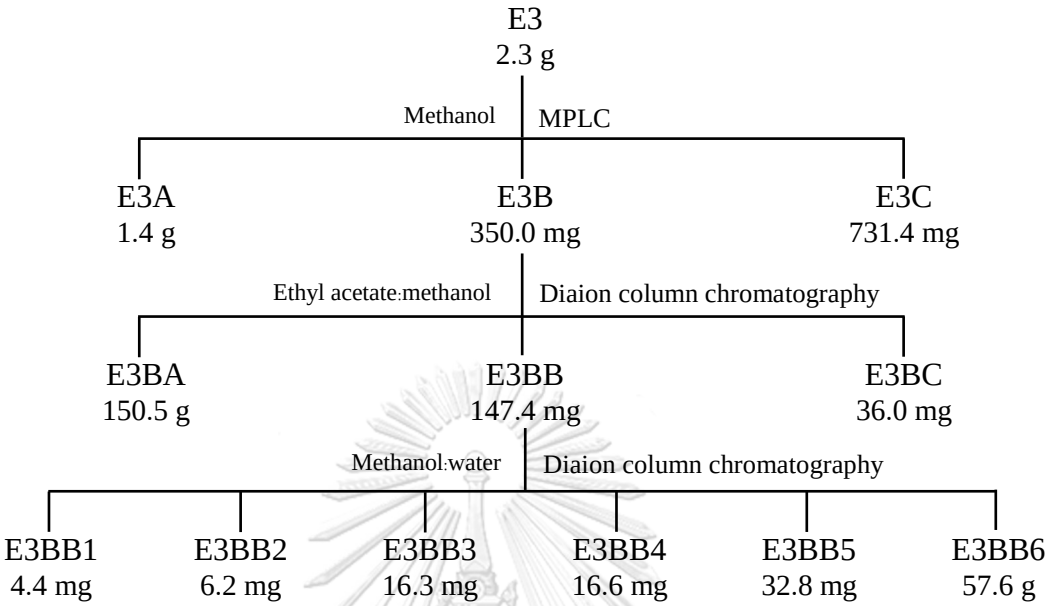

Figure 26 Isolation procedure of fraction E3

CHAPTER IV
RESULTS AND DISCUSSION

4.1 Extraction of different parts of *M. kauki*

The dried powder of fruits, leaves, seeds, stem barks and woods of *M. kauki* were extracted with methanol and water. Methanol and aqueous crude extracts of five different parts of *M. kauki* were afforded percentage yield of crude extracts in the range of 3.39-19.08% w/w of dry plant. Aqueous crude extract of fruits of *M. kauki* got the highest percent yield with 19.08% w/w of dry weight. While, methanol crude extract of woods of *M. kuaki* got the lowest percent yield with 3.39% w/w of dry weight. The characteristic and percent yield of methanol and aqueous crude extracts of different parts of *M. kauki* are shown in Tables 4.1 and 4.2, respectively.

Table 4.1 Characteristic and percentage yield of methanol crude extract of different parts of *M. kauki*

Part of plant	Dry weight (g)	Methanol crude extract	
		Characteristic	Yield (g) (% w/w of dry weight)
Fruits	10.62	Light brown gum	1.17 (11.02)
Leaves	29.77	Green solid	3.45 (11.59)
Seeds	7.86	Brown solid	0.42 (5.34)
Stem barks	34.13	Brown solid	2.02 (5.92)
Woods	24.43	Yellow gum	0.83 (3.39)

Table 4.2 Characteristic and percentage yield of aqueous crude extract of different parts of *M. kauki*

Part of plant	Dry weight (g)	Aqueous crude extract	
		Characteristic	Yield (g) (% w/w of dry weight)
Fruits	11.69	Brown gum	2.23 (19.08)
Leaves	19.39	Dark green solid	1.74 (8.97)
Seeds	10.70	Brown solid	0.93 (8.69)
Stem barks	32.52	Brown solid	1.92 (5.92)
Woods	24.70	Yellow gum	1.12 (4.53)

4.2 Phytochemical compositions of different parts of *M. kauki*

4.2.1 Total phenolic content

The results of total phenolic content of methanol and aqueous crude extracts of different parts of *M. kauki* are presented in Table 4.3. Methanol crude extract of

leaves of *M. kauki* exhibited the highest amount of total phenolic content (11.79 ± 0.04 mg GAE/g of dry weight) and followed by methanol crude extract of stem barks, aqueous crude extract of leaves, aqueous crude extract of stem barks, methanol crude extract of woods, aqueous and methanol crude extracts of fruits, aqueous crude extract of woods, aqueous and methanol crude extracts of seeds with values of 10.45 ± 0.03, 9.50 ± 0.08, 4.00 ± 0.02, 2.83 ± 0.05, 2.83 ± 0.01, 1.92 ± 0.02, 1.91 ± 0.03, 0.95 ± 0.02 and 0.79 ± 0.01 mg GAE/g of dry weight, respectively.

The previous researches showed that methanol and aqueous crude extracts of barks of *M. elengi* exhibited total phenolic content with values of 154.36 ± 0.51 and 72.60 ± 1.10 mg GAE/g of dry weight [66]. Methanol:water (70:30 v/v) crude extract of leaves of *A. spinosa* exhibited total phenolic content with value of 2.88 mg GAE/g of dry weight [67]. Aqueous and ethanol crude extracts of seeds of *M. zapota* showed total phenolic content with values of 115.89 ± 4.52 and 1.00 ± 0.01 g GAE/g of dry weight [68]. These plants are trees in Sapotaceae family. Consequently, crude extracts of barks of *M. elengi* and seeds of *M. zapota* exhibited higher total phenolic content values than crude extracts of stem barks of *M. kauki* but methanol and aqueous crude extracts of leaves and stem barks of *M. kauki* exhibited higher total phenolic content than leaves of *A. spinosa*.

Table 4.3 Total phenolic content of methanol and aqueous crude extracts of different parts of *M. kauki*

Part of plant	Total phenolic content			
	Methanol crude extract		Aqueous crude extract	
	(mg GAE/g of crude extract)	(mg GAE/g of dry weight)	(mg GAE/g of crude extract)	(mg GAE/g of dry weight)
Fruits	17.52 ± 0.19	1.92 ± 0.02	14.83 ± 0.07	2.83 ± 0.01
Leaves	101.75 ±1.15	11.79 ± 0.04	105.98 ± 0.38	9.50 ± 0.08
Seeds	14.83 ± 0.11	0.79 ± 0.01	10.88 ± 0.14	0.95 ± 0.02
Stem barks	176.56 ± 0.70	10.45 ± 0.03	99.73 ± 0.51	4.00 ± 0.02
Woods	101.75 ± 0.61	2.83 ± 0.05	47.71 ± 0.42	1.91 ± 0.03

4.2.2 Total flavonoid content

The results of total flavonoid content of methanol and aqueous crude extracts of different parts of *M. kauki* are presented in Table 4.4. The highest total flavonoid content was obtained in methanol crude extract of leaves of with value of 89.84 ± 0.19 mg QE/g of dry weight and followed by aqueous crude extract of leaves, aqueous and methanol crude extracts of stem barks, aqueous and methanol crude extracts of fruits, aqueous crude extract of woods, aqueous and methanol crude extracts of seeds and methanol crude extract of woods which showed total flavonoid content values of 66.60 ± 0.22, 58.07 ± 0.32, 48.62 ± 0.21, 20.17 ± 0.16, 10.72 ± 0.08, 4.54 ± 0.21, 3.66 ± 0.14, 2.04 ± 0.07 and 0.46 ± 0.07 mg QE/g of dry weight, respectively.

The previous reports showed that total methanol and aqueous crude extracts of barks of *M. elengi* exhibited high total flavonoid content with values of 54.7 ± 0.22 and 23.5 ± 0.80 mg QE/g of dry weight, respectively [66]. Methanol:water (70:30 v/v) crude extract of leaves of *A. spinosa* exhibited total flavonoid content with value of 0.869 mg QE/g of dry weight [67]. Aqueous and ethanol crude extracts of *M. zapota* showed total flavonoid content with values of 7.26 ± 1.86 and 7.2 ± 1.40 mg QE/ g dry weight, respectively [68]. These plants are trees in Sapotaceae family. Consequently, the crude extract of *M. elengi* exhibited higher total flavonoid content value than *M. kauki* crude extract but crude extracts of *M. kauki* exhibited higher total flavonoid content than *A. spinosa* and methanol and aqueous crude extracts of leaves and stem barks of *M. kauki* showed higher total flavonoid content than crude extract of seeds of *M. zapota.*

Table 4.4 Total flavonoid content of methanol and aqueous crude extracts of *M. kauki*

Part of plant	Total flavonoid content			
	Methanol crude extract		Aqueous crude extract	
	(mg QE/g of crude extract)	(mg QE/g of dry weight)	(mg QE/g of crude extract)	(mg QE/g of dry weight)
Fruits	98.00 ± 0.72	10.72 ± 0.08	105.67 ± 0.82	20.17 ± 0.16
Leaves	775.33 ± 1.81	89.84 ± 0.19	743.33 ± 2.14	66.60 ± 0.22
Seeds	38.33 ± 1.41	2.04 ± 0.07	42.00 ± 1.15	3.66 ± 0.14
Stem barks	820.67 ± 1.98	48.62 ± 0.21	799.67 ± 2.96	58.07 ± 0.32
Woods	13.67 ± 0.72	0.46 ± 0.07	113.33 ± 1.27	4.54 ± 0.21

4.3 Biological activities of different parts of *M. kauki*

4.3.1 Antioxidant activities

4.3.1.1 DPPH radical scavenging activity

The DPPH free radical scavenging activity of different parts of *M. kauki* was investigated by spectrophotometric method. The results of DPPH free radical scavenging activity are presented in Table 4.5. The highest DPPH radical scavenging activity was found in methanol crude extract of stem barks with value of 257.02 ± 0.26 mg TE/g of crude extract. Secondly, aqueous crude extract of leaves showed DPPH radical scavenging activity with value of 243.19 ± 1.24 mg TE/g of crude extract and followed by aqueous crude extract of stem barks, methanol crude extract of leaves, methanol and aqueous crude extracts of woods, methanol crude extracts of fruits and seeds, aqueous crude extracts of fruits and seeds which exhibited DPPH radical scavenging activity with values of 219.19 ± 0.13, 208.60 ± 0.98, 194.38 ± 0.70, 66.04 ± 0.57, 45.28 ± 0.51, 16.08 ± 0.31, 13.01 ± 0.51 and 10.32 ± 0.38 mg TE/g of crude extract, respectively. These results indicated that both methanol and aqueous crude extracts of stem barks and leaves of *M. kauki* exhibited strong DPPH

radical scavenging activity. Whereas, fruits and seeds of *M. kauki* showed low activity of DPPH radical scavenging.

Methanol and aqueous crude extracts of *Bidens tripartita* exhibited DPPH radical scavenging activity with values of 504.87 ± 4.58 and 260.69 ± 6.36 mg TE/g of crude extract, respectively [69]. It showed higher DPPH radical scavenging activity than crude extracts of *M. kauki*. Butanol crude extract of aerial parts of *Bidens humilis* showed DPPH radical scavenging activity with value of 173.8 ± 6.2 mg TE/g of crude extract. (2S)-Isookanin 7-*O*-*α*-*L*-arabinopyranoside, (2S)-isookanin 7-*O*-(2″-acetyl)-*α*-Larabinopyranoside and luteolin 7-*O*-*β*-*D*-glucopyranosyl-(1→6)-*β*-*D*-galactopyranoside were isolated from butanol crude extract of *B. humiliis* and showed DPPH radical scavenging with values of 513.7 ± 28.7, 484.7 ± 21.3 and 357.8 ± 17.5 mg TE/g of crude extract, respectively [70]. Methanol and aqueous crude extracts of leaves and stem barks of *M. kauki* showed higher DPPH radical scavenging activity than butanol crude extract of aerial parts of *B. humilis*. Thus, methanol and aqueous crude extracts of leaves and stem barks of *M. kauki* might be contained excellent active compounds.

Table 4.5 DPPH radical scavenging activity of methanol and aqueous crude extracts of different parts of *M. kauki*

Part of plant	DPPH			
	Methanol crude extract		Aqueous crude extract	
	(mg TE/g of crude extract)	Percentage of inhibition (%)	(mg TE/g of crude extract)	Percentage of inhibition (%)
Fruits	45.28 ± 0.51	8.53 ± 0.09	13.01 ± 0.51	0.99 ± 0.08
Leaves	208.60 ± 0.98	46.68 ± 0.21	243.19 ± 1.24	54.76 ± 0.32
Seeds	16.08 ± 0.31	1.71 ± 0.02	10.32 ± 0.38	0.36 ± 0.04
Stem barks	257.02 ± 0.26	57.99 ± 0.05	219.19 ± 0.13	49.19 ± 0.03
Woods	194.38 ± 0.70	43.36 ± 0.23	66.04 ± 0.57	13.38 ± 0.19

4.3.1.2 FRAP activity

The results of FRAP activity of different parts of *M. kauki* are presented in Table 4.6. Aqueous crude extract of leaves showed the highest FRAP activity with value of 219.56 ± 0.89 mg TE/g of crude extract and followed by methanol crude extract of leaves, methanol and aqueous crude extracts of stem barks, methanol and aqueous crude extracts of woods, methanol crude extract of seeds and fruits and aqueous crude extracts fruits and seeds which exhibited FRAP activity with values of 210.94 ± 1.37, 210.94 ± 0.89, 107.89 ± 0.79, 72.61 ± 0.98, 42.06 ± 0.98, 15.93 ± 0.98, 11.78 ± 0.96, 5.11 ± 0.79 and 4.56 ± 0.81 mg TE/g of crude extract, respectively.

The previous researches, methanol and aqueous crude extracts of *B. tripartita* exhibited FRAP activity with values of 299.21 ± 3.87 and 193.44 ± 6.22 mg TE/g of

crude extract, respectively [69]. Chlorogenic acid, *epi*-catechin and luteolin-7-glucoside were main phenolic components of *B. tripartita* extracts. Correlation between total phenolic content with DPPH radical scavenging and FRAP activities were reported in previous study. Phenolic compounds were investigated to be the most important antioxidants of plant materials [71]. Methanol and aqueous crude extracts of leaves and stem barks of *M. kauki* exhibited DPPH radical scavenging and FRAP activities values nearly *B. tripartita* crude extracts. Thus, methanol and aqueous crude extracts of leaves and stem barks of *M. kauki* might be contained high amount of phenolic compounds and antioxidant inhibitors.

Table 4.6 FRAP activity of methanol and aqueous crude extracts of different parts of *M. kauki*

Part of plant	FRAP (mg TE/g of crude extract)	
	Methanol crude extract	Aqueous crude extract
Fruits	11.78 ± 0.96	5.11 ± 0.79
Leaves	210.94 ± 1.37	219.56 ± 0.69
Seeds	15.93 ± 0.98	4.56 ± 0.81
Stem barks	210.94 ± 0.89	107.89 ± 0.79
Woods	72.61 ± 0.98	42.06 ± 0.98

4.3.2 Tyrosinase inhibitory activity

Methanol and aqueous crude extracts of fruits, leaves, seeds, stem barks and woods of *M. kauki* were evaluated for their tyrosinase inhibitory activity using *L*-tyrosine as the a substrate (Table 4.7). Kojic acid and *α*-arbutin were used as positive controls. The methanol crude extract of stem exhibited the strongest tyrosinase inhibitory activity with IC_{50} value of 0.26 ± 0.05 mg/mL and followed by methanol crude extract of leaves and aqueous crude extracts of stem barks, leaves and fruits, methanol crude extract of fruits, methanol and aqueous crude extracts of seeds exhibited tyrosinase inhibitory activity with IC_{50} values of 0.32 ± 0.08, 0.41 ± 0.11, 0.49 ± 0.12, 0.49 ± 0.11, 0.75 ± 0.14, 3.86 ± 0.12 and 3.88 ± 0.17 mg/mL, respectively. Whereas, methanol and aqueous crude extracts of woods of *M. kauki* showed no tyrosinase inhibitory activity. Methanol and aqueous crude extract of fruits, leaves and stem barks of *M. kauki* exhibited stronger tyrosinase inhibitory activity than *α*-arbutin which was used as a positive control.

Tyrosinase inhibitors from natural sources have been reported and their mechanisms of inhibition have been investigated. Acetone extract of *Koelreuteria henryi, Camellia sinensis* and *Rhodiola rosea* demonstrated tyrosinase inhibitory activity with IC_{50} values of 289.00 ± 0.50, 232.50 ± 3.30 and 181.80 ± 11.00 μg/mL, respectively. In comparison, kojic acid was used as a positive control (IC_{50} value of 6.20 ± 0.40 μg/mL) [72]. Acetone extract of seeds of *Alpinia zerumbet* exhibited tyrosinase inhibitory activity with IC_{50} value of 2.30 ± 0.02 μg/mL and found that

cholest-4-ene-3,6-dione was isolated from this extract as a potent steroid for this activity [73]. Methanol and ethyl acetate extracts of woods of *M. alba* exhibited potent tyrosinase inhibitory activity with IC_{50} values of 0.40 ± 0.02 and 1.30 ± 0.10 µg/mL, respectively [74]. Likewise, the twigs of *M. alba* showed strong tyrosinase inhibitory activity [75]. Methanol extract of leaves of *Hypericum laricifolium* showed strong tyrosinase inhibitory activity with IC_{50} value of 120.90 µg/mL [76]. *S.inerme*, a tree in the family Sapotaceae, was reported on tyrosinase inhibitory activity using *L*-tyrosine as a substrate. Acetone and methanol crude extracts of *S. inerme* barks exhibited tyrosinase inhibitory activity with IC_{50} values of 63.00 ± 2.10 and 82.10 ± 2.70 µg/mL, respectively [48]. Moreover, *epi*-gallocatechin gallate and procyanidin B1 were isolated from this methanol crude extract and exhibited potent tyrosinase inhibitory activity with IC_{50} values of 30 ± 1.9 and 200 ± 2.2 µg/mL, respectively. Various plants demonstrated significant tyrosinase inhibition. Therefore, natural tyrosinase inhibitors should be further investigated for potent tyrosinase inhibitors. Methanol crude extract of stem barks exhibited the strongest tyrosinase inhibitory activity, so it was further isolated to find potent tyrosinase inhibitors.

Table 4.7 Tyrosinase inhibitory activity (IC_{50}) of methanol and aqueous crude extracts of different parts of *M. kauki*

Parts of plant	IC_{50}	
	Methanol crude extract	Aqueous crude extract
Fruits	0.75 ± 0.14*	0.49 ± 0.11*
Leaves	0.32 ± 0.08*	0.49 ± 0.12*
Seeds	3.86 ± 0.12*	3.88 ± 0.17*
Stem barks	0.26 ± 0.05*	0.41 ± 0.11*
Woods	No activity*	No activity*
Kojic acid	8.17 ± 0.03**	
α-Arbutin	1.92 ± 0.09*	

* IC_{50} value (mg/mL)
**IC_{50} value (µg/mL)

Stem barks and leaves of *M. kauki* showed high total phenolic and total flavonoid contents and also strong antioxidant activity. Stem barks of *M. kauki* exhibited the strongest tyrosinase inhibitory activity. Thus, the evaluation of total phenolic and total flavonoid contents showed relationship between total phenolic and flavonoid contents and antioxidant and tyrosinase inhibitory activities. The highest levels of phenolic and flavonoid components likewise, the previous research [77]. It was demonstrated that stem barks of *M. kauki* might be contained high amount of antioxidant and tyrosinase inhibitors.

4.4 Extraction of stem barks of *M. kauki*

The stem barks of *M. kauki* were extracted with *n*-hexane, ethyl acetate and methanol at room temperature (30 ± 2 °C) for 72 hours and water at 60 °C for 20

minutes, respectively. The extracts were filtered and evaporated to give four crude extracts as *n*-hexane crude extract (165.45 g, 3.27% w/w of dry weight, yellow gum), ethyl acetate crude extract (77.52 g, 1.54% w/w of dry weight, green gum), methanol crude extract (847.63 g, 16.85% w/w of dry weight, brown solid) and aqueous crude extract (495.25 g, 9.84% w/w of dry weight, brown gum). The different polarities of solvents were used for classification of chemical constituents in stem barks. The characteristic and percentage yield of crude extracts of stem barks of *M. kauki* are shown in Table 4.8. All of different polarities of crude extracts of stem barks were tested on total phenolic and flavonoid contents, antioxidant and tyrosinase inhibitory activities.

Table 4.8 Characteristic and percentage yield of crude extracts of stem barks of *M. kauki*

Crude extract	Characteristic	Yield (g) (%, w/w of dry weight)
n-Hexane	Yellow gum	164.45 (3.27)
Ethyl acetate	Green gum	77.52 (1.54)
Methanol	Brown solid	847.63 (16.85)
Aqueous	Brown gum	495.25 (9.84)

4.5 Phytochemical compositions of crude extracts of stem barks of *M. kauki*

Phytochemical compositions of the crude extracts of stem barks of *M. kauki* were determined as total phenolic and flavonoid contents.

4.5.1 Total phenolic content

Methanol crude extract of stem barks of *M. kauki* exhibited the highest total phenolic content with value of 160.12 ± 0.27 mg GAE/g of crude extract and followed by ethyl acetate crude extract (111.46 ± 0.38 mg GAE/g of crude extract), aqueous crude extract (66.17 ± 0.26 mg GAE/g of crude extract) and *n*-hexane crude extract (10.98 ± 0.14 mg GAE/g of crude extract) of stem barks of *M. kauki*, respectively. Total phenolic content of crude extracts of stem barks of *M. kauki* is shown in Table 4.9.

4.5.2 Total flavonoid content

Ethyl acetate crude extract of stem barks of *M. kauki* exhibited the highest total flavonoid content with value of 755.33 ± 1.53 mg QE/g of crude extract and followed by methanol crude extract (527.33 ± 1.00 mg QE/g of crude extract), aqueous crude extract (516.67 ± 1.73 mg QE/g of crude extract) and *n*-hexane crude extract (283.67 ± 1.52 mg QE/g of crude extract) of stem barks, respectively. Total flavonoid content of crude extracts of stem barks of *M. kauki* is shown in Table 4.9.

Table 4.9 Phytochemical compositions of crude extracts of stem barks of *M. kauki*

Crude extract	Total phenolic content (mg GAE/g of crude extract)	Total flavonoid content (mg QE/g of crude extract)
n-Hexane	10.98 ± 0.14	283.67 ± 1.52
Ethyl acetate	111.46 ± 0.38	755.33 ± 1.53
Methanol	160.12 ± 0.27	527.33 ± 1.00
Aqueous	66.17 ± 0.26	516.67 ± 1.73

4.6 Biological activities of crude extracts of stem barks of *M. kauki*

4.6.1 Antioxidant activities

4.6.1.1 DPPH radical scavenging activity

Ethyl acetate crude extract of stem barks of *M. kauki* exhibited the highest DPPH radical scavenging with DPPH radical scavenging value of 249.33 ± 0.25 mg TE/g of crude extract and followed by methanol crude extract (241.26 ± 0.32 mg TE/g of crude extract), aqueous crude extract (39.52 ± 0.25 mg TE/g of crude extract) and *n*-hexane crude extract (11.85 ± 0.67 mg TE/g of crude extract) of stem barks of *M. kauki*, respectively. DPPH radical scavenging activity of stem barks of *M. kauki* is shown in Table 4.10.

4.6.1.2 FRAP activity

Methanol crude extract of stem barks of *M. kauki* exhibited the highest FRAP activity with FRAP activity value of 221.50 ± 0.78 mg TE/g of crude extract and followed by ethyl acetate crude extract (179.28 ± 0.59 mg TE/g of crude extract), aqueous (50.94 ± 0.20 mg TE/g of crude extract) and *n*-hexane crude extract (10.39 ± 0.59 mg TE/g of crude extract) of stem barks of *M. kauki*, respectively. FRAP activity of stem barks of *M. kauki* is shown in Table 4.10.

Table 4.10 Antioxidant activities of stem barks of *M. kauki*

Crude extract	DPPH		FRAP
	(mg TAE/g crude extract)	Percentage of inhibition (%)	(mg TAE/g crude extract)
n-Hexane	11.85 ± 0.67	0.72 ± 0.03	10.39 ± 0.59
Ethyl acetate	249.33 ± 0.25	56.19 ± 0.04	179.28 ± 0.59
Methanol	241.26 ± 0.32	54.31 ± 0.06	221.50 ± 0.78
Aqueous	39.52 ± 0.25	7.18 ± 0.04	50.94 ± 0.20

4.6.2 Tyrosinase inhibitory activity

Ethyl acetate crude extract exhibited the strongest tyrosinase inhibitory activity (IC_{50} values of 0.24 ± 0.02 and 0.28 ± 0.04 mg/mL for *L*-tyrosine and *L*-DOPA, respectively) and followed by methanol crude extract (IC_{50} value of 1.66 ±

0.07 and 1.25 ± 0.05 for *L*-tyrosine and *L*-DOPA, respectively), aqueous crude extract (IC_{50} value of 1.89 ±0.09 and 1.89 ±0.09 mg/mL for *L*-tyrosine and *L*-DOPA, respectively) and *n*-hexane crude extract (IC_{50} value of 9.58 ± 0.17 and 9.23 ± 0.28 mg/mL for *L*-tyrosine and *L*-DOPA, respectively). The tyrosinase inhibitory activity of crude extracts of stem barks of *M. kauki* is shown in Table 4.11.

The previous published studies, (+)-*epi*-syringaresinol and *N-trans*-feruloyltyramine were isolated from methanol crude extract of stems of *S. dulcificum*. (+)-*epi*-Syringaresinol and *N-trans*-feruloyltyramine exhibited DPPH radical scavenging activity with IC_{50} values of 100.2 and 154.7 µM, respectively and these compounds exhibited tyrosinase inhibitory activity with IC_{50} values of 200.5 and 215.5 µM, respectively [60]. The ethyl acetate crude extract of *Peucedanum knappii* showed the highest antioxidant with SC_{50} value of 36.4 mg/mL and tyrosinase inhibitory activity with IC_{50} value of 517 mg/mL. Isorhamnetin-3-*O*-*β*-*D*-glucopyranoside was isolated from ethyl acetate crude extract of *P. knappii*. This compound exhibited DPPH radical scavenging with SC_{50} value of 2.9 µg/mL and tyrosinase inhibitory activity with IC_{50} value of 27.95 µg/mL [77]. After reviewing the previous researches, they show significant results which can be found in this research.

Table 4.11 Tyrosinase inhibitory activity of stem barks of *M. kauki*

Crude extract	Tyrosinase inhibitory activity (IC_{50})	
	L-tyrosine	*L*-DOPA
n-Hexane	9.58 ± 0.17*	9.23 ± 0.28*
Ethyl acetate	0.24 ± 0.02*	0.28 ± 0.04*
Methanol	1.66 ± 0.07*	1.25 ± 0.05*
Aqueous	1.89 ±0.09*	1.58± 0.11*
Kojic acid	8.17 ± 0.03 **	8.43 ± 0.05**
α-Arbutin	1.92 ± 0.09*	1.73 ± 0.11*

* IC_{50} value (mg/mL)
**IC_{50} value (µg/mL)

Several polyphenols including flavanones, flavones and isoflavones have been isolated from plants. Some of these compounds were identified and reported as tyrosinase inhibitors [78]. Thus, ethyl acetate crude extract of stem barks have potential to be excellent source for potent tyrosinase inhibitors.

4.7 Isolation of ethyl acetate crude extract of stem barks of *M. kauki*

The ethyl acetate crude extract of stem barks of *M. kauki* was isolated using silica gel quick column chromatography with a mixture of *n*-hexane:ethyl acetate, ethyl acetate and a mixture of ethyl acetate:methanol to obtain three fractions (E1-E3). All three fractions were tested on tyrosinase inhibitory activity using *L*-tyrosine as a substrate. Fraction E1 showed the strongest tyrosinase inhibitory activity with percent inhibition of 74.64 ± 0.74% and followed by fractions E2 and E3 with percent

inhibition of 71.46 ± 0.70% and 70.56 ± 0.82%, respectively. The isolation and tyrosinase inhibitory activity of ethyl acetate crude extract are shown in Table 4.12.

Table 4.12 Isolation and tyrosinase inhibitory activity of fraction E

Fraction	Characteristic	Yield (g) (% w/w of ethyl acetate crude extract)	Tyrosinase inhibitory activity (%)
E1	Yellow green gum	19.60 (32.67)	74.64 ± 0.74*
E2	Dark brown solid	9.15 (15.25)	71.46 ± 0.70*
E3	Dark brown solid	23.38 (38.96)	70.56 ± 0.82*
Kojic acid [a]			98.19 ± 0.12**

[a] Positive control

* at concentration 1 mg/mL

** at concentration 0.1 mg/mL

The fraction E1 was further isolated using silica column chromatography with gradient elution of mixture of *n*-hexane and dichloromethane to obtain ten fractions (E1A-E1J). All ten fractions were tested on tyrosinase inhibitory activity using *L*-tyrosine as a substrate. The fractions E1D, E1I and E1J showed strong tyrosinase inhibitory activity with percent inhibition of 73.51 ± 0.76%, 79.70 ± 4.65% and 75.69 ± 1.04%, respectively. The fractions E1B, E1C, E1E, E1F and E1H showed moderate tyrosinase inhibitory activity with percent inhibition of 41.01 ± 6.89%, 62.76 ± 1.54%, 64.14 ± 2.36%, 58.87 ± 1.83% and 41.38 ± 4.42%, respectively. The fraction E1G showed weak tyrosinase inhibitory activity with percent inhibition of 11.01 ± 3.78% and E1A showed no tyrosinase inhibitory activity. The isolation and tyrosinase inhibitory activity of fraction E1 are shown in Table 4.13.

Table 4.13 Isolation and tyrosinase inhibitory activity of fraction E1

Fraction	Characteristic	Yield (mg) (% w/w of fraction E1)	Tyrosinase inhibitory activity (%)
E1A	White wax	0.4 (0.00)	No activity
E1B	White powder	30.0 (0.15)	41.01 ± 6.89*
E1C	Yellow wax	7,480.0 (38.16)	62.76 ± 1.54*
E1D	White solid	750.0 (3.83)	73.51 ± 0.76*
E1E	Crystal colorless	90.0 (0.46)	64.14 ± 2.36*
E1F	Crystal colorless	50.0 (0.26)	58.87 ± 1.83*
E1G	Yellow solid	1,190.0 (6.07)	11.01 ± 3.78*
E1H	Gold solid	2,520.0 (12.86)	41.38 ± 4.42*
E1I	Green solid	720.0 (3.67)	79.70 ± 4.65*
E1J	Yellow wax	6,450.0 (32.91)	75.69 ± 1.04*
Kojic acid [a]			98.19 ± 0.09**

[a] Positive control

* at concentration 1 mg/mL

** at concentration 0.1 mg/mL

The fraction E1B was further isolated using silica gel column chromatography with gradient elution of mixture of *n*-hexane and dichloromethane to get six fractions (E1BA-E1BF). The isolation and tyrosinase inhibitory activity of fraction E1B are shown in Table 4.14.

Table 4.14 Isolation and tyrosinase inhibitory activity of fraction E1B

Fraction	Characteristic	Yield (mg) (% w/w of fraction E1B)	Tyrosinase inhibitory activity (%)
E1BA	White solid	4.0 (13.33)	ND
E1BB	White solid	0.8 (2.67)	ND
E1BC	White solid	24.8 (82.67)	40.02 ± 01.02
E1BD	White solid	0.1 (0.33)	ND
E1BE	White solid	0.2 (0.67)	ND
E1BF	White solid	1.1 (0.04)	ND

ND = no detection

The fraction E1BC was a major component of fraction E1B. It was isolated using silica gel column chromatography with gradient elution of mixture of *n*-hexane and dichloromethane to obtain five fractions (E1BC1-E1BC5). The isolation of fraction E1BC is shown in Table 4.15.

Table 4.15 Isolation of fraction E1BC

Fraction	Characteristic	Yield (mg) (% w/w of fraction E1BC)
E1BC1	White solid	1.4 (5.64)
E1BC2	White solid	21.6 (0.87)
E1BC3	White solid	0.6 (0.02)
E1BC4	White solid	0.7 (1.49)
E1BC5	White solid	1.4 (5.64)

The fraction E1BC2 was a major component of fraction E1BC. It further was isolated by MPLC using gradient system of *n*-hexane and ethyl acetate with flow rate 10 mL/min to afford six fractions (E1BC2A-E1BC2F). The isolation of fraction E1BC2 is shown in Table 4.16.

Table 4.16 Isolation of fraction E1BC2

Fraction	Characteristic	Yield (mg) (% w/w of fraction E1BC2)
E1BC2A	White solid	0.5 (2.31)
E1BC2B	White solid	0.8 (3.70)
E1BC2C	White solid	19.2 (88.89)
E1BC2D	White solid	0.1 (0.46)
E1BC2E	White solid	0.7 (3.24)
E1BC2F	White solid	0.9 (4.17)

The fraction E1BC2C was a major component of fraction E1BC2. It was separated by MPLC using gradient system of *n*-hexane and ethyl acetate as eluent with flow rate 10 mL/min to obtain three fractions (E1BC2C1-E1BC2C3). The isolation of fraction E1BC2C is shown in Table 4.17.

Table 4.17 Isolation of fraction E1BC2C

Fraction	Characteristic	Yield (mg) (% w/w of fraction E1BC2C)
E1BC2C1	White solid	0.2 (1.04)
E1BC2C2	White solid	18.8 (97.92)

The fraction E1BC2C2 was a major component of fraction E1BC2C. It was separated by PTLC using *n*-hexane and ethyl acetate as developing solvent to afford three fractions (E1BC2C2A-E1BC2C2C). The isolation of fraction E1BC2C2 is shown in Table 4.18. Unfortunately, isolation of fraction E1BC2C2 did not succeed to get pure compound.

Table 4.18 Isolation of fraction E1BC2C2

Fraction	Characteristic	Yield (mg) (% w/w of fraction E1BC2C2)
E1BC2C2A	White solid	10.1 (53.72)
E1BC2C2B	White solid	1.3 (6.91)
E1BC2C2C	White solid	1.2 (6.38)

The fraction E1C showed moderate tyrosinase inhibitory activity. The fraction E1C was separated by MPLC using gradient system of *n*-hexane and dichloromethane with flow rate 10 mL/min to get ten fractions (E1CA-E1CJ). The isolation of fraction E1C is shown in Table 4.19.

Table 4.19 Isolation of fractions E1C

Fraction	Characteristic	Yield (mg) (% w/w of fraction E1C)
E1CA	White wax	2.2 (0.03)
E1CB	White solid	0.1 (0.00)
E1CC	White solid	0.6 (0.01)
E1CD	White wax	14.1 (0.20)
E1CE	White wax	1,932.1 (27.6)
E1CF	White solid	1,299.7 (18.56)
E1CG	White wax	574.2 (8.20)
E1CH	Yellow wax	82.6 (1.18)
E1CI	Yellow wax	70.8 (1.01)
E1CJ	Yellow oil	2,920.8 (41.72)

The fraction E1CG was separated by PTLC using petroleum ether and dichloromethane as developing solvent to obtain three fractions (E1CG1-E1CG3). The isolation of fraction E1CG is shown in Table 4.20. Unfortunately, isolation of fraction E1CG did not succeed to get pure compound.

Table 4.20 Isolation of fraction E1CG

Fraction	Characteristic	Yield (mg) (% w/w of fraction E1CG)
E1CG1	White wax	4.5 (22.50)
E1CG2	White wax	7.0 (35.00)
E1CG3	White wax	6.2 (31.00)

The fraction E1D showed strong tyrosinase inhibitory activity. The fraction E1D was separated by silica gel column chromatography with gradient system of *n*-hexane and dichloromethane to get ten fractions (E1DA-E1DJ). The isolation and tyrosinase inhibitory activity of fraction E1D are shown in Table 4.21.

Table 4.21 Isolation and tyrosinase inhibitory activity of fraction E1D

Fraction	Characteristic	Yield (mg) (% w/w of fraction E1D)	Tyrosinase inhibitory activity (%)
E1DA	White solid	6.0 (0.82)	ND
E1DB	White solid	1.0 (0.14)	ND
E1DC	White solid	0.9 (0.12)	ND
E1DD	White solid	13.8 (1.89)	ND
E1DE	White solid	2.0 (0.27)	ND
E1DF	White solid	1.2 (0.16)	ND
E1DG	White solid	6.2 (0.85)	ND
E1DH	White solid	135.4 (18.55)	66.64 ± 1.24
E1DI	White solid	479.8 (65.73)	67.32 ± 0.87
E1DJ	White solid	60.2 (8.25)	39.23 ± 2.32

ND = No detection

Fraction E1DI was a major component of fraction E1D. It was separated by silica gel column chromatography with gradient system of *n*-hexane and dichloromethane to obtain six fractions (E1DIA-E1DIE). The isolation of fraction E1DI is shown in Table 4.22.

Table 4.22 Isolation of fraction E1DI

Fraction	Characteristic	Yield (mg) (% w/w of fraction E1DI)
E1DIA	White solid	0.7 (0.14)
E1DIB	White solid	2.9 (0.60)
E1DIC	White solid	1.2 (0.31)
E1DID	White solid	339.0 (70.65)
E1DIE	White solid	5.2 (1.09)
E1DIF	White solid	10.8 (2.25)

Fraction E1DID was a major component of fraction E1DI. It was further separated with gradient system of *n*-hexane and acetone to afford four fractions (E1DID1-E1DID4). Fraction E1DID3 (compound **I**) was obtained as white solid (339.0 mg, 0.57% w/w of ethyl acetate crude extract)**.** Other fractions showed more than one spot on TLC and did not have enough amounts for separation. The isolation of fraction E1DID is shown in Table 4.23.

Table 4.23 Isolation of fraction E1DID

Fraction	Characteristic	Yield (mg) (% w/w of fraction E1DID)
E1DID1	White solid	1.1 (0.32)
E1DID2	White solid	2.1 (0.62)
E1DID3	White solid	319.2 (94.16)
E1DID4	White solid	3.1 (0.91)

The fraction E1E (90.4 mg) showed strong tyrosinase inhibitory activity. The fraction E1E was separated by silica gel column chromatography with gradient elution of *n*-hexane and dichloromethane to afford eight fractions (E1EA-E1EH). The isolation of fraction E1E is shown in Table 4.24.

Table 4.24 Isolation and tyrosinase inhibitory activity of fraction E1E

Fraction	Characteristic	Yield (mg) (% w/w of fraction E1E)	Tyrosinase inhibitory activity (%)
E1EA	White solid	1.3 (1.44)	ND
E1EB	White solid	2.1 (2.32)	ND
E1EC	White solid	0.0 (0.00)	ND
E1ED	White solid	0.2 (0.22)	ND
E1EE	White solid	2.7 (2.99)	ND
E1EF	White solid	74.2 (82.08)	60.27 ± 0.52
E1EG	White solid	5.6 (6.19)	ND
E1EH	White solid	4.8 (5.31)	ND

ND = No detection

The fraction E1EF was a major component of fraction E1E. It was further separated by silica gel column chromatography with gradient system of *n*-hexane and dichloromethane to get five fractions (E1EF1-E1EF5). The isolation fraction E1EF is shown in Table 4.25.

Table 4.25 Isolation of fraction E1EF

Fraction	Characteristic	Yield (mg) (% w/w of fraction E1EF)
E1EF1	White solid	0.0 (0.00)
E1EE2	White solid	3.2 (4.31)
E1EF3	White solid	2.6 (3.50)
E1EF4	White solid	68.5 (92.32)
E1EF5	White solid	2.7 (3.64)

The fraction E1EF4 was a major component of fraction E1EF. It was further separated by silica gel column chromatography with *n*-hexane and acetone to obtain five fractions (E1EF4A-E1EF4E). The isolation of fraction E1EF4 is shown in Table 4.26.

Table 4.26 Isolation of fraction E1EF4

Fraction	Characteristic	Yield (mg) (% w/w of fraction E1EF4)
E1EF4A	White solid	0.2 (0.29)
E1EE4B	White solid	55.5 (0.81)
E1EF4C	White solid	0.3 (0.43)
E1EF4D	White solid	0.2 (0.29)
E1EF4E	White solid	4.0 (5.84)

The fraction E1EF4B was a major component of fraction E1EF4. It was separated by silica gel column chromatography with gradient system of *n*-hexane and acetone to afford E1EF4B1-E1EF4B5. Fraction E1EF4B2 (compound **I)** was obtained as white solid (54.9 mg, 0.09% w/w of ethyl acetate crude extract). Other fractions showed more than one spot on TLC and did not have enough amounts for separation. The isolation of fraction E1EF4B is shown in Table 4.27.

Table 4.27 Isolation of fraction E1EF4B

Fraction	Characteristic	Yield (mg) (% w/w of fraction E1EF4B)
E1EF4B1	White solid	1.5 (2.70)
E1EE4B2	White solid	54.9 (98.92)
E1EF4B3	White solid	1.2 (2.16)

The fraction E1F showed moderate tyrosinase inhibitory activity. It was separated by PTLC using *n*-hexane:dichloromethane as developing solvent to afford four fractions (E1FA-E1FD). Fraction E1FB (compound **I)** was obtained as white solid (9.2 mg, 0.02% w/w of ethyl acetate crude extract. Other fractions showed more than one spot on TLC and did not have enough amounts for separation. The isolation of fraction E1F is shown in Table 4.28.

Table 4.28 Isolation of fraction E1F

Fraction	Characteristic	Yield (mg) (% w/w of fraction E1F)
E1FA	White solid	15.3 (30.60)
E1FB	White solid	9.2 (18.40)
E1FC	White solid	5.6 (11.20)
E1FD	White solid	2.2 (4.40)

The fraction E1H showed moderate tyrosinase inhibitory activity. It was separated by column chromatography with mixture of *n*-hexane and ethyl acetate to obtain six fractions (E1HA-E1HF). The isolation of fraction E1H is shown in Table 4.29.

Table 4.29 Isolation of fraction E1H

Fraction	Characteristic	Yield (mg) (% w/w of fraction E1H)
E1HA	White wax	37.8 (6.30)
E1HB	White wax	111.0 (18.50)
E1HC	White wax	70.0 (11.67)
E1HD	White wax	177.6 (29.60)
E1HE	White wax	22.1(3.68)
E1HF	Yellow wax	154.1 (25.68)

The fraction E1HA was separated by PTLC using *n*-hexane and dichloromethane as developing solvent to obtain two fractions (E1HA1-E1HA2). The

isolation of fraction E1HA is shown in Table 4.30. Unfortunately, isolation of fraction E1HA did not succeed to get pure compound.

Table 4.30 Isolation of fraction E1HA

Fraction	Characteristic	Yield (mg) (% w/w of fraction E1HA)
E1HA1	White wax	19.8 (52.38)
E1HA2	White wax	1.6 (0.42)

The fraction E1HB was a major component of fraction E1H. It was separated by MPLC using gradient system of *n*-hexane and ethyl acetate with flow rate 1 mL/min to obtain nine fractions (E1HB1-E1HB9). The isolation of fraction E1HB is shown in Table 4.31. Unfortunately, isolation of fraction E1HB did not succeed to afford pure compound.

Table 4.31 Isolation of fraction E1HB

Fraction	Characteristic	Yield (mg) (% w/w of fraction E1HB)
E1HB1	White wax	0.6 (1.62)
E1HB2	White wax	0.6 (1.62)
E1HB3	White wax	0.6 (1.62)
E1HB4	White wax	14.2 (38.38)
E1HB5	White wax	10.3 (27.84)
E1HB6	White wax	1.6 (4.32)
E1HB7	White wax	2.8 (7.57)
E1HB8	White wax	4.3 (11.62)
E1HB9	White wax	0.3 (0.81)

The fraction E1HC was separated by silica gel column chromatography with gradient system of *n*-hexane and ethyl acetate to get four fractions (E1HC1-E1HC5). The isolation of fraction E1HC is shown in Table 4.32.

Table 4.32 Isolation of fraction E1HC

Fraction	Characteristic	Yield (mg) (% w/w of fraction E1HC)
E1HC1	White wax	1.3 (1.86)
E1HC2	White wax	1.1 (1.57)
E1HC3	White wax	1.8 (2.57)
E1HC4	White wax	33.6 (48.00)
E1HC5	White wax	21.4 (30.57)

The fraction E1HC4 was a major component of fraction E1HC. It was separated by PTLC using petroleum ether and ethyl acetate as developing system to get five fractions (E1HC4A-E1HC4E). The isolation of fraction E1HC4 is shown in Table 4.33. Unfortunately, isolation of fraction E1HC4 did not succeed to obtain pure compound.

Table 4.33 Isolation of fraction E1HC4

Fraction	Characteristic	Yield (mg) (% w/w of fraction E1HC4)
E1HC4A	White wax	7.9 (23.51)
E1HC4B	White wax	7.5 (22.32)
E1HC4C	White wax	0.6 (1.78)
E1HC4D	White wax	2.7 (8.04)
E1HC4E	White wax	4.5 (13.39)

The fraction E1HE was separated by column chromatography with mixture of dichloromethane and acetone to obtain four fractions (E1HE1-E1HE4). The isolation of fraction E1HE is shown in Table 4.34. Unfortunately, isolation of fraction E1HE did not succeed to obtain pure compound. The fractions E1HE1-E1HE4 showed more than one spot on TLC and did not have enough amounts for separation.

Table 4.34 Isolation of fractions E1HE

Fraction	Characteristic	Yield (mg) (% w/w of fraction E1HE)
E1HE1	White wax	1.6 (7.24)
E1HE2	White wax	7.3 (33.03)
E1HE3	White wax	1.5 (6.79)
E1HE4	White wax	6.2 (28.05)

The fraction E1I showed the strongest tyrosinase inhibitory activity among fractions E1A-E1I. The fraction E1I was separated by silica gel column chromatography with *n*-hexane and ethyl acetate to get six fractions (E1IA-E1IF). The isolation and tyrosinase inhibitory activity of fraction E1I are shown in Table 4.35.

Table 4.35 Isolation and tyrosinase inhibitory activity of fraction E1I

Fraction	Characteristic	Yield (mg) (% w/w of fraction E1I)	Tyrosinase inhibitory activity (%)
E1IA	Yellow wax	9.9 (1.65)	ND
E1IB	Yellow solid	184.1 (30.85)	23.29 ± 1.1
E1IC	Yellow solid	55.3 (9.22)	76.26 ± 0.2
E1ID	Yellow solid	192.5 (32.08)	33.23 ± 2.1
E1IE	Yellow wax	34.3 (5.72)	ND
E1IF	Yellow wax	45.0 (7.50)	ND

ND = No detection

The fraction E1IC exhibited the strongest tyrosinase inhibitory activity among fractions E1IA-E1IF. It was further separated by PTLC using *n*-hexane and acetone as developing solvent to afford five fractions (E1IC1-E1IC5). Fraction E1IC5 (compound **II**) was obtained as a yellow solid (7.8 mg, 0.01% w/w of ethyl acetate

crude extract). Other fractions showed weak tyrosinase inhibitory activity. The isolation of fraction E1IC is shown in Table 4.36.

Table 4.36 Isolation of fraction E1IC

Fraction	Characteristic	Yield (mg) (% w/w of fraction E1IC)
E1IC1	Yellow solid	2.4 (4.34)
E1IC2	Yellow solid	6.6 (11.93)
E1IC3	Yellow solid	20.0 (36.17)
E1IC4	Yellow solid	0.6 (1.08)
E1IC5	Yellow solid	7.8 (14.10)

The fraction E2 showed moderate tyrosinase inhibitory activity. The fraction E2 was separated by MPLC using gradient system of *n*-hexane and acetone with flow rate 36 mL/min to get six fractions (E2A-E2F). The fraction E2B showed the strongest tyrosinase inhibitory activity with percent inhibition of 70.39 ± 0.38% and followed by fractions E2F, E2D, E2A, E2C and E2E showed tyrosinase inhibitory activity with percent inhibition of 62.80 ± 0.17 %, 62.30 ± 0.29 %, 61.79 ± 0.14 %, 58.26 ± 0.12 % and 58.18 ± 0.16 %, respectively. The isolation and tyrosinase inhibitory activity of fraction E2 are shown in Table 4.37.

Table 4.37 Isolation and tyrosinase inhibitory activity of fraction E2

Fraction	Characteristic	Yield (mg) (% w/w of fraction E2)	Tyrosinase inhibitory activity (%)
E2A	White solid	112.2 (1.50)	61.79 ± 0.14*
E2B	White solid	68.3 (0.91)	70.39 ± 0.38*
E2C	White wax	127.7 (1.70)	58.26 ± 0.12*
E2D	White wax	297.2 (3.96)	62.30 ± 0.29*
E2E	Brown solid	721.4 (9.62)	58.18 ± 0.16*
E2F	Brown solid	3,263.3 (43.51)	62.80 ± 0.17*
Kojic acid [a]			98.19 ± 0.12**

[a] Positive control

* at concentration 1 mg/mL

** at concentration 0.1 mg/mL

The fraction E2A showed moderate tyrosinase inhibitory activity. It was separated by MPLC using gradient system of *n*-hexane and dichloromethane with flow rate 10 mL/min to obtain seven fractions (E2AA-E2AG). Isolation of fraction E2A is shown in Table 4.38.

Table 4.38 Isolation of fraction E2A

Fraction	Characteristic	Yield (mg) (% w/w of fraction E2A)
E2AA	White solid	2.7 (2.41)
E2AB	White solid	5.2 (4.63)
E2AC	White solid	13.5 (12.03)
E2AD	White solid	13.5 (12.03)
E2AE	White solid	6.9 (6.15)
E2AF	White solid	45.0 (40.11)
E2AG	White solid	12.3(10.96)

The E2AD was a major component of fraction E2A. It was further separated by PTLC using *n*-hexane and dichloromethane as developing solvent to get three fractions (E2AD1-E2AD3). The isolation of fraction E2AD is shown in Table 4.39. Unfortunately, isolation of fraction E2AD did not succeed to afford pure compound.

Table 4.39 Isolation of fraction E2AD

Fraction	Characteristic	Yield (mg) (% w/w of fraction E2AD)
E2AD1	White solid	0.2 (1.48)
E2AD2	White solid	1.9 (14.07)
E2AD3	White solid	2.8 (20.74)

The fraction E2AE was separated by PTLC using *n*-hexane and dichloromethane as developing solvent to afford three fractions (E2AE1-E2AE3). The isolation of fraction E2AE is shown in Table 4.40. Unfortunately, isolation of fraction E2AE did not succeed to get pure compound. The fraction E2AE1 showed one spot on TLC. Then, there were detected by NMR spectroscopy that showed spectrum of mixture compound.

Table 4.40 Isolation of fraction E2AE

Fraction	Characteristic	Yield (mg) (% w/w of fraction E2AE)
E2AE1	White solid	0.6 (8.70)
E2AE2	White solid	2.5 (36.23)
E2AE3	White solid	3.7 (53.62)

The fraction E2B showed strong tyrosinase inhibitory activity. The fraction E2B was separated by MPLC using gradient system of *n*-hexane and acetone with flow rate 10 mL/min to afford seven fractions (E2BA-E2BG). The isolation of fraction E2B is shown in Table 4.41.

Table 4.41 Isolation of fraction E2B

Fraction	Characteristic	Yield (mg) (% w/w of fraction E2B)
E2BA	White solid	1.3 (2.17)
E2BB	White solid	0.8 (1.33)
E2BC	White solid	5.8 (9.67)
E2BD	White solid	9.9 (16.50)
E2BE	White solid	18.9 (31.50)
E2BF	White solid	2.4 (4.00)
E2BG	White solid	17.4 (29.00)

The fraction E2BD was separated by PTLC using *n*-hexane and acetone as developing solvent to get two fractions (E2BD1-E2BD2). The isolation of fraction E2BD is shown in Table 4.42. Unfortunately, isolation of fraction E2BD did not succeed to get pure compound.

Table 4.42 Isolation of fraction E2BD

Fraction	Characteristic	Yield (mg) (% w/w of fraction E2BD)
E2BD1	White solid	3.8 (38.38)
E2BD2	White solid	3.7 (37.37)

The fraction E2BE was a major component of fraction E2B. It was separated by MPLC using gradient system of dichloromethane and ethyl acetate with flow rate 10 mL/min to obtain three fractions (E2BE1-E2BE3). The isolation of fraction E2BE is shown in Table 4.43.

Table 4.43 Isolation of fraction E2BE

Fraction	Characteristic	Yield (mg) (% w/w of fraction E2BE)
E2BE1	White solid	9.6 (50.79)
E2BE2	White solid	0.3 (1.59)
E2BE3	White solid	5.9 (31.22)

The fraction E2BE1 was a major component of fraction E2BE. It was separated by PTLC using dichloromethane and ethyl acetate as developing solvent to get three fractions (E2BE1A-E2BE1C). The isolation of fraction E2BE1 is shown in Table 4.44 Unfortunately, isolation of fraction E2BE1 did not succeed to afford pure compound. The fractions E2BE1A-E2BE1C showed more than one spot on TLC and did not have enough amounts for separation.

Table 4.44 Isolation of fraction E2BE1

Fraction	Characteristic	Yield (mg) (% w/w of fraction E2BE1)
E2BE1A	White solid	0.9 (9.38)
E2BE1B	White solid	6.6 (68.75)
E2BE1C	White solid	0.7 (7.29)

The fraction E2C showed moderate tyrosinase inhibitory activity. It was separated by MPLC using gradient system of *n*-hexane and acetone with flow rate 5 mL/min to afford eight fractions (E2CA-E2CH). The isolation of fraction E2C is shown in Table 4.45.

Table 4.45 Isolation of fraction E2C

Fraction	Characteristic	Yield (mg) (% w/w of fraction E2C)
E2CA	White solid	0.5 (0.39)
E2CB	White solid	0.3 (0.23)
E2CC	White solid	8.9 (6.97)
E2CD	White wax	3.6 (2.82)
E2CE	White wax	15.0 (11.75)
E2CF	White wax	62.9 (49.26)
E2CG	White wax	9.7 (7.60)
E2CH	White wax	7.1 (5.56)

The fraction E2CC was further separated by MPLC using gradient system of *n*-hexane and acetone with flow rate 5 mL/min to get four fractions (E2CC1-E2CC4). The isolation of fraction E2CC is shown in Table 4.46.

Table 4.46 Isolation of fraction E2CC

Fraction	Characteristic	Yield (mg) (% w/w of fraction E2CC)
E2CC1	White solid	0.2 (2.25)
E2CC2	White solid	0.3 (3.37)
E2CC3	White solid	1.2 (13.48)
E2CC4	White solid	7.0 (78.65)

The fraction E2CC4 was a major component of fraction E2CC. It was separated by PTLC using *n*-hexane and acetone as developing solvent to get four fractions (E2CC4A-E2CC4D). The isolation of fraction E2CC4 is shown in Table 4.47. Unfortunately, isolation of fraction E2CC4 did not succeed to get pure compound.

Table 4.47 Isolation of fraction E2CC4

Fraction	Characteristic	Yield (mg) (% w/w of fraction E2CC4)
E2CC4A	White solid	0.2 (2.86)
E2CC4B	White solid	0.1 (1.43)
E2CC4C	White solid	3.4 (48.57)
E2CC4D	White solid	0.2 (2.86)

The fraction E2CE was further separated by PTLC using a mixture of *n*-hexane and acetone as developing solvent to get three fractions (E2CE1-E2CE3). The isolation of fraction E2CE is shown in Table 4.48. Unfortunately, isolation of fraction E2CE did not succeed to afford pure compound.

Table 4.48 Isolation of fraction E2CE

Fraction	Characteristic	Yield (mg) (% w/w of fraction E2CE)
E2CE1	White solid	6.2 (41.33)
E2CE2	White solid	3.0 (20.00)
E2CE3	White solid	1.8 (12.00)

The fraction E2CF showed moderate tyrosinase inhibitory activity. It was separated by MPLC using gradient system of dichloromethane and ethyl acetate with flow rate 5 mL/min to obtain three fractions (E2CF1-E2CF3). The isolation of fraction E2CF is shown in Table 4.49. Unfortunately, isolation of fraction E2CF did not succeed to obtain pure compound.

Table 4.49 Isolation of fraction E2CF

Fraction	Characteristic	Yield (mg) (% w/w of fraction E2CF)
E2CF1	White solid	1.0 (1.59)
E2CF2	White solid	0.3 (0.47)
E2CF3	White solid	1.9 (3.02)

The fraction E2D showed moderate tyrosinase inhibitory activity. It was separated by MPLC using gradient system of *n*-hexane and ethyl acetate with flow rate 10 mL/min to get three fractions (E2DA-E2DC). The isolation of fraction E2D is shown in Table 4.50. The fraction E2DA-E2DC showed more than one spot on TLC and did not have enough amounts for separation.

Table 4.50 Isolation of fraction E2D

Fraction	Characteristic	Yield (mg) (% w/w of fraction E2D)
E2DA	White wax	2.7 (1.06)
E2DB	White wax	10.5 (4.12)
E2DC	White wax	206.9 (81.14)

The fraction E2DC was a major component of fraction E2D. It was further separated by MPLC using gradient system of dichloromethane and ethyl acetate with flow rate 10 mL/min to get six fractions (E2DC1-E2DC6). The isolation of fraction E2DC is shown in Table 4.51.

Table 4.51 Isolation of fraction E2DC

Fraction	Characteristic	Yield (mg) (% w/w of fraction E2DC)
E2DC1	White wax	0.7 (0.34)
E2DC2	White wax	2.8 (1.35)
E2DC3	White wax	20.4 (9.86)
E2DC4	White wax	39.6 (19.14)
E2DC5	White wax	65.6 (31.71)
E2DC6	White wax	50.0 (24.17)

The fraction E2DC4 was a major component of fraction E2DC. It was separated by MPLC using gradient system of *n*-hexane and acetone with flow rate 2 mL/min to obtain five fractions (E2DC4A-E2DC4E). The isolation of fraction E2DC4 is shown in Table 4.52. Unfortunately, isolation of fraction E2DC4 did not succeed to obtain pure compound.

Table 4.52 Isolation of fraction E2DC4

Fraction	Characteristic	Yield (mg) (% w/w of fraction E2DC)
E2DC4A	White wax	0.0 (0.00)
E2DC4B	White wax	0.4 (1.01)
E2DC4C	White wax	0.3 (0.76)
E2DC4D	White wax	1.8 (4.54)
E2DC4E	White wax	35.4 (89.39)

The fraction E2DC5 was a major component of fraction E2DC. It was further separated by MPLC using gradient system of *n*-hexane and ethyl acetate with flow rate 5 mL/min to get three fractions (E2DC5A-E2DC5C). The isolation of fraction E2DC5 is shown in Table 4.53.

Table 4.53 Isolation of fraction E2DC5

Fraction	Characteristic	Yield (mg) (% w/w of fraction E2DC5)
E2DC5A	White wax	1.5 (2.29)
E2DC5B	White wax	16.3 (24.85)
E2DC5C	White wax	45.2 (68.90)

The fraction E2DC5C was a major component of fraction E2DC5. It was separated by PTLC using mixture of petroleum ether and ethyl acetate as developing solvent to afford two fractions (E2DC5CA-E2DC5CB). The isolation of fraction

E2DC5C is shown in Table 4.54. Unfortunately, isolation of fraction E2DC5C did not succeed to get pure compound.

Table 4.54 Isolation of fraction E2DC5C

Fraction	Characteristic	Yield (mg) (% w/w of fraction E2DC4CA)
E2DC5CA	White wax	27.4 (60.62)
E2DC5CB	White wax	10.4 (23.01)

The fraction E2E showed moderate tyrosinase inhibitory activity. It was separated by MPLC using gradient system of *n*-hexane and ethyl acetate with flow rate 10 mL/min to get seven fractions (E2EA-E2EG). The isolation of fraction E2E is shown in Table 4.55.

Table 4.55 Isolation of fraction E2E

Fraction	Characteristic	Yield (mg) (% w/w of fraction E2E)
E2EA	White wax	1.7 (1.7)
E2EB	White wax	3.0 (3.0)
E2EC	White wax	1.6 (1.6)
E2ED	White wax	12.7 (12.7)
E2EE	White wax	25.8 (25.8)
E2EF	White wax	28.6 (28.6)
E2EG	White wax	18.4 (18.4)

The fraction E2ED was further separated by PTLC using mixture of *n*-hexane and acetone as developing solvent to get four fractions (E2ED1-E2ED4). The isolation of fraction E2ED is shown in Table 4.56. Unfortunately, isolation of fraction E2ED did not succeed to afford pure compound.

Table 4.56 Isolation fraction E2ED

Fraction	Characteristic	Yield (mg) (% w/w of fraction E2ED)
E2ED1	White wax	0.8 (6.30)
E2ED2	White wax	0.0 (0.00)
E2ED3	White wax	0.7 (5.51)
E2ED4	White wax	6.6 (51.97)

The fraction E2EE was separated by MPLC using gradient system of dichloromethane and acetone with flow rate 10 mL/min to afford three fractions (E2EE1-E2EE3). The isolation of fraction E2EE is shown in Table 4.57.

Table 4.57 Isolation of fraction E2EE

Fraction	Characteristic	Yield (mg) (% w/w of fraction E2EE)
E2EE1	White wax	2.7 (10.46)
E2EE2	White wax	2.1 (8.14)
E2EE3	White wax	19.1 (74.03)

The fraction E2EF was a major component of fraction E2E. It was further separated by MPLC using gradient system of *n*-hexane and acetone with flow rate 2 mL/min to obtain six fractions (E2EFA-E2EFF). The isolation of fraction E2EF is shown in Table 4.58. Unfortunately, isolation of fraction E2EF did not succeed to obtain pure compound. The fractions E2EFA-E2EFF showed more than one spot on TLC and did not have enough amounts for separation.

Table 4.58 Isolation of fraction E2EF

Fraction	Characteristic	Yield (mg) (% w/w of fraction E2EF)
E2EFA	White solid	1.7 (5.94)
E2EFB	White solid	3.4 (11.89)
E2EFC	White solid	11.1 (38.81)
E2EFD	White solid	2.1 (7.34)
E2EFE	White solid	5.9 (20.63)
E2EFF	White solid	0.3 (1.05)

The fraction E2F showed moderate tyrosinase inhibitory activity. It was separated by MPLC using gradient system of *n*-hexane and ethyl acetate with flow rate 5 mL/min to obtain 10 fractions (E2FA-E2FJ). The isolation of fraction E2F is shown in Table 4.59. Unfortunately, isolation of fraction E2F did not succeed to obtain pure compound.

Table 4.59 Isolation of fraction E2F

Fraction	Characteristic	Yield (mg) (% w/w of fraction E2EF)
E2FA	White solid	3.3 (2.2)
E2FB	White solid	17.0 (11.3)
E2FC	White solid	12.6 (8.4)
E2FD	White solid	8.7 (5.8)
E2FE	White solid	12.2 (8.13)
E2FF	White solid	8.9 (5.93)
E2FG	White solid	8.5 (5.67)
E2FH	White solid	8.5 (5.67)
E2FI	White solid	16.8 (11.2)
E2FJ	White solid	50.0 (33.33)

The fraction E3 was separated by MPLC using isocratic elution of methanol with flow rate 10 mL/min to obtain three fractions (E3A-E3C). Fraction E3B showed

strong tyrosinase inhibitory activity with percent inhibition of 74.74 ± 2.79%. Fraction E3C showed moderate tyrosinase inhibitory activity with percent inhibition of 48.22 ± 1.50%. While, E3A showed weak tyrosinase inhibitory activity with percent inhibition of 29.32 ± 2.47%. The tyrosinase inhibitory activity and isolation of fraction E3 are shown in Table 4.60.

Table 4.60 Isolation and tyrosinase inhibitory activity of fraction E3

Fraction	Characteristic	Yield (mg) (% w/w of fraction E3)	Tyrosinase inhibitory activity (%)
E3A	Brown solid	1,436.2 (62.44)	29.32 ± 2.47*
E3B	Brown solid	350.0 (15.22)	74.74 ± 2.79*
E3C	Brown solid	731.4 (31.80)	48.22 ±1.50*
Kojic acid [a]			95.19 ± 0.07**

[a] Positive control

* concentration at 1 mg/mL

** concentration at 0.1 mg/mL

The fraction E3B showed strong tyrosinase inhibitory activity. It was separated using diaion column chromatography with gradient system of ethyl acetate and methanol to get three fractions (E3BA-E3BC). The isolation of fraction E3B is shown in Table 4.61.

Table 4.61 Isolation of fraction E3B

Fraction	Characteristic	Yield (mg) (% w/w of fraction E3B)
E3BA	Brown solid	150.5 (43.00)
E3BB	Brown solid	147.4 (42.11)
E3BC	Brown solid	36.0 (10.28)

The fraction E3BB was showed a major component of fraction E3B. It was separated by diaion column chromatography with isocratic system of water and methanol as eluent to obtain six fractions (E3BB1-E3BB6). The isolation of fraction E3BB is shown in Table 4.62. Unfortunately, isolation of fraction E3BB did not succeed to obtain pure compound.

Table 4.62 Isolation of fraction E3BB

Fraction	Characteristic	Yield (mg) (%, w/w of fraction E3BB)
E3BB1	Brown solid	4.4 (2.98)
E3BB2	Brown solid	6.2 (4.20)
E3BB3	Brown solid	16.3 (11.04)
E3BB4	Brown solid	16.6 (11.24)
E3BB5	Brown solid	32.8 (22.21)
E3BB6	Brown solid	57.6 (39.00)

Compounds **I** and **II** were isolated from fraction E1 of ethyl acetate crude extract. Isolation of fractions E2 and E3 did not succeed to afford pure compound. The summary of isolation of ethyl acetate crude extract of stem barks of *M. kauki* is showed in Figure 27.

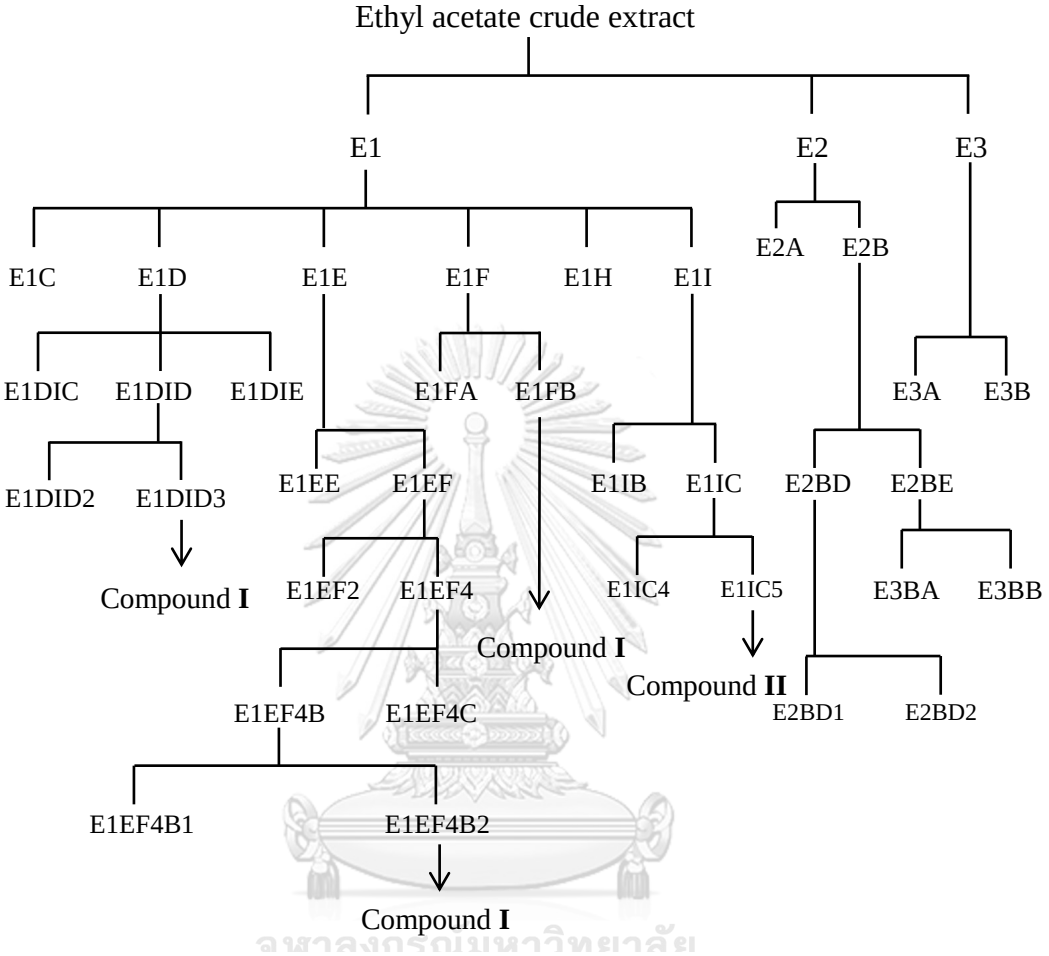

Figure 27 Summary of isolation of ethyl acetate crude extract of stem barks of *M. kauki*

4.8 Elucidation of isolated compounds of ethyl acetate crude extract of stem barks of *M. kauki*

4.8.1 Compound **I**

Compound **I** was obtained as white solid. It was isolated from ethyl acetate crude extract of stem barks of *M. kauki* (403.1 mg, 0.67 % w/w of ethyl acetate crude extract). The melting point was 272-274 °C. The actual melting point is nearly with the standard melting point of 278-280 °C [79]. The HR-ESI-MS spectrum of compound **I** (Figure 46) showed $[M+Na]^+$ at m/z 449.3603. A molecular formula of compound **I** was assigned as $C_{30}H_{50}O$ and calculated for $C_{30}H_{50}O$ as m/z 426.3849.

The ^{1}H (300 MHz) and ^{13}C NMR (75 MHz) data of compound **I** are shown in Table 4.63. The ^{1}H-NMR signals of eight methyl protons displayed at δ 0.93 ppm (s, H-23), 0.91 ppm (s, H-24), 0.98 ppm (s, H-25), 1.09 ppm (s, H-26), 0.82 ppm (s, H-27), 0.80 ppm (s, H-28), 0.95 ppm (s, H-29) and 0.91 ppm (s, H-30). The ^{1}H-NMR signals of one methylene proton displayed at δ 5.53 ppm (dd, J = 8.2, 3.2 Hz, H-14). The ^{1}H-NMR signals of four methine protons displayed at δ 3.19 ppm (m, H-3), 1.40 ppm (m, H-5), 1.41 ppm (m, H-9) and 1.44 ppm (m, H-18). The ^{1}H-NMR spectrum of compound **I** is shown in Figure 38.

The ^{13}C-NMR signals of eight methyl groups displayed at δ 27.8 ppm (C-23), 15.4 ppm (C-24), 15.4 ppm (C-25), 29.8 ppm (C-26), 25.9 ppm (C-27), 29.9 ppm (C-28), 33.3 ppm (C-29) and 21.3 ppm (C-30). The ^{13}C-NMR signal of one methylene group displayed at δ 158.1 ppm (C-14). The ^{13}C-NMR signal of one carbon attached to hydroxyl group at δ 79.1 ppm (C-3). The ^{13}C-NMR signal of six quaternary carbons displayed at δ 38.7 ppm (C-4), 39.0 ppm (C-8), 35.9 ppm (C-10), 37.5 ppm (C-13), 38.0 ppm (C-17) and 28.8 ppm (C-20). The ^{13}C-NMR spectrum of compound **I** is shown in Figure 39.

The HMBC spectrum is correlation between protons and carbons. The HMBC spectrum (Figure 43) showed correlation signals of H-3 (3.19)/C-1 (37.7), 2 (27.1) and C-4 (38.7), H-5 (1.40)/C-6 (18.8) and C-10 (35.9), H-7 (1.31, 0.98)/C-6 (18.8) and C-8 (39.0), H-9 (1.41)/C-10 (35.9) and C-11 (17.5), H-15 (1.63 , 1.22)/C-14 (158.1) and C-16 (36.5), H-18 (1.44)/C-13 (37.5) and C-19 (41.3), H-23 (0.98)/C-3 (79.1), C-4 (38.7) and C-5 (55.5), H-24 (15.4)/C-3 (79.1), C-4 (38.7) and C-5 (55.5), H-25 (0.93)/C-1 (37.7), C-5 (55.5) and C-10 (35.9), H-26 (29.8)/C-7 (35.1), C-8 (39.0) and C-9 (48.7), H-27 (25.9)/C-11 (17.5), C-12 (37.7) and C-13 (37.5), H-28 (0.80)/C-16 (36.5), C-17 (38.0) and C-22 (33.1), H-29 (33.33)/C-18 (49.2), C-19 (41.3) and C-20 (28.8), H-30 (0.91)/C-20 (28.8), C-21 (33.7) and C-22 (33.1). HMBC correlation of compound **I** is shown in Figure 28.

Compound **I** was identified as taraxerol by comparison of spectroscopic data with published literature [80]. The spectrums of DEPT90 (Figure 40), DEPT135 (Figure 41), HSQC (Figure 42), COSY (Figure 44) and NOESY (Figure 45) were confirmed the structure of compound **I**. The structure of compound **I** is shown in Figure 29.

Table 4.63 Comparison of ^{1}H- and ^{13}C-NMR of compound **I** and taraxerol

	Compound **I**			Taraxerol [80]	
Position	δ_H (multiplicity, J_{HH})	δ_C	HMBC correlations	δ_H	δ_C
1	1.62 (m), 1.57 (m)	37.7			38.0
2	1.68 (m), 1.40 (m)	27.1			27.1
3	3.19 (m)	79.1	C-1, 2, 4	3.20	79.1
4	-	38.7			39.0
5	1.40 (m)	55.5	C-6, 10		55.5
6	1.52 (m), 1.47 (m)	18.8			18.8
7	1.31 (m), 0.98 (m)	35.1	C-6, 8		35.1
8	-	39.0			38.8
9	1.41 (m)	48.7	C-10, 11		48.7
10	-	35.9			37.6
11	1.64 (m), 1.27 (m)	17.5			17.5
12	1.28 (m), 1.95 (m)	37.7			35.8
13	-	37.5			37.7
14	5.53 (dd, J = 8.2, 3.2 Hz)	158.1		5.52	158.1
15	1.63 (m), 1.22 (m)	116.9	C-14, 16		116.9
16	-	36.5			36.7
17	-	38.0			37.7
18	1.44 (m)	49.2	C-13, 19		49.3
19	2.03 (m), 1.33 (m)	41.3			41.3
20	-	28.8			28.8
21	1.55 (m), 1.46 (m)	33.7			33.7
22	1.51 (m), 1.43 (m)	33.1			33.1
23	0.98 (s)	28.0	C-3, 4, 5	0.92 (s)	28.0
24	0.82 (s)	15.4	C-3, 4, 5	0.90 (s)	15.4
25	0.93 (s)	15.4	C-1, 5, 10	0.97 (s)	15.4
26	1.09 (s)	29.8	C-7, 8, 9	1.08 (s)	29.8
27	0.91 (s)	25.9	C-11, 12, 13	0.82 (s)	25.9
28	0.80 (s)	29.9	C-16, 17, 22	0.80 (s)	29.9
29	0.95 (s)	33.3	C-18, 19, 20	0.94 (s)	33.3
30	0.91 (s)	21.35	C-20, 21, 22	0.90 (s)	21.3

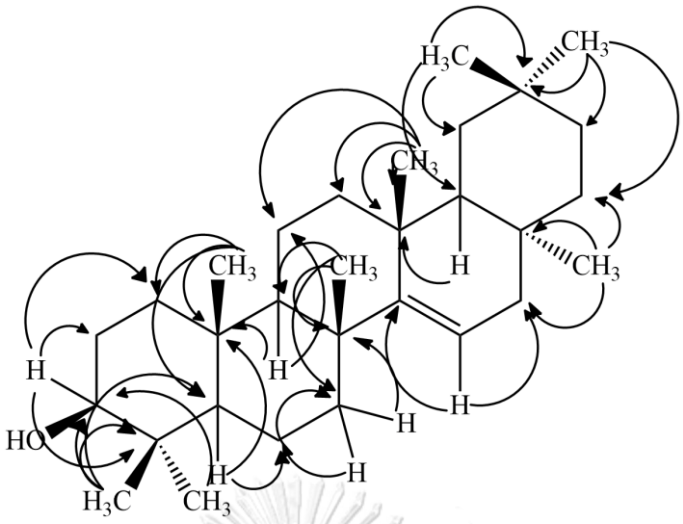

Figure 28 HMBC correlation of taraxerol (compound **I**)

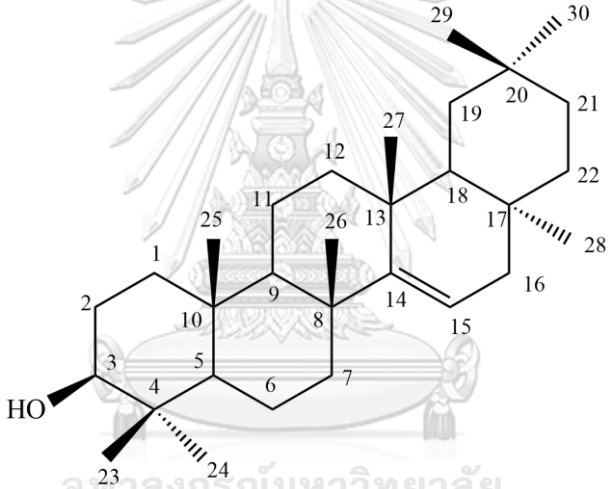

Figure 29 The structure of taraxerol (compound **I**)

In previous researches, taraxerol was isolated from various plants such as leaves crude extracts of *Jatropha tanjorensis* [79], *Rhizophora mangle* and *Rhizophora racemose* [81], roots crude extract of *Taraxacum officinale* [82], seed oils of *Catharanthus roseus, Nymphaea nelumbo, Casuarina equisetifolia, Acrocarpus fraxinifolius* [83] and barks of *Cupania dentate* [84]. Furthermore, taraxerol was isolated from Sapotaceae family such as seed oils of *M. hexandra*, leaves of *P. ramiflora* [45], barks of *M. elengi* which showed antibacterial activity [85]. Taraxerol has been reported to exhibit antibacterial [85], antigiardial [84], mulluscicidal [28] and antimicrobial activities [86].

4.8.2 Compound **II**

Compound **II** was obtained as yellow solid. It was isolated from ethyl acetate crude extract of stem bark of *M. kauki* (7.8 mg, 0.013% w/w of ethyl acetate crude

extract). The melting point was 184-186 °C. The actual melting point is nearly with the standard melting point of 221-223 °C [87]. The HR-ESI-MS spectrum of compound **II** (Figure 54) displayed $[M+Na]^+$ at m/z 311.214. A molecular formula of compound **II** was assigned as $C_{15}H_{12}O_6$ and calculated for $C_{15}H_{12}O_6$ as m/z 288.0630. ^{1}H-NMR and ^{13}C NMR data of compound **II** are shown in Table 4.64. The ^{1}H-NMR signals of four aromatic protons displayed at δ 7.42 ppm (d, J = 8.6 Hz, H-2' and H-6'), 6.89 ppm (d, J = 8.6 Hz, H-3' and H-5'), 5.99 ppm (d, J = 2.1 Hz, H-8) and 5.95 ppm (d, J = 2.1 Hz, H-6), respectively. The ^{1}H-NMR signals of two methine protons displayed at δ 5.08 ppm (d, J = 11.5 Hz, H-2) and 4.67 ppm (d, J = 11.5 Hz, H-3). The ^{1}H-NMR signals of hydroxyl group signal displayed at δ 11.71 ppm. The ^{1}H-NMR spectrum of compound **II** is shown in Figure 47.

The ^{13}C-NMR signals of one ketone group displayed at δ 198.81 ppm (C-4) and six methylene groups were displayed at δ 96.42, 97.47, 116.3, 116.3, 130.70 and 130.70 ppm (C-6, C-8, C-2', C-3', C-5' and C-6', respectively). The ^{13}C-NMR spectrum of compound **II** is shown in Figure 48.

The HMBC spectrum is correlation between protons and carbons. The HMBC spectrum (Figure 52) showed correlation signals of H-3 (4.67)/C-2 (84.8), C-3 (73.5) and C-4 (198.81), H-6 (5.95)/C-5 (165.4), C-6 (96.4) and C-7 (168.4), H-8 (5.99)/C-7 (168.4), C-8 (97.5) and C-9 (164.6), H-2' (7.42)/C-1' (129.5), C-3' (116.3), and C-6' (130.7), H-3' (6.89)/C-2' (130.7), C-4' (159.3) and C-5' (116.3), H-5' (6.89)/C-3' (116.3), C-4' (159.26) and C-6' (130.70) and H-6' (5.95)/C-1' (129.5), C-2' (130.7) and C-5' (116.3). The HMBC correlation of compound **II** is showed in Figure 30.

Compound **II** was identified by comparison of spectroscopic data with published literature [88]. The spectrums of DEPT90 (Figure 49), DEPT135 (Figure 50), HSQC (Figure 51) and COSY (Figure 53) were confirmed the structure of compound **II.** The structure of compound **II** is shown in Figure 31.

Table 4.64 Comparison of ^{1}H and ^{13}C NMR of compound **II** and dihydrokaempferol

	Compound **II**			Dihydrokaempferol [88]	
Position	δ_H (multiplicity, J_{HH})	δ_C	HMBC correlations	δ_H (multiplicity, J_{HH})	δ_C
1	-	-		-	-
2	5.08 (d, J = 11.5 Hz)	84.8		4.97 (d, J = 11.6 Hz)	85.00
3	4.67 (d, J = 11.5 Hz)	73.5	C-2, 4	4.54 (d, J = 11.6 Hz)	73.6
4	-	198.8		-	198.5
5	-	165.4		-	165.3
6	5.95 (d, J = 2.1 Hz)	96.4	C-5, 7	5,87 (d, J = 1.59 Hz)	97.3

Table 4.64 Comparison of ^{1}H- and ^{13}C-NMR of compound **II** and dihydrokaempferol

	Compound **II**			Dihydrokaempferol [88]	
Position	δ_H (multiplicity, J_{HH})	δ_C	HMBC correlations	δ_H (multiplicity, J_{HH})	δ_C
7		168.4			168.8
8	5.99 (d, J = 2.1 Hz)	97.5	C-7, 9	5.91 (d, J = 1.59 Hz)	96.3
9	-	164.6		-	164.6
10	-	101.9		-	101.9
1'	-	129.5		-	129.3
2'	7.42 (d, J = 8.6 Hz)	130.7	C-1', 3', 6'	7.35 (d, J = 8.56 Hz)	130.4
3'	6.89 (d, J = 8.6 Hz)	116.3	C-2', 4', 5'	6.82 (d, J = 8.56 Hz)	116.1
4'	-	159.3		-	159.2
5'	6.89 (d, J = 8.6 Hz)	116.3	C-3', 4', 6'	6.82 (d, J = 8.56 Hz)	116.1
6'	7.42 (d, J = 8.6 Hz)	130.7	C-1', 2', 5'	7.35 (d, J = 8.56 Hz)	130.3

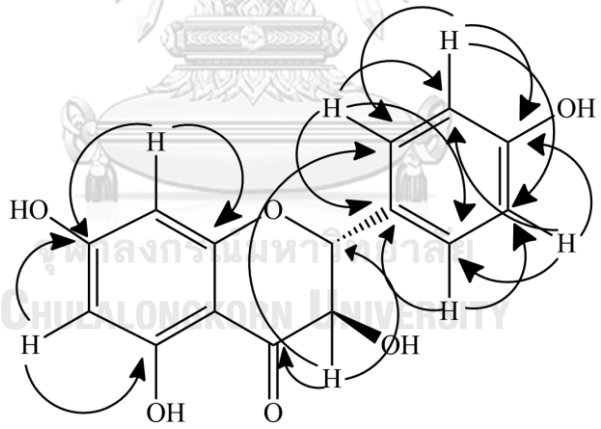

Figure 30 HMBC correlation of dihydrokaempferol (compound **II**)

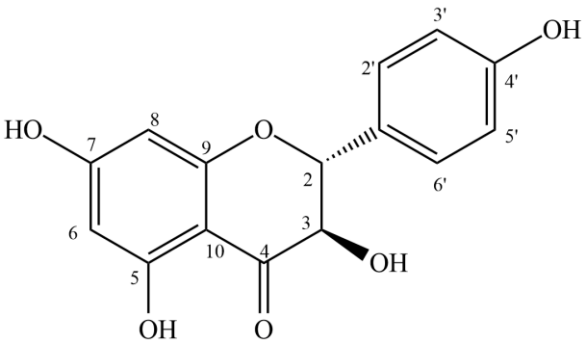

Figure 31 The structure of dihydrokaempferol (compound **II**)

In previous researches, dihydrokaempferol was isolated from various plants such as leaves of *C. sinensis* [89], fruits of *Maclura pomifera* [90], flowers of *Paeonia ostia* [88], aerial part of *Euphorbia cuneate* [87], fruits of *Citrus unshiu* [91], woods of *Annona ambotay* [92], knotwood of *Pinus banksiana* [93], roots of *Polygonum amplexicaule* [94] and branches of *Gracinia schomburgkiana* [95]. Dihydrokaenferol exhibited antioxidant (DPPH activity with IC_{50} = 34.2 ± 0.98 µg/mL) [88], antiulcerogenic [87], lipid peroxidation (IC_{50} = 5.4 nM) [93] and anti-HIV-1 [96] activities.

4.9 Tyrosinase inhibitory activity of isolated compounds

The compounds **I** and **II** were isolated from stem barks of *M. kauki.* They were tested on *in vitro* tyrosinase inhibitory activity. Compounds **I** and **II** were prepared for seven dilutions as 0.10, 0.25, 0.50, 1.00, 1.25, 1.50 and 2.00 mg/mL for calculation of IC_{50} value. Compound **I** exhibited moderate tyrosinase inhibitory activity with IC_{50} values of 0.99 ± 0.14 and 1.13 ± 0.28 mg/mL for *L*-tyrosine and *L*-DOPA, respectively. Calibration plots of compound **I** for *L*-tyrosine and *L*-DOPA are shown in Figures 32 and 33, respectively. Compound **II** exhibited strong tyrosinase inhibitory activity with IC_{50} values of 0.33 ± 0.14 and 0.05 ± 0.11 mg/mL for *L*-tyrosine and *L*-DOPA, respectively. Calibration plots of compound **II** for *L*-tyrosine and *L*-DOPA are shown in Figures 33 and 34, respectively. Kojic acid (IC_{50} value 8.17 ± 0.03 and 8.43 ± 0.05 µg/mL for *L*-tyrosine and *L*-DOPA, respectively) and *α*-arbutin (IC_{50} value 1.92 ± 0.09 and 1.73 ± 0.11 mg/mL for *L*-tyrosine and *L*-DOPA, respectively) were used as reference compounds. Tyrosinase inhibitory activity of isolated compounds of stem barks of *M. kauki* is shown in Table 4.65. Compounds **I** and **II** exhibited lower tyrosinase inhibitory activity than kojic acid. On the other hand, compounds **I** and **II** exhibited higher tyrosinase inhibitory activity than *α*-arbutin which was usually used in commercial whitening cosmetic.

Table 4.65 Tyrosinase inhibitory activity values of isolated compounds of stem barks of *M. kauki*

Compound	Characteristic	IC_{50} (mg/mL) (mM)	
		L-tyrosine	*L*-DOPA
Compound **I**	White solid	0.99 ± 0.14 (2.32 ± 0.06) *	1.13 ± 0.28 (2.65 ± 0.03) *
Compound **II**	Yellow solid	0.33 ± 0.14 (1.15 ± 0.06) *	0.50 ± 0.11 (1.74 ± 0.05) *
Kojic acid [a]		8.17 ± 0.03 (57.49 ± 0.02) **	8.43 ± 0.05 (59.32 ± 0.01) **
α-Arbutin [a]		1.92 ± 0.09 (7.05 ± 0.02) *	1.73 ± 0.11 (6.35 ± 0.01)

[a] Positive control

*IC_{50} value (mg/mL) (mM)

**IC_{50} value (μg/mL) (μM)

When comparison this results with previous studies, dihydrokaempferol which was isolated from twigs of *M. alba* [75], twigs of *Cudrania tricuspidata* [97], bark of *Peltophorum dasyrachis* [98] and barks of *M. zapota* [59] exhibited tyrosinase inhibitory activity with IC_{50} values of >200 μM (*L*-tyrosine as substrate), >100 μM (*L*-tyrosine as substrate), 126 ± 0.32 μM (*L*-DOPA as substrate) and 32.17 ± 0.32 and 31.60 ± 0.73 μM (*L*-tyrosine and *L*-DOPA as substrates, respectively), respectively. In addition, it was isolated from ethanol crude extract of vine stems of *Spatholobus suberectus* and showed tyrosinase inhibitory activity with percent inhibition of 15.18 ± 6.47% at concentration 100 μM using *L*-DOPA as a substrate. Taraxerol is widely distributed among several plants. It was isolated from barks of *M. zapota* that exhibited tyrosinase inhibitory activity with IC_{50} values of 103.37 ± 0.22 and 272.10 ± 0.16 μM for *L*-tyrosine and *L*-DOPA as substrates, respectively [59]. It is a triterpenoid compound. Triterpenoid compounds from various plants were reported as tyrosinase inhibitors. (22*R*)-Cycloart-20,25-dien-2*α*,3*β*,22*α*-triol; (22*R*)-cycloart-23-ene-3*β*,22*α*,25-triol; cycloart-23-ene-3*β*,25-diol; cycloart-20-ene-3*β*,25-diol, cycloart-25-ene-3*β*,(22*R*)22-diol; 3*β*,21,22,23-tetrahydroxy-cycloart-24,25(26)-diene and (23*R*)-5*α*-cycloart-24-ene-3*β*,21,23-triol were isolated from whole plant of *Amberboa ramose* and exhibited tyrosinase inhibitory activity with IC_{50} values of 7.92 ± 0.39, 15.94 ± 1.93, 8.32 ± 0.097, 12.09 ± 1.03, 22.21 ± 1.94, 1.32 ± 0.373 and 4.93 ± 0.197 μM, respectively. [99]. Moreover, erythrodiol, betulinic acid, maslinic acid, 2*α*,3*α*,23-trihydroxyolean-12-en-28-oic acid, bayogenin, arjunilic acid, methyl arjunolate, arjungenin and 3*β*,23,24-trihydroxyolean-12-en-28-oic acid were isolated from methanol crude extract of aerial parts of *Rhododendron collettianum* and showed tyrosinase inhibitory activity with IC_{50} values of 3.12 ± 0.25, 2.14 ± 0.37, 1.70 ± 0.34, 1.12 ± 0.13, 1.10 ± 0.10, 1.0 ± 0.37, 2.34 ± 0.41, 6.58 ± 0.85 and 11.02 ± 1.37 μM, respectively [100]. These compounds were evaluated for tyrosinase inhibitory activity

towards *L*-DOPA as the substrate. It was found that compounds **I** and **II** exhibited tyrosinase inhibitory activity lower than the previous studies. Because of difference in assay conditions may cause different reactivity of test sample to the enzyme reaction. The phosphate buffer (pH 6.8) was used in the reported studies; whereas, the phosphate buffer (pH 6.5) was utilized in this study. Furthermore, the incubation temperature in the reported studies was 25 °C. Whereas, incubation temperature in this study was 30 ± 2 °C.

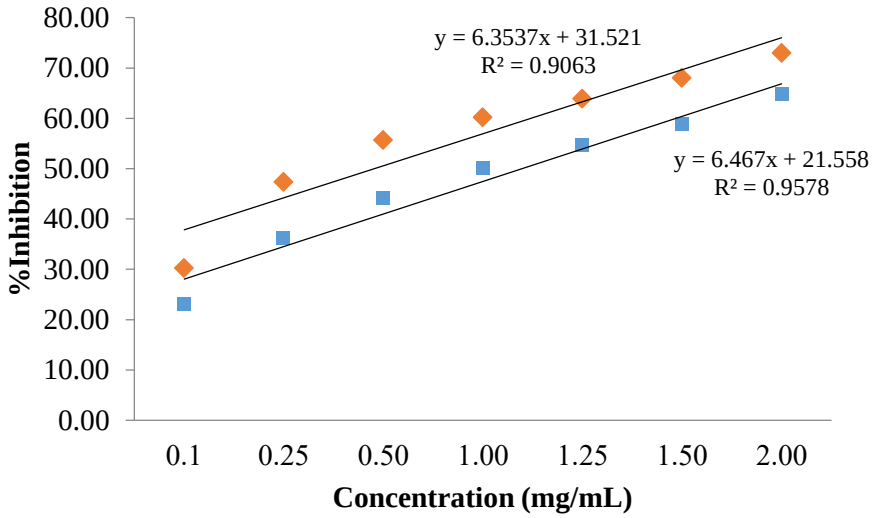

Figure 32 Calibration plots of tyrosinase inhibitory activity of compounds **I** and **II** using *L*-tyrosine as a substrate

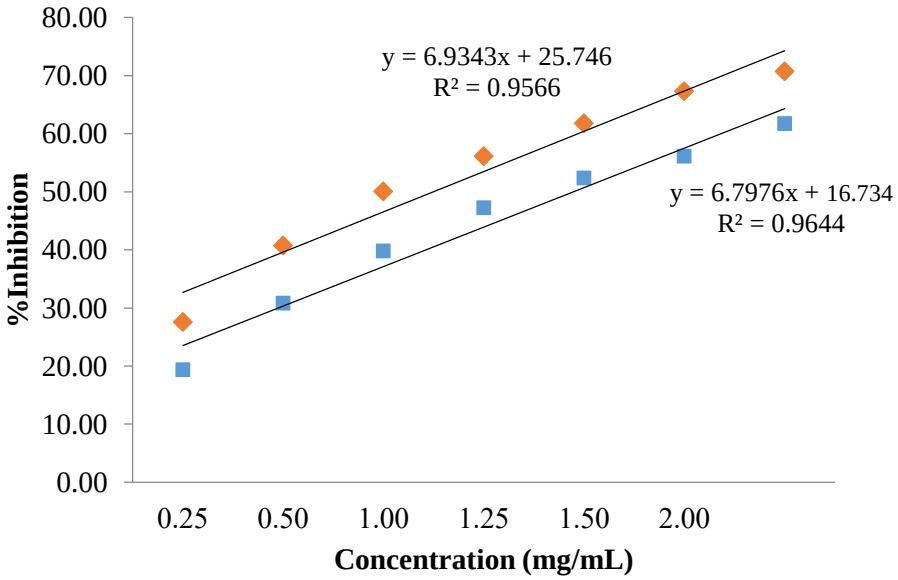

Figure 33 Calibration plots of tyrosinase inhibitory activity of compounds **I** and **II** using *L*-DOPA as a substrate

CHAPTER V
CONCLUSION

The methanol and aqueous crude extracts of fruits, leaves, seeds, stem barks and woods of *M. kauki* were evaluated for their total phenolic and flavonoid contents, antioxidant and tyrosinase inhibitory activities. Methanol crude extract of leaves exhibited the highest amount of total phenolic content (11.79 ± 0.04 mg GAE/g of dry weight) and followed by methanol crude extract of stem barks, aqueous crude extract of leaves, aqueous crude extract of stem barks, methanol crude extract of woods, aqueous and methanol crude extracts of fruits, aqueous crude extract of woods, aqueous and methanol crude extracts of seeds with total phenolic content values of 10.45 ± 0.03, 9.50 ± 0.08, 4.00 ± 0.02, 2.83 ± 0.01, 2.83 ± 0.01, 1.92 ± 0.02, 1.91 ± 0.03, 0.95 ± 0.02 and 0.79 ± 0.01 mg GAE/g of dry weight, respectively. Then, the crude extracts of different parts of *M. kauki* were evaluated for total flavonoid content. The highest total flavonoid content was obtained in methanol crude extract of leaves of with value of 89.84 ± 0.19 mg QE/g of dry weight and followed by aqueous crude extract of leaves, aqueous and methanol crude extracts of stem barks, aqueous and methanol crude extracts of fruits, aqueous crude extract of woods, aqueous and methanol crude extracts of seeds and methanol crude extract of woods which showed total flavonoid content values of 66.60 ± 0.22, 58.07 ± 0.32, 48.62 ± 0.21, 20.17 ± 0.16, 10.72 ± 0.08, 4.54 ± 0.21, 3.66 ± 0.14, 2.04 ± 0.07 and 0.46 ± 0.07 mg QE/g of dry weight, respectively. The antioxidant activities of different parts of *M. kauki* were investigated by DPPH radical scavenging and FRAP methods. The results of DPPH radical scavenging and FRAP activities were used trolox equivalent as standard regression curve. The highest DPPH radical scavenging activity was found in methanol crude extract of stem barks with value of 257.02 ± 0.26 mg TE/g of crude extract. Secondly, aqueous crude extract of leaves showed DPPH radical scavenging activity with value of 243.19 ± 1.24 mg TE/g of crude extract and followed by aqueous crude extract of stem barks, methanol crude extract of leaves, methanol and aqueous crude extracts of woods, methanol crude extracts of fruits and seeds, aqueous crude extracts of fruits and seeds which exhibited DPPH radical scavenging activity with values of 219.19 ± 0.13, 208.60 ± 0.98, 194.38 ± 0.70, 66.04 ± 0.57, 45.28 ± 0.51, 16.08 ± 0.31, 13.01 ± 0.51 and 10.32 ± 0.38 mg TE/g of crude extract, respectively. From the results of FRAP activity, aqueous crude extract of leaves showed the highest FRAP activity with value of 219.56 ± 0.89 mg TE/g of crude extract and followed by methanol crude extract of leaves, methanol and aqueous crude extracts of stem barks, methanol and aqueous crude extracts of woods, methanol crude extract of seeds and fruits and aqueous crude extracts fruits and seeds which exhibited FRAP activity with values of 210.94 ± 1.37, 210.94 ± 0.89, 107.89 ± 0.79, 72.61 ± 0.98, 42.06 ± 0.98, 15.93 ± 0.98, 11.78 ± 0.96, 5.11 ± 0.79 and 4.56 ±

0.81 mg TE/g of crude extract, respectively. The methanol and aqueous crude extracts of fruits, leaves, seeds, stem barks and woods of *M. kauki* were evaluated on tyrosinase inhibitory activity. Tyrosinase inhibitory activity was determined using *L*-tyrosine as a substrate. Methanol crude extract of stem barks exhibited the highest tyrosinase inhibitory activity with IC_{50} value 0.26 ± 0.05 mg/mL and followed by methanol crude extract of leaves, aqueous crude extract of stem barks and leaves, aqueous and methanol crude extracts of fruits, methanol and aqueous crude extract seeds which showed tyrosinase inhibitory activity with IC_{50} values of 0.32 ± 0.08, 0.41 ± 0.11, 0.49 ± 0.12, 0.49 ± 0.11, 0.75 ± 0.14, 3.86 ± 0.12 and 3.88 ± 0.11 mg/mL, respectively. Whereas, methanol and aqueous crude extracts of woods of *M. kauki* showed no activity. These results indicated that stem barks and leaves of *M. kauki* contained high amount of phenolic compounds and flavonoids and expressed strong DPPH radical scavenging, FRAP and tyrosinase inhibitory activities. These results suggested that the crude extracts of stem barks and leaves can be sources of antioxidant and tyrosinase inhibitors. This study further investigated the tyrosinase inhibitors from stem barks of *M. kauki.*

The stem barks of *M. kauki* were extracted by maceration method with *n*-hexane, ethyl acetate, methanol and water, respectively. All crude extracts were tested on total phenolic and flavonoid contents, antioxidant and tyrosinase inhibitory activities. Methanol crude extract exhibited the highest total phenolic content with value of 160.12 ± 0.27 mg GAE/g of crude extract and followed by ethyl acetate, aqueous and *n*-hexane crude extracts with values of 111.46 ± 0.38, 66.17 ± 0.26 and 10.98 ± 0.14 mg GAE/g of crude extract, respectively. The highest total flavonoid content was found in ethyl acetate crude extract with value of 755.33 ± 1.53 mg QE/g of crude extract and followed by methanol, aqueous and *n*-hexane crude extracts with values of 527.33 ± 1.00, 516.67 ± 1.73 and 283.67 ± 1.52 mg QE/g of crude extract, respectively. Ethyl acetate crude extract showed the highest DPPH radical scavenging activity with value of 249.33 ± 0.25 mg TE/g of crude extract and followed by methanol, aqueous and *n*-hexane crude extracts with values of 241.26 ± 0.32, 39.52 ± 0.25 and 11.85 ± 0.67 mg TE/g of crude extract, respectively. The highest FRAP activity was obtained in methanol crude extract with value of 221.50 ± 0.78 mg TE/g of crude extract and followed by ethyl acetate, aqueous and *n*-hexane crude extracts with values of 179.28 ± 0.59, 50.94 ± 0.20 and 10.39 ± 0.59 mg TE/g of crude extract, respectively. All crude extracts were also tested on tyrosinase inhibitory activity. The ethyl acetate crude extract exhibited the highest tyrosinase inhibitory activity with IC_{50} values of 0.24 ± 0.02 and 0.28 ± 0.04 for *L*-tyrosine and *L*-DOPA, respectively and followed by methanol crude extract (IC_{50} values of 1.66 ± 0.07 and 1.25 ± 0.05 mg/mL for *L*-tyrosine and *L*-DOPA, respectively), aqueous crude extract (IC_{50} values of 1.89 ± 0.09 and 1.58 ± 0.11 mg/mL for *L*-tyrosine and *L*-DOPA, respectively) and *n*-hexane crude extract (IC_{50} values of 9.58 ± 0.17 and 9.23 ± 0.28 mg/mL for *L*-tyrosine and *L*-DOPA, respectively). Hence, ethyl acetate crude extract of stem barks

of *M. kauki* exhibited high amount of phenolic compounds and flavonoids and strong antioxidant activity along with tyrosinase inhibitory activity.

Ethyl acetate crude extract of stem barks of *M. kauki* was isolated by activity guided-fractionation. Compounds **I** and **II** were isolated from ethyl acetate crude extract of stem barks. Compound **I** was elucidated as taraxerol ($C_{30}H_{50}O$) which exhibited tyrosinase inhibitory activity with IC_{50} values of 2.32 ± 0.06 and 2.65 ± 0.03 mM for *L*-tyrosine and *L*-DOPA, respectively. Compound **II** was elucidated as dihydrokaempferol ($C_{15}H_{12}O_6$) which showed tyrosinase inhibitory activity with IC_{50} values of 1.15 ± 0.06 and 1.74 ± 0.05 mM for *L*-tyrosine and *L*-DOPA, respectively. Compounds **I** and **II** exhibited lower tyrosinase inhibitory activity than kojic acid (IC_{50} vales of 57.49 ± 0.02 and 59.32 ± 0.01 µM for *L*-tyrosine and *L*- DOPA as substrates, respectively) but they exhibited higher tyrosinase inhibitory activity than α-arbutin (IC_{50} vales of 7.05 ± 0.02 and 6.35 ± 0.01 mM for *L*-tyrosine and *L*- DOPA as substrates, respectively). These results suggested that stem barks of *M. kauki* should be further investigated to purify tyrosinase inhibitors, especially ethyl acetate crude extract of stem barks. It should be further investigated for others biological activities including anti-allergic, cytotoxicity and *in vitro* tyrosinase inhibitory activities to evaluate it before using as a potential ingredient in whitening cosmetic.

REFERENCES

[1] Rees, J.L. The genetics of human pigmentary disorders. Journal of Invesigative Dermatology 131(3) (2011): E12-E13.

[2] Marmol, V., and Beermann, F. Tyrosinase and related proteins in mammalian pigmentation. Ferderation of European Biochemical Societies 318(3) (1996): 165-168.

[3] Isabelle, M., Lee, B.L., Lim, M.T., Koh, W.P., Huang, D., and Ong, C.N. Antioxidant activity and profiles of common fruits in Singapore. Food Chemistry 123(1) (2010): 77-84.

[4] Fernandes, C.P., Correa, A.L., Lobo, J.F.R., Caramel, O.P., Almeida, F.B., Castro, E.S., Souza, K.F.C.S., Burth, P., Amorim, L.M.F., Santos, M.G., Ferreira, J.L.P., Falcão, D.Q., Carvalho, J.C.T., and Rocha, L. Triterpene esters and biological activities from edible fruits of *Manilkara subsericea* (Mart.) Dubard, Sapotaceae. BioMed Research International 2013(1) (2013): 1-7.

[5] Rhourri-Frih, B., Renimel, I., Chaimbault, P., André, P., Herbette, G., and Lafosse, M. Pentacyclic triterpenes from *Manilkara bidentata* resin. isolation, identification and biological properties. Fitoterapia 88(1) (2013): 101-108.

[6] Baky, M.H., Kamal, A.M., Elgindi, M.R., and Haggag, E.G. A review on phenolic compounds from family sapotaceae. Journal of Pharmacognosy and Phytochemistry 5(2) (2016): 280-287.

[7] Chantaranothai, P. Sapotaceae. in Santisuk, T. and Balslev, H. (eds.), Flora of Thailand, pp. 625-629. Bangkok: Department of National Parks, Wildlife and Plant Conservative, 2014.

[8] Fenske, N.A., and Lober, C.W. Structural and functional changes of normal aging skin. Journal of the American Academy of Dermatology 15(4) (1986): 571-585.

[9] Toledo, A.V., Franco, M.E.E., Lopez, S.M.Y., Troncozo, M.I., Saparrat, M.C.N., and Balatti, P.A. Melanins in fungi: types, localization and putative biological roles. Physiological and Molecular Plant Pathology 99(1) (2017): 2-6.

[10] Clausa, H., and Deckerb, H. Bacterial tyrosinases. Systematic and Applied Microbiology 29(1) (2006): 3-14.

[11] Ito, S. and Wakamatsu, K. Quantitative analysis of eumelanin and pheomelanin in humans, mice, and other animals: a comparative review. Pigment Cell Research 16(5) (2003): 523-531.

[12] Hearing, V.J., and Jimenez, M. Mammalian tyrosinase -the critical regulatory control point in melanocyte pigmentation. International Journal of Biochemistry 19(12) (1987): 1141-1147.

[13] Hearing, V.J. Determination of melanin synthetic pathways. Journal of Investigative Dermatology 131(3) (2011): E8-E11.

[14] Jimbow, K., Alena, F., Dixon, W., and Hara, H. Regulatory factors of pheomelanogenesis and eumelanogenesis in melanogenic compartment. Pigment Cell Research 3(S2) (1992): 36-42.

[15] Benefits plant for health. *Manilkara kauki* a good fruit to traditional healing [Online]. 2017. Available from: https://benefitsplantforhealth.blogspot.com/2017/01/manilkara-kauki-sawo-kecik-benefits-for-health-Habitat-and-Distribution-Classification-traits-a-good-fruit-to-traditional-healing.html [2017, December 12]

[16] Khare, C.P. *Manilkara kauki*. In Khare, C.P. Indian medicinal plants, pp. 397-398. Heidelberg: Springer, 2007.

[17] Chopra, R.N., Nayara, S.L., and Chopra, I.C. Glossary of Indian medicinal plants. New Delhi: Council of Scientific & Industrial Research, 1956.

[18] Dejadisai, S., Meechai, I., Puripattanavong, J., and Kummee, S. Antityrosinase and antimicrobial activities from Thai medicinal plants. Archives of Phamacal Research 37(4) (2014): 473–483.

[19] Tengamnuay, P., Pengrungruangwong, K., Pheansri, I., and Likhitwitayawuid, K. *Artocarpus lakoocha* heartwood extract as a novel cosmetic ingredient: evaluation of the *in vitro* anti-tyrosinase and *in vivo* skin whitening activities. International Journal of Cosmetic Science 28(4) (2006): 269-276.

[20] Homklob, J., Winitchai, S., Rimkeeree, H., and Luangprasert, N. Free radical scavenging, tyrosinase inhibition activity and total phenolics content of ethyl acetate extracts from Indian gooseberry (*Phyllanthus emblica* L.) in Thailand. In Proceedings of the 48th Kasetsart University Annual Conference, Kasetsart, 3-5 March, 2010. Subject: Agro-Industry, pp. 91-99. Bangkok, 2010.

[21] Malik, W., Ahmed, D., and Izhar, S. Tyrosinase inhibitory activities of *Carissa opaca* Stapf ex Haines roots extracts and their phytochemical analysis. Pharmacognosy Magazine 13(51) (2017): S544-S548.

[22] Krishnappa, K., and Elumalai, K. Mosquitocidal activity of indigenenous plants of Western Ghats, *Achras sapota* Linn. (Sapotaceae) and *Cassia auriculata* L. (Fabaceae) against a common malarial vector, *Anopheles stephensi* Liston (Culicidae: Diptera). Journal of Coastal Life Medicine 2(5) (2014): 402-410.

[23] Adebayo, A.H., Abolaji, A.O., Kela, R., Ayepola, O.O., Olorunfemi, T.B., and Taiwo, O.S. Antioxidant activities of the leves of *Chrysophyllum albidun* G. Pakistan Journal of Pharmaceutical Sciences 24(4) (2011): 545-551.

[24] Purnima, S., and Swarnalatha. *In vitro* antimicrobial activity of *Madhuca Longifolia* leaf extract. The International Journal of Engineering and Science 7(4) (2018): 9-12.

[25] Sharma, S., Sharmaa, M.C., and Kohlib, D.V. Wound healing activity and formulation of ether-benzene-95% ethanol extract of herbal drug *Madhuca longifolia* leaves in Albino rats. Journal of Optoelectronics and Biomedical Materials 1(1) (2010): 13-15.

[26] Patel, K., Ali, A.K., Nair, N., and Kothari, V. *In vitro* antibacterial activity of *Manilkara hexandra* (Sapotaceae) seed extracts and violacein against multidrug resistant *Streptococcus mutans.* Journal of Natural Remedies 15(1) (2015): 1-11.

[27] Rodrigues, K., Ramos, D.F., Carrion, L.L., Cursino, L.M.C., Jefreys, M.F., Pedroza, L.S., Osório, M.I.C., Oliveira, J.L., Andrade, J.I.A., Fernandes, C.C., Nunez, C.V., and Silva, P.E.A. Antifungal activity of Brazilian amazon plantas extracts against some species of *Candida* spp. International Journal of Phytopharmacology 5(6) (2014): 445-453.

[28] Fariaa, R.X., Rochab, L.M., Eloísa Portugal Barros Silva Soares Souzab, Almeidac, F.B., Fernandesc, C.P., and Santosd, J.A.A. Molluscicidal activity of *Manilkara subsericea* (Mart.) dubard on *Biomphalaria glabrata* (Say, 1818). Acta Tropica 178(1) (2018): 163-168.

[29] Sumithra, P., Shoba, F.G., Vimala, G., Sathya, J., Sankar, V., Saraswathi, R., and Jayapriya, G. Anti-cancer activity of *Annona squamosa* and *Manilkara zapota* flower extract against MCF-7 cell line. Der Pharmacia Sinica 5(6) (2014): 98-104.

[30] Islam, M.R., Parvin, M.S., Islam, M.S., Hasan, S.M.R., and Islam, M.E. Antioxidant activity of the ethanol extract of *Manilkara zapota* leaf. Journal of Scientific Research 4(1) (2012): 193-202.

[31] Mewara, D., Tamakuwala, H., and Desai, B. Antifungal activity and phytochemical screening from leaf extract of *Manilkara zapota* and *Averrhoa carambola.* International Journal of Ethnobiology & Ethnomedicine 3(1) (2017): 1-9.

[32] Nair, R., and Sumitra, C. Antimicrobial activity of *Terminalia catappa, Manilkara zapota* and *Piper betel* leaf extract. Indian Journal of Pharmaceutical Science 70(3) (2008): 390-393.

[33] Fomani, M., Nouga, A.B., Toze, F.A.A., Ndom, J.C., Waffo, A.F.K., and Wansi, J.D. Bioactive phenylethanoids from the seeds of *Manilkara zapota.* British Journal of Pharmaceutical Research 8(5) (2015): 1-5.

[34] Krishna, P.S., Babu, P.S., and Karthikeyan, R. Anti-inflammatory activity of ethanolic extract of flowers *Manilkara zapota* L. by HRBC membrane stabilization method. Journal of Pharmaceutical Sciences 6(1) (2017): 19-21.

[35] Sathishkumar, T., Anitha, S., Sharon, R.E., Santhi, V., Sukanya, M., Kumaraesan, K., and Rapheal, V.S. Evaluation of *in vitro* invertase inhibitory activity of *Manilkara zapota* seeds - a novel strategy to manage diabetes mellitus. Journal of Food Biochemistry 39(5) (2015): 517-527.

[36] Mistry, K.S., Sanghvi, Z., Parmar, G., and Shah, S. The antimicrobial activity of *Azadirachta indica, Mimusops elengi, Tinospora cardifolia, Ocimum sanctum* and 2% chlorhexidine gluconate on common endodontic pathogens: An *in vitro* study. European Journal of Dentistry 8(2) (2014): 172-177.

[37] Koti, B.C., and Ashok, P. Diuretic activity of extracts of *Mimusops elengi* Linn. bark. International Journal of Green Pharmacy 4(2) (2010): 90-92.

[38] Reddy, L.J., and Jose, B. Evaluation of antibacterial activity of *Mimusops elengi* L. flowers and *Thichosanthes cucumerina* L. fruits from South India. International Journal of Pharmacy and Pharmaceutical Sciences 5(3) (2013): 362-364.

[39] Suedee, A., Tewtrakul, S., and Panichayupakaranant, P. Anti-HIV-1 integrase activity of *Mimusops elengi* leaf extracts. Pharmaceutical Biology 52(1) (2013): 58-61.

[40] Bardhan, A., Mukhopadhyay, R., Bhattacharya, S., and Biswas, M. *In vitro* free radical scavenging activity of leaf extracts from *Mimusops elengi.* Journal of Advanced Pharmacy Education & Research 4(4) (2014): 426-429.

[41] Zahid, H., Rizwani, G.H., Kamil, A., Shareef, H., Tasleem, S., and Khan, A. Anti-urease activity of *Mimusops elengi* Linn (Sapotaceae). European Journal of Medicinal Plants 6(4) (2015): 223-230.

[42] Shahwar, D., and Raza, M.A. *In vitro* antibacterial activity of extracts of *Mimusops elengi* against gram positive and gram negative bacteria. African Journal of Microbiology Research 3(3) (2009): 458-462.

[43] Rahman, U., Rahman, T.U., Zeb, M.A., Khattak, K.F., Qaisar, M., and Ullah, S. Phytochemical screening, antibacterial and antioxidant activity of *Monoteheca buxifolia* stem. International Journal of Biosciences 11(1) (2017): 198-203.

[44] Manosroi, A., Saraphanchotiwitthaya, A., and Manosroi, J. Effects of *Pouteria cambodiana* extracts on *in vitro* immunomodulatory activity of mouse immune system. Fitoterapia 77(3) (2006): 189-193.

[45] Rodrigues, P.M., Gomes, J.V.D., Jamal, C.M., Neto, A.C., Santos, M.L., Fagg, C.W., Fonseca-Bazzo, Y.M., Magalhaes, P.O., Sales, P.M., and Silveira, P. Triterpenes from *Pouteria ramiflora* (Mart.) Radlk. leaves (Sapotaceae). Food and Chemical Toxicology 109(2) (2017): 1063-1068.

[46] Yahia, E.M., Orozco, F.G., and Leon, C.A. Phytochemical and antioxidant characterization of mamey (*Pouteria sapot*a Jacq. H.E. Moore & Stearn) fruit. Food Research International 44(1) (2011): 2175–2181.

[47] Dua, L., Shen, Y., Zhang, X., Prinyawiwatkul, W., and Xu, Z. Antioxidant-rich phytochemicals in miracle berry (*Synsepalum dulcificum*) and antioxidant activity of its extracts. Food Chemistry 153(1) (2014): 279-284.

[48] Momtaza, S., Mapunyaa, B.M., Houghtonb, P.J., Edgerlyb, C., Husseina, A., Naidooc, S., and Lalla, N. Tyrosinase inhibition by extracts and constituents of

Sideroxylon inerme L. stem bark, used in South Africa for skin lightening. Journal of Ethnopharmacology 119(3) (2008): 507-512.

[49] Kuete, V., Tangmouob, J.G., Benga, V.P., Ngounoub, F.N., and Lontsi, D. Antimicrobial activity of the methanolic extract from the stem bark of *Tridesmostemon omphalocarpoides* (Sapotaceae). Journal of Ethnopharmacology 104(1-2) (2006): 5-11.

[50] Einbond, L.S., Reynertson, K.A., Luo, X.D., Basile, M.J., and Kennelly, E.J. Anthocyanin antioxidants from edible fruits. Food Chemistry 28(1) (2005): 23-28.

[51] Misra, G., and Mitra, C.R. *Mimusops hexandra*-ll. Constituents of bark and seed. Phytochemistry 5(3) (1966): 535-538.

[52] Misra, G., and Mitra, C.R. *Mimusops manilkara*, contituents of fruit and seed. Phytochemistry 8(1) (1969): 249-252.

[53] França, C.V., Perfeito, J.P.S., Resck, I.S., Gomes, S.M., Fagg, C.W., Castro, C.F.S., Simeoni, L.A., and Silveira, D. Potential radical-scavenging activity of *Pouteria caimito* leaves extracts. Journal of Applied Pharmaceutical Science 6(7) (2016): 184-188.

[54] Sotes, G.J., Urzu, A., and Sebastia, B. Chemistry of *Pouteria splendens* and its ecological situation. Biochemical Systematics and Ecology 34(4) (2006): 338-340.

[55] Perfeito, J.P., Santos, M.L., López, K.S.E., Paula, J.E., and Silveira, D. Characterization and biological properties of *Pouteria torta* extracts: a preliminary study. Revista Brasileira de Farmacognosia Brazilian Journal of Pharmacognosy 15(3) (2005): 183-186.

[56] Costa, D.L.M.G., Rinaldo, D., Varanda, E.A., Sousa, J.F., Nasser, A.L.M., Silva, A.C.Z., Baldoqui, D.C., Vilegas, W., and Santos, L.C. Flavonoid detection in hydroethanolic extract of *Pouteria torta* (Sapotaceae) leaves by HPLC-DAD and the determination of its mutagenic activity. Journal of Medicainal Food 17(10) (2014): 1103-1112.

[57] Zhang, J., Kurita, M., Shinozaki, T., Ukiya, M., Yasukawa, K., Shimizu, N., Tokuda, H., Masters, E.T., Akihisa, M., and Akihisa, T. Triterpene glycosides and other polar constituents of shea (*Vitellaria paradoxa*) kernels and their bioactivities. Phytochemistry 108(1) (2014): 157-170.

[58] Rao, G.V., Sahoo, M.R., Madhavi, M.S.L., and Mukhopadhyay, T. Phytoconstituents from the leaves and seeds of *Manilkara zapota* Linn. Der Pharmacia Lettre 6(2) (2014): 69-73.

[59] Chunhakant, S. Tyrosinase inhibitors from sapodilla plum *Manilkara zapota* L. Doctoral dissertation, Program in Biotechnology, Graduate School, Chulalongkorn University, 2017.

[60] Wang, H.M., Chou, Y.T., Hong, Z.L., Chen, H.A., Chang, Y.C., Yang, W.L., Chang, H.C., Mai, C.T., and Chen, C.Y. Bioconstituents from stems of

Synsepalum dulcificum Daniell (Sapotaceae) inhibit human melanoma proliferation, reduce mushroom tyrosinase activity and have antioxidant properties. Journal of the Taiwan Institute of Chemical Engineers 42(2) (2011): 204-211.

[61] Ainsworth, E.A., and Gillespie, K.M. Estimation of total phenolic content and other oxidation substrates in plant tissues using Folin–Ciocalteu reagent. Nature Protocols 2(4) (2007): 875-877.

[62] Tohidi, B., Rahimmalek, M., and Arzani, A. Essential oil composition, total phenolic, flavonoid contents, and antioxidant activity of *Thymus* species collected from different regions of Iran. Food Chemistry 220 (2017): 153-161.

[63] Thaiponga, K., Boonprakoba, U., Crosbyb, K., Zevallosc, L.C., and Byrnec, D.H. Comparison of ABTS, DPPH, FRAP, and ORAC assays for estimating antioxidant activity from guava fruit extracts. Journal of Food Composition and Analysis 19(1) (2006): 669–675.

[64] Benzie, I.F.F., and Strain, J.J. The ferric reducing ability of plasma (FRAP) as a measure of ‘‘Antioxidant Power’’: The FRAP assay. Analytical Biochemistry 239(1) (1996): 70-76.

[65] Ishihara, A., Ide, Y., Bito, T., Ube, N., Endo, N., Sotome, K., Maekawa, N., Ueno, K., and Nakagiri, A. Novel tyrosinase inhibitors from liquid culture of *Neolentinus lepideus.* Bioscience, Biotechnology and Biochemistry 82(1) (2018): 22-30.

[66] Mathur, R., and Vijayvergia, R. Determination of total flavonoid and phenol content in *Mimosops elengi* Linn. International Journal of Pharmaceutical Sciences and Research 8(12) (2017): 5282-5285.

[67] Dakiche, H., Khali, M., Abu-el-Haija, A.K., Al-Maaytah, A., and Al-Balas, Q.A. Biological activities and phenolic contents of *Argania spinosa* L. (Sapotaceae) leaf extract. Tropical Journal of Pharmaceutical Research 15(12) (2016): 2563-2570.

[68] Kothari, V., Pathan, S., and Seshadri, S. Antioxidant activity, free radical scavenging activity, phenol and flavonoid contents of *Manilkara zapota* and *Citrus limon* seeds. Journal of Natural Remedies 10(1) (2010): 175-180.

[69] Uysal, S., Ugurlu, A., Zengin, G., Baloglu, M.C., Altunoglu, Y.C., Mollica, A., Custodio, L., Neng, N.R., Nogueira, J.M.F., and Mahomoodally, M.F. Novel *in vitro* and *in silico* insights of the multi-biological activities and chemical composition of *Bidens tripartita* L. Food and Chemical Toxicology 111(1) (2018): 525-536.

[70] Saltos, M.B.V., Puente, B.F.N., Milella, L., Tommasi, N.D., Piaz, F.D., and Braca, A. Antioxidant and free radical savenging activity of phenolics from *Bidens humilis.* Planta Medica Journal 81(12-13) (2015): 1-9.

[71] Sulaiman, S.F., Yusoff, N.A.M., Eldeen, I.M., Seow, E.M., Sajak, A.A.B., Supriatno, and Ooi, K.L. Correlation between total phenolic and mineral

contents with antioxidant activity of eight Malaysian bananas (*Musa* sp.). Journal of Food Composition and Analysis 24(1) (2011): 1-10.

[72] Chen, C.H., Chan, H.C., Chu, Y.T., Ho, H.Y., Chen, P.Y., Lee, T.H., and Lee, C.K. Antioxidant activity of some plant extracts towards xanthine oxidase, lipoxygenase and tyrosinase. Molecules 14(8) (2009): 2947-2958.

[73] Chompoo, J., Upadhyay, A., Gima, S., Fukuta, M., and Tawata, S. Antiatherogenic properties of acetone extract of *Alpinia zerumbet* seeds. Molecules 17(6) (2012): 6237-6248.

[74] Chaita, E., Lambrinidis, G., Cheimonidi, C., Agalou, A., Beis, D., Trougakos, I., Mikros, E., Skaltsounis, A.L., and Aligiannis, N. Anti-melanogenic properties of Greek plants. A novel depigmenting agent from *Morus alba* wood. Molecules 22(4) (2017).

[75] Zhang, L., Tao, G., Chen, J., and Zheng, Z.P. Characterization of a new flavone and tyrosinase inhibition constituents from the twigs of *Morus alba* L. Molecules 21(9) (2016): 1-9.

[76] Quispe, Y.N.G., Hwang, S.H., Wang, Z., and Lim, S.S. Screening of peruvian medicinal plants for tyrosinase inhibitory properties: Identification of tyrosinase inhibitors in *Hypericum laricifolium* Juss. Molecules 22(402) (2017): 1-15.

[77] Sarkhail, P., Sarkheil, P., Khalighi-Sigaroodi, F., Shafiee, A., and Ostad, N. Tyrosinase inhibitor and radical scavenger fractions and isolated compounds from aerial parts of *Peucedanum knappii* Bornm. Natural Product Research 27(10) (2013): 896-899.

[78] Chang, T.S. An updated review of tyrosinase inhibitors. International Journal of Molecular Sciences 10(6) (2009): 2440-2475.

[79] Oladoye, S.O., Ayodele, E.T., Abdul-Hammed, M., and Idowu, O.T. Characterisation and identification of taraxerol and taraxer-14-en-3-one from *Jatropha tanjorensis* (Ellis and Saroja) leaves. Pakistan Journal of Science and Industrial Research 58(1) (2015): 46-50.

[80] Ebajo, V.D., Brkljača, R., Urban, S., and Ragasa, C.Y. Chemical constituents of *Hoya buotii* Kloppenb. Journal of Applied Pharmaceutical Science 5(11) (2015): 69-72.

[81] Versteegh, G.J.M., Schefub, E., Dupont, L., Marret, F., and Jansen, J.H.F. Taraxerol and *Rhizophora* pollen as proxies for tracking past mangrove ecosystems. Geochimica et Cosmochimica Acta 68(3) (2004): 411-422.

[82] Sharma, K., and Zafar, R. Simultaneous estimation of taraxerol and taraxasterol in root callus cultures of *Taraxacum officinale* weber. International Journal of Pharmacognosy and Phytochemical Research 6(3) (2014): 540-546.

[83] Saeed, M.T., Agarwal, R., Khan, M.W.Y., Ahmad, F., Osman, S.M., Akihisa, T., Suzuki, K., and Matsumoto, T. Unsaponifiable lipid constituents of ten

Indian seed oils. Journal of the American Oil Chemists Society 68(3) (1991): 193-197.

[84] Hernández-Chávez, I., Torres-Tapia, L.W., Simá-Polanco, P., Cedillo-Rivera, R., Moo-Puc, R., and Peraza-Sánchez, S.R. Antigiardial activity of *Cupania dentata* bark and its constituents. Journal of the Mexican Chemical Society 56(2) (2012): 105-108.

[85] Amir, F., Wong, K.C., Eldeen, I., Asmawi, M.Z., and Osman, H. Evaluation of biological activities of extracts and chemical constituents of *Mimusops elengi.* Tropical Journal of Pharmaceutical Research 12(4) (2013): 591-596.

[86] Mokoka, T.A., McGaw, L.J., Mdee, L.K., Bagla, V.P., Iwalewa, E.O., and Eloff, J.N. Antimicrobial activity and cytotoxicity of triterpenes isolated from leaves of *Maytenus undata* (Celastraceae). BMC Complementary and Alternative Medicine 13(111) (2013): 1-9.

[87] Awaad, A.S., Al-Jaber, N.A., Moses, J.E., El-Meligy, R.M., and Zain, M.E. Antiulcerogenic activities of the extracts and isolated flavonoids of *Euphorbia cuneata* Vahl. Phytotherapy Research 27(1) (2013): 126-130.

[88] Zhang, H., Li, X., Wu, K., Wang, M., Liu, P., Wang, X., and Deng, R. Antioxidant activities and chemical constituents of flavonoids from the flower of *Paeonia ostii.* Molecules 22(5) (2017): 1-15.

[89] Punyasiri, P.A.N., Abeysinghe, I.S.B., Kumar, V., Treutter, D., Duy, D., Gosch, C., Martens, S., Forkmann, G., and Fischer, T.C. Flavonoid biosynthesis in the tea plant *Camellia sinensis*: properties of enzymes of the prominent epicatechin and catechin pathways. Archives of Biochemistry and Biophysics 431(1) (2004): 22-30.

[90] Tian, L., Blount, J.W., and Dixon, R.A. Phenylpropanoid glycosyltransferases from osage orange (*Maclura pomifera*) fruit. Federation of European Biochemical Societies 580(30) (2006): 6915-6920.

[91] Lukacin, R., Wellmann, F., Britsch, L., Martens, S., and Matern, U. Flavonol synthase from *Citrus unshiu* is a bifunctional dioxygenase. Phytochemistry 62(3) (2003): 287-292.

[92] Oliveir, A.B., Oliveira, G.G., Carazza, F., and Maia, J.G.S. Geovanine, a new azaanthiracene alkaloid from *Annona ambotay* Aubl. Phytochemistry 26(9) (1987): 2650-2651.

[93] Neacsu, M., Eklund, P.C., Sjoholm, R.E., Pietarinen, S.P., Ahotupa, M.O., Holmbom, B.R., and Willfor, S.M. Antioxidant flavonoids from knotwood of Jack pine and European aspen. European Journal of Wood and Wood Products 65(1) (2007): 1-6.

[94] Xiang, M., Su, H., Hu, J., and Yan, Y. Isolation, identification and determination of methyl caffeate, ethyl caffeate and other phenolic compounds from *Polygonum amplexicaule* var. sinense. Journal of Medicinal Plants Research 5(9) (2011): 1685-1691.

[95] Meechai, I., Phupong, W., Chunglok, W., and Meepowpan, P. Anti-radical activities of xanthones and flavonoids from *Garcinia schomburgkiana.* International Journal of Pharmacy and Pharmaceutical Sciences 8(9) (2016): 235-238.

[96] Wang, W.X., Qian, J.Y., Wang, X.J., Jiang, A.P., and Jia, A.Q. Anti-HIV-1 activities of extracts and phenolics from *Smilax china* L. Pakistan Journal of Pharmaceutical Sciences 27(1) (2014): 147-151.

[97] Zheng, Z.P., Tan, H.Y., Chen, J., and Wang, M. Characterization of tyrosinase inhibitors in the twigs of *Cudrania tricuspidata* and their structure-activity relationship study. Fitoterapia 84(1) (2013): 242-247.

[98] Fujiwara, M., Yagi, N., and Miyazawa, M. Tyrosinase inhibitory constituents from the bark of *Peltophorum dasyrachis* (yellow batai). Natural Product Research 25(16) (2011): 1540-1548.

[99] Khan, M.T.H., Khan, S.B., and Ather, A. Tyrosinase inhibitory cycloartane type triterpenoids from the methanol extract of the whole plant of *Amberboa ramosa* Jafri and their structure–activity relationship. Bioorganic and Medicinal Chemistry 14(4) (2006): 938-943.

[100] Ullah, F., Hussain, H., Hussain, J., Bukhari, I.A., Khan, M.T.H., Choudhary, M.I., Gilani, A.H., and Ahmad, V.U. Tyrosinase inhibitory pentacyclic triterpenes and analgesic and spasmolytic activities of methanol extracts of *Rhododendron collettianum.* Phytotherapy Research 21(11) (2007): 1076-1081.

APPENDIX

1. Preparation of reagents for quantitative analysis of total phenolic content assay

1.1 Preparation of 350 mM Na_2CO_3 solution

3.71 g of Na_2CO_3 was dissolved in 100 mL of DI water.

1.2 Preparation of 10% Folin–Ciocalteu reagent

5 mL of Folin–Ciocalteu reagent was dissolved in 45 mL of DI water.

1.3 Preparation of 10 mM gallic acid stock solution

0.0188 g of Gallic acid monohydrate was dissolved in 10 mL of methanol:water (19:1 v/v).

1.4 Preparation of standard calibration curve

Gallic acid was used as a standard for calculation of total phenolic content. Serial dilution was performed for the preparation of 1000, 900, 800, 700, 600, 500, 400, 300, 200 and 100 µM of gallic acid concentration (Table A).

Table A Serial dilutions of gallic acid equivalent

Concentration (µM)	Gallic acid stock solution	1000 µM Gallic acid solution	Methanol:water (19:1 v/v)
1000	1 mL	-	9 mL
900	-	900 µL	100 µL
800	-	800 µL	200 µL
700	-	700 µL	300 µL
600	-	600 µL	400 µL
500	-	500 µL	500 µL
400	-	400 µL	600 µL
300	-	300 µL	700 µL
200	-	200 µL	800 µL
100	-	100 µL	900 µL

2. Preparation of reagents for quantitative analysis of total flavonoid content assay

2.1 Preparation of 1 M NaOH

40.00 g of NaOH was dissolved in 1 L of DI water.

2.2 Preparation of 5% $NaNO_3$ solution

5 g of $NaNO_3$ was dissolved in 100 mL of DI water.

2.3 Preparation of 10% $AlCl_3$ solution

10 g of $AlCl_3$ was dissolved in 100 mL of DI water.

2.4 Preparation of standard calibration curve

Quercetin was used as a standard for the calculation of total flavonoid content. Serial dilutions were performed for the preparation of 1000, 900, 800, 700, 600, 500, 400, 300, 200 and 100 µg/mL of quercetin concentration (Table B).

Table B Serial dilutions of quercetin equivalent

Concentration (µg/mL)	Quercetin	1000 µg/mL quercetin solution	Methanol
1000	10 mg	-	10 mL
900	-	900 µL	100 µL
800	-	800 µL	200 µL
700	-	700 µL	300 µL
600	-	600 µL	400 µL
500	-	500 µL	500 µL
400	-	400 µL	600 µL
300	-	300 µL	700 µL
200	-	200 µL	800 µL
100	-	100 µL	900 µL

3. Preparation of reagents for quantitative analysis of DPPH radical scavenging assay

3.1 Preparation of 0.6 mM DPPH stock solution

12 mg of DPPH was dissolved in 50 mL of methanol (in the dark) and filtered with No.1 filter paper. The solution was stored at -20 °C.

3.2 Preparation of DPPH working solution

10 mL of 0.6 mM DPPH stock solution was dissolved in 45 mL of methanol:water (19:1 v/v).

3.3 Preparation of 10 mM trolox stock solution

2.5 mg of Trolox was dissolved in 1 mL of methanol:water (19:1 v/v)

3.4 Preparation of trolox equivalent for standard calibration curve.

Trolox was used as a standard for the calculation of DPPH radical scavenging activity. Serial dilutions were performed for the preparation of 1000, 800, 600, 400, 200, 100, 50 and 25 µM of trolox concentration (Table C).

4. Preparation of reagents for quantitative analysis of FRAP assay

4.1 Preparation of 300 mM acetate buffer, pH 3.6

3.10 g of $NaCH_3COO \cdot 3H_2O$ was added 16 mL of glacial acetic acid and dissolved in 1 L of DI water. Then the soluble was adjusted to pH 3.6 and stored at 4 °C.

4.2 Preparation of 20 mM $FeCl_3 \cdot 6H_2O$

0.0541 g of $FeCl_3 \cdot 6H_2O$ was dissolved in 10 mL of DI water.

4.3 Preparation of 1M HCl

16.47 mL 0f 37% HCl was dissolved in 183.53 mL of DI water.

4.4 Preparation of 40 mM HCl

8 mL of 1 M HCl was dissolved in 192 mL of DI water.

4.5 Preparation of 10 mM TPTZ

0.031 g of TPTZ was dissolved in 10 mL of 40 mM HCl at 50 °C.

4.6 Preparation of FRAP working solution

FRAP working solution was contained 10 mL of 300 mM acetate buffer, 1 mL of 20 mM $FeCl_3 \cdot 6H_2O$ solution and 1 mL of 10 mM TPTZ solution.

4.7 Preparation of trolox equivalent for standard calibration curve.

Trolox was used as a standard for the calculation of FRAP scavenging activity. Serial dilutions were performed for the preparation of 1000, 800, 600, 400, 200, 100, 50 and 25 µM of trolox concentration (Table C).

Table C Serial dilutions of trolox equivalent

Concentration (µM)	Trolox stocks solution	1000 µM trolox solution	Methanol:water (19:1 v/v)
1000	100 µL	-	900 mL
800	-	80 µL	20 µL
600	-	60 µL	40 µL
400	-	40 µL	60 µL
200	-	20 µL	80 µL
100	-	10 µL	90 µL
50	-	50 µL	950 µL
25	-	25 µL	975 µL

5. Preparation of reagents for quantitative analysis of tyrosinase inhibitory assay

5.1 Preparation of 0.1 M phosphate buffer, pH 6.5

12.48 g of $NaH_2PO_4 \cdot H_2O$ and 3.20 g of $Na_2HPO_4 \cdot H_2O$ were dissolved in 1 L of DI water. Then the soluble was adjusted slightly as necessary to pH 6.5 using 40 mM HCl or 1 M NaOH.

5.2 Preparation of 2.5 mM *L*-tyrosine

0.45 mg of *L*-tyrosine was dissolved in 1 mL of 0.1 M phosphate buffer, pH 6.5.

5.3 Preparation of 2.5 mM *L*-DOPA

0.49 mg of *L*-DOPA was dissolved in 1 mL of 0.1 M phosphate buffer, pH 6.5.

5.4 Preparation of mushroom tyrosinase (14.7 Units/mg)

1.2 mg of mushroom tyrosinase was dissolved in 1 mL of 0.1 M phosphate buffer pH 6.5.

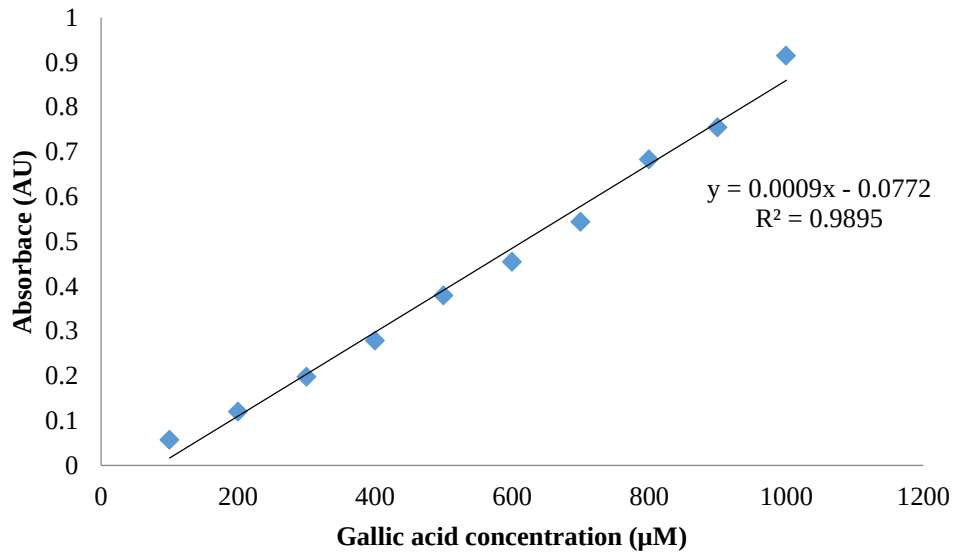

Figure 34 Standard curve of total phenolic content

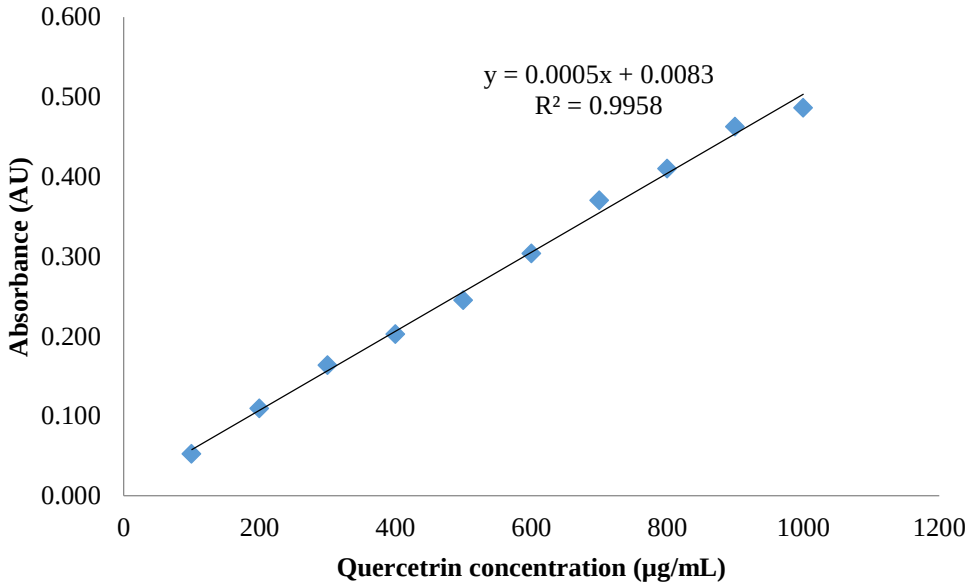

Figure 35 Standard curve of total flavonoid content

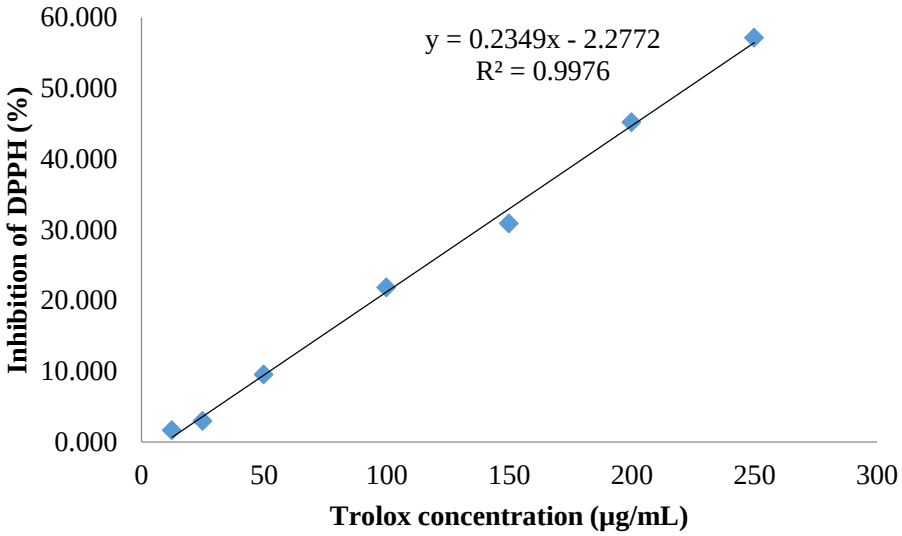

Figure 36 Standard curve of DPPH radical scavenging assay

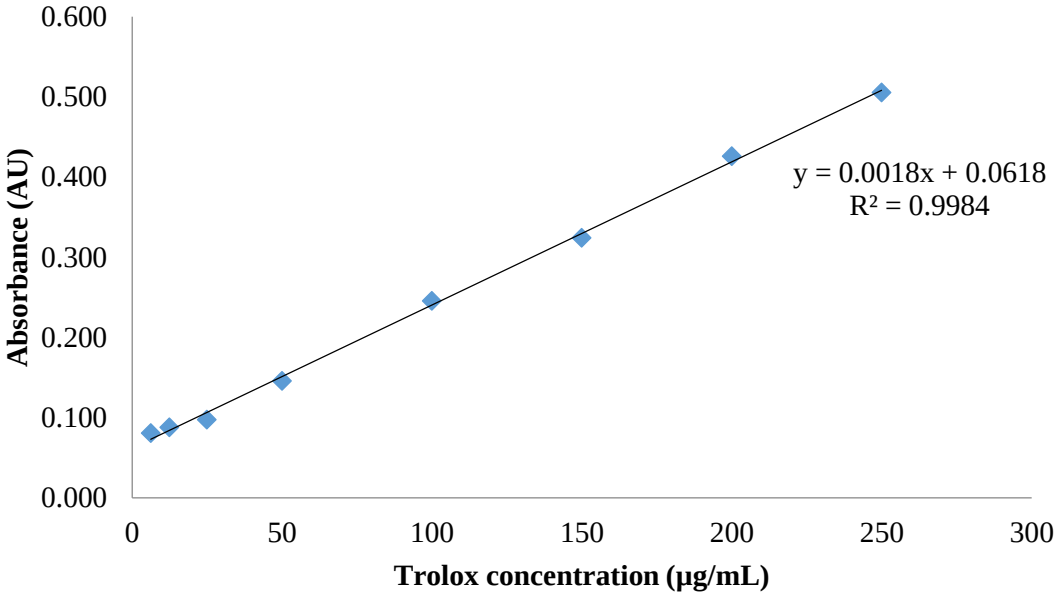

Figure 37 Standard curve of FRAP assay

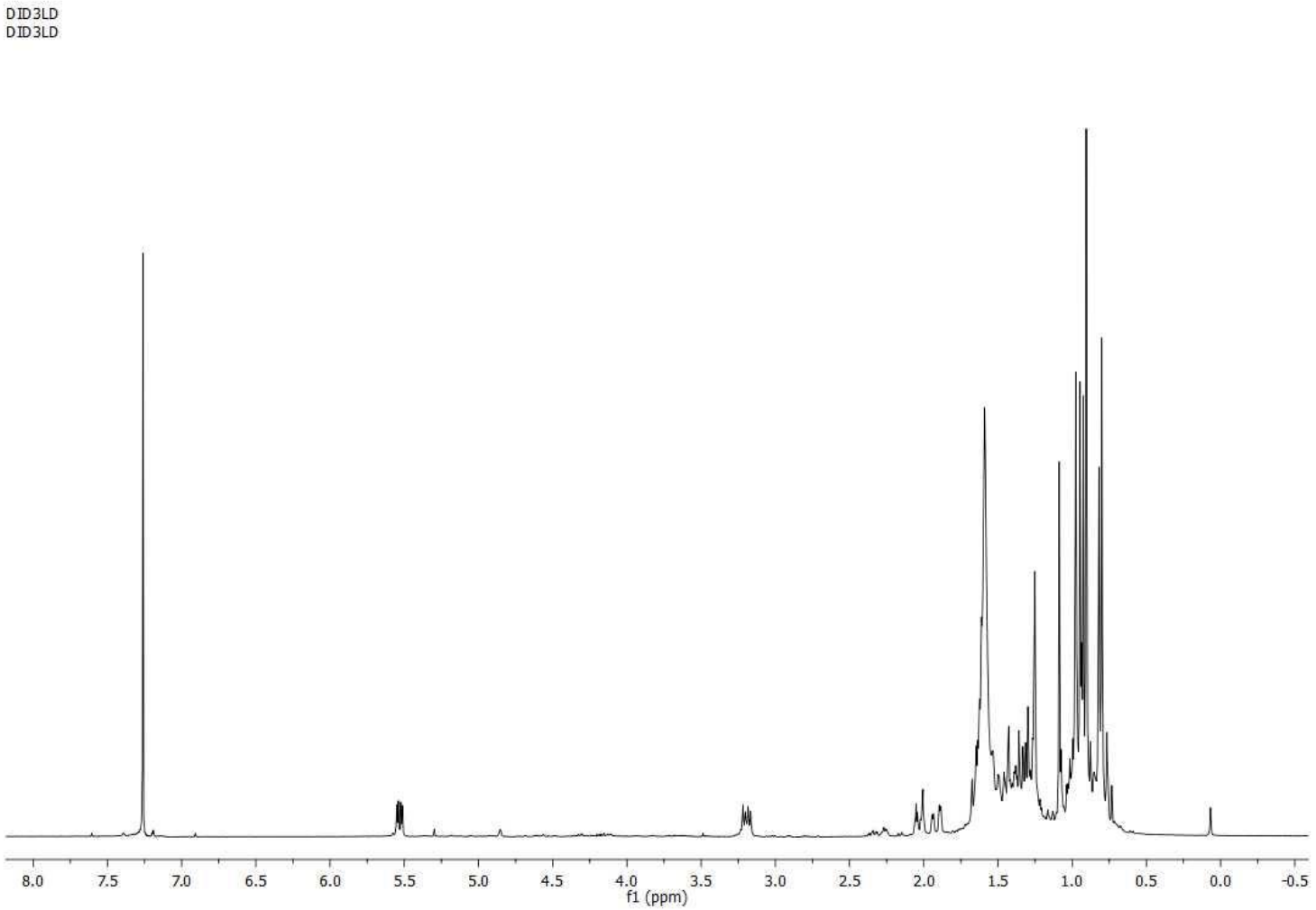

Figure 38 ^{1}H-NMR spectrum ($CDCl_3$) of compound **I**

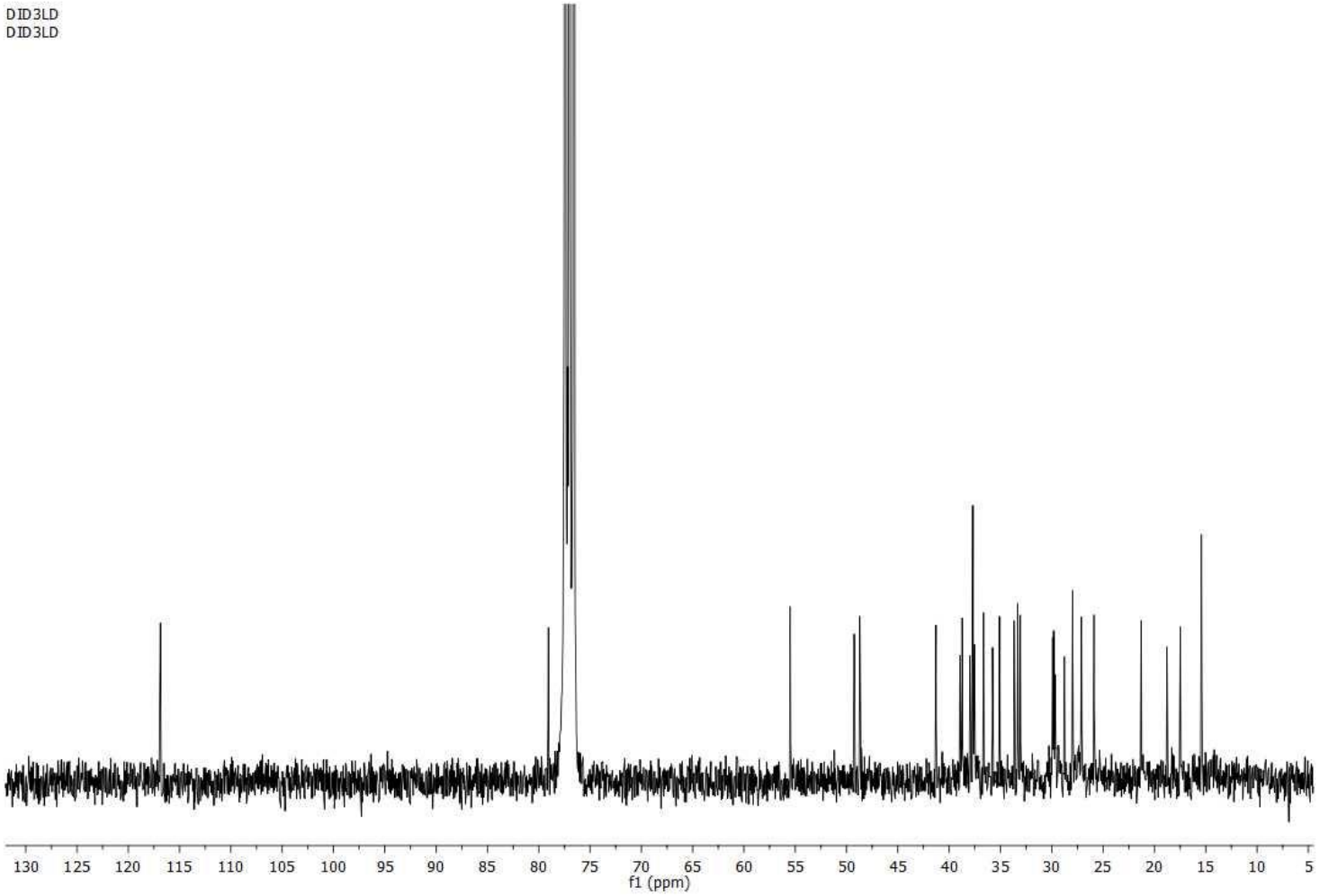

Figure 39 ^{13}C-NMR spectrum ($CDCl_3$) of compound **I**

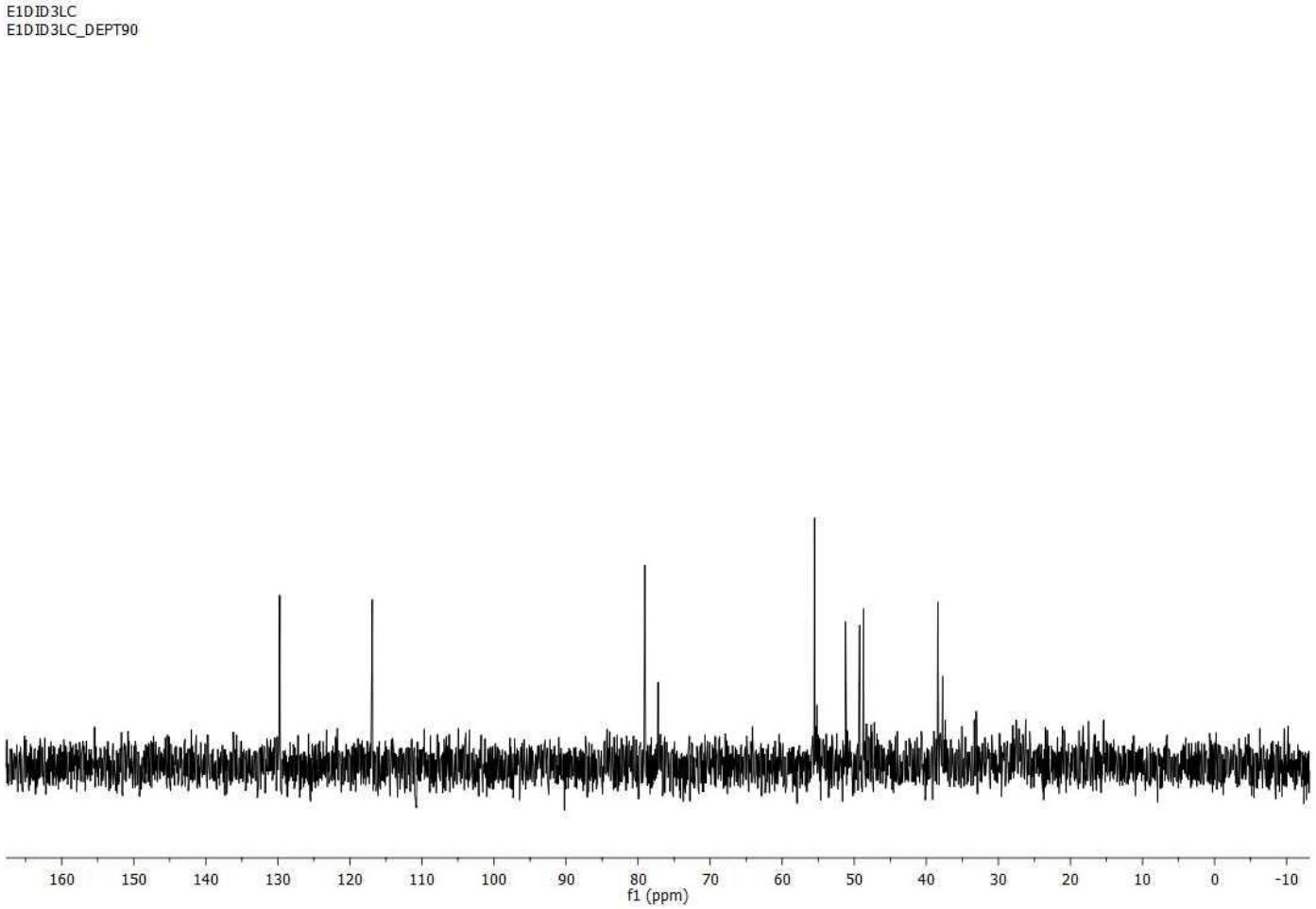

Figure 40 DEPT90 spectrum ($CDCl_3$) of compound **I**

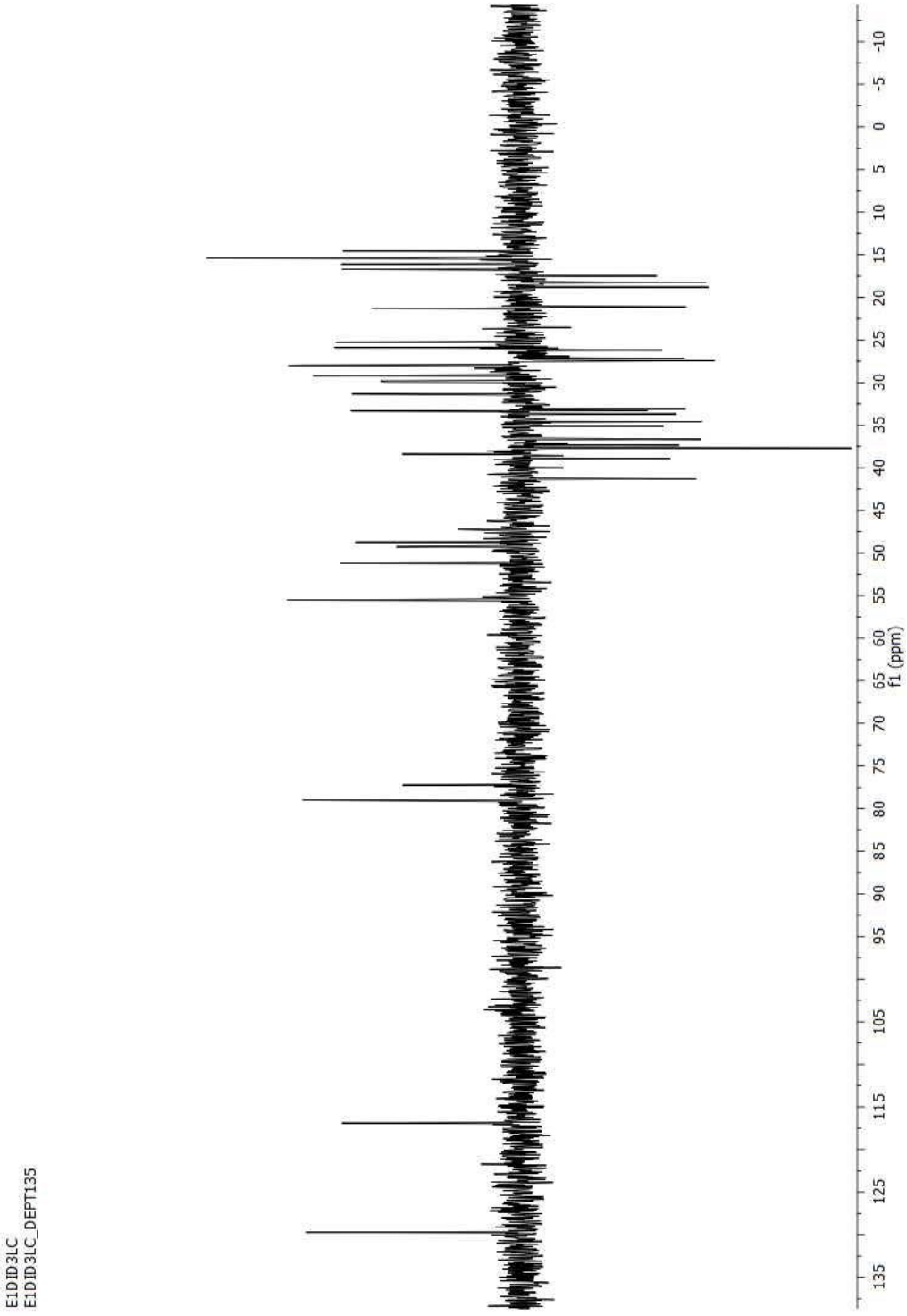

Figure 41 DEPT135 spectrum ($CDCl_3$) of compound **I**

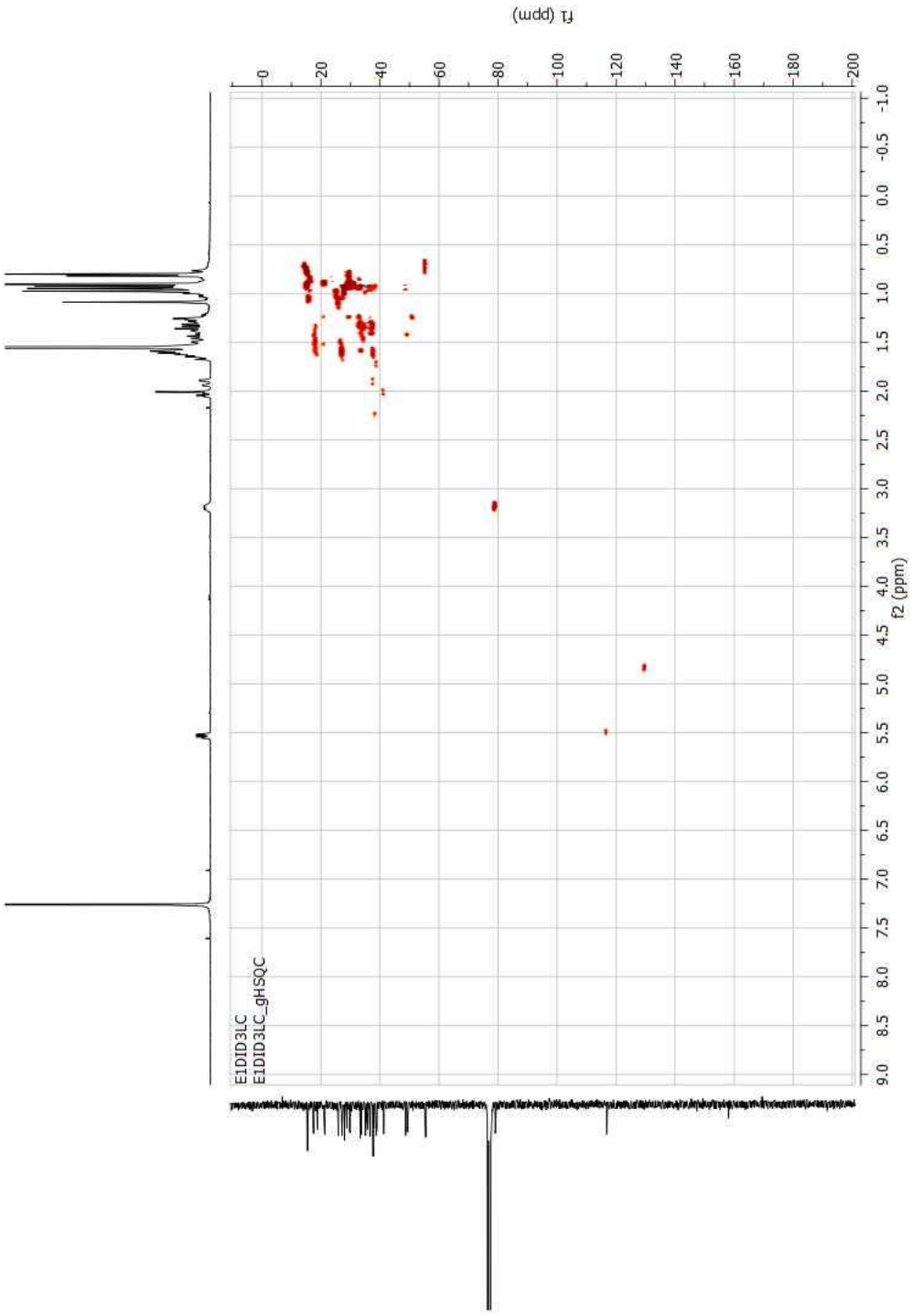

Figure 42 HSQC spectrum ($CDCl_3$) of compound **I**

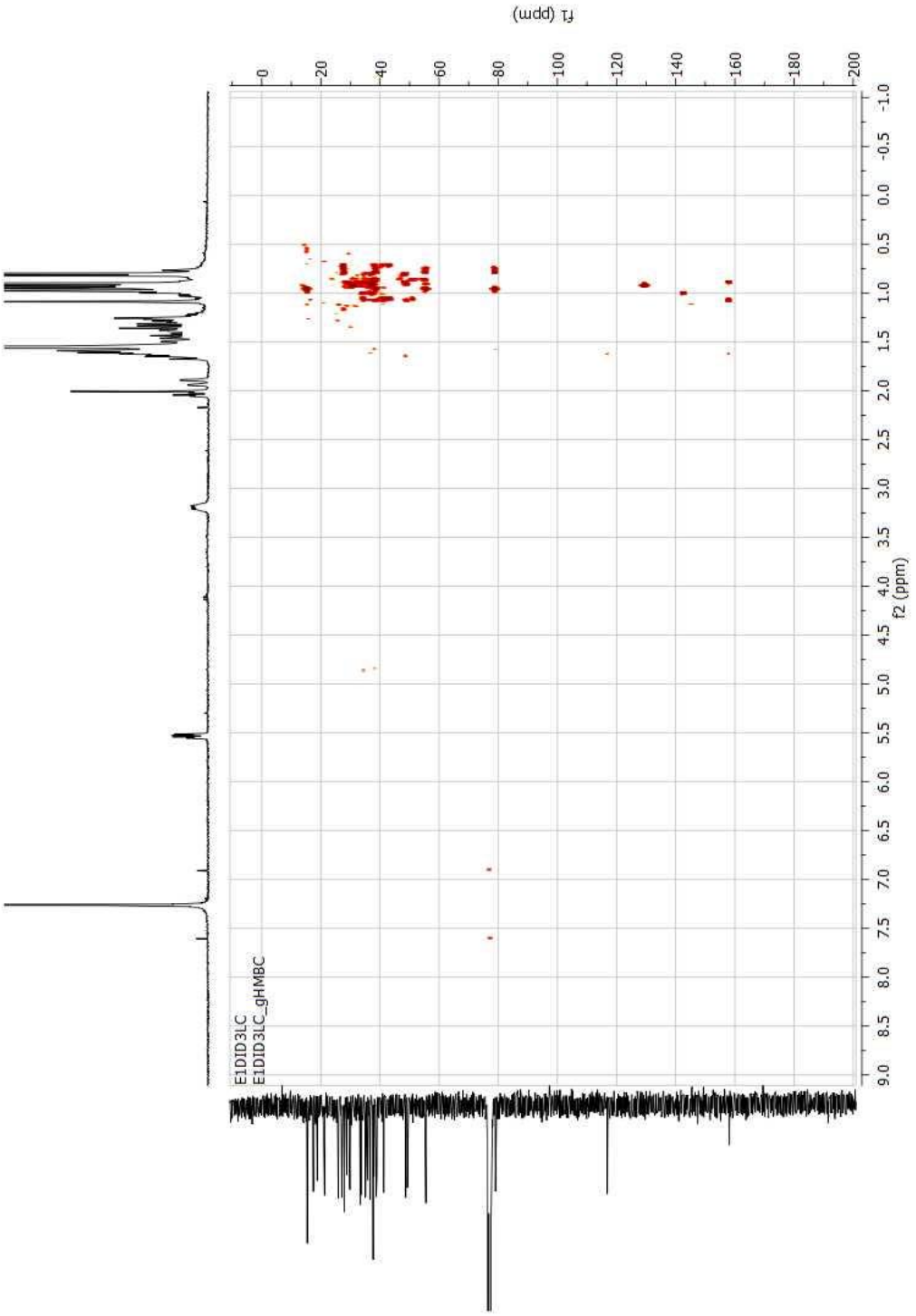

Figure 43 HMBC spectrum ($CDCl_3$) of compound **I**

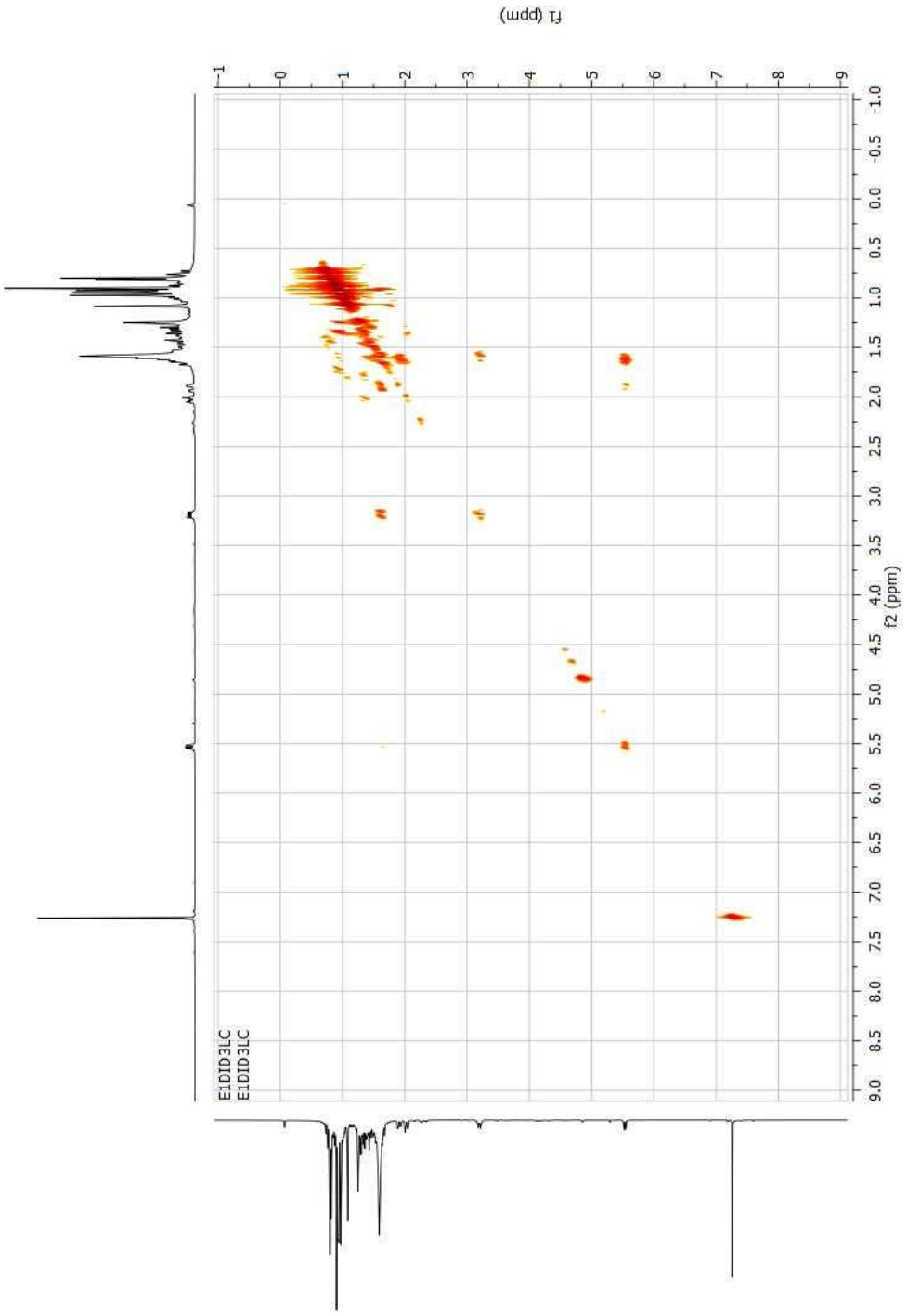

Figure 44 COSY spectrum ($CDCl_3$) of compound **I**

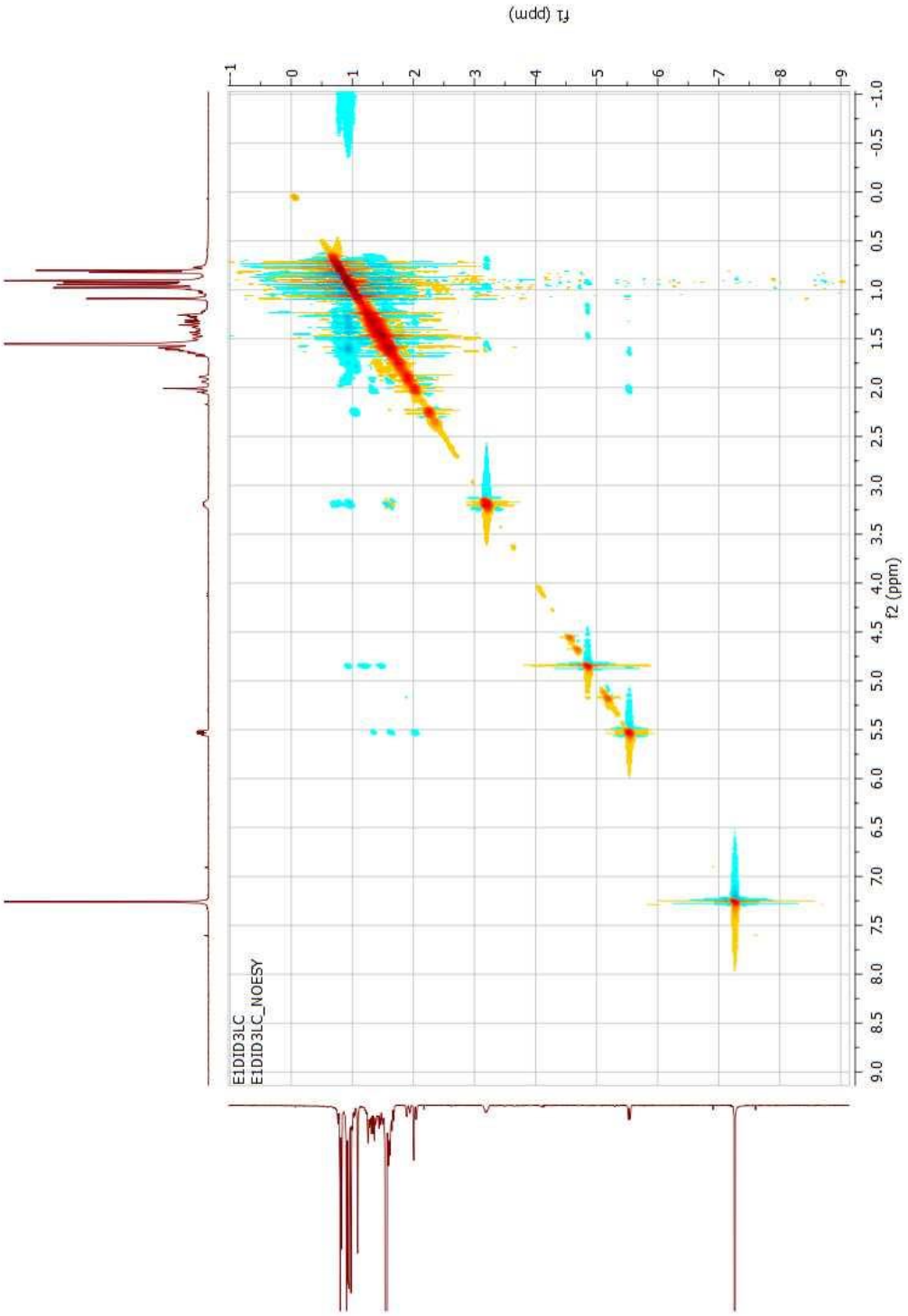

Figure 45 NOESY spectrum ($CDCl_3$) of compound **I**

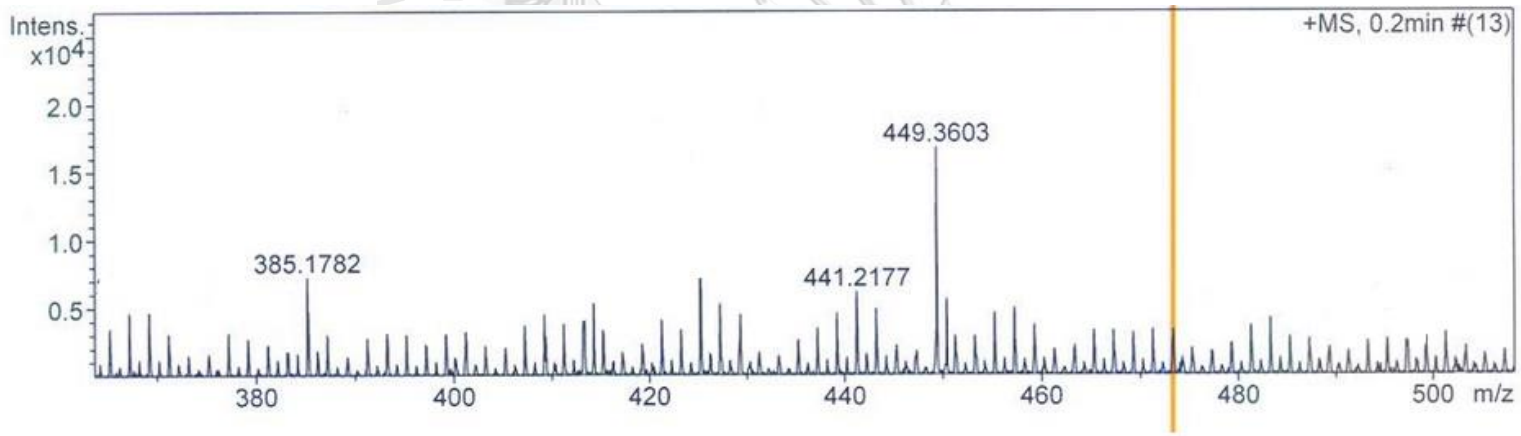

Figure 46 HR-ESI-MS spectrum of compound **I**

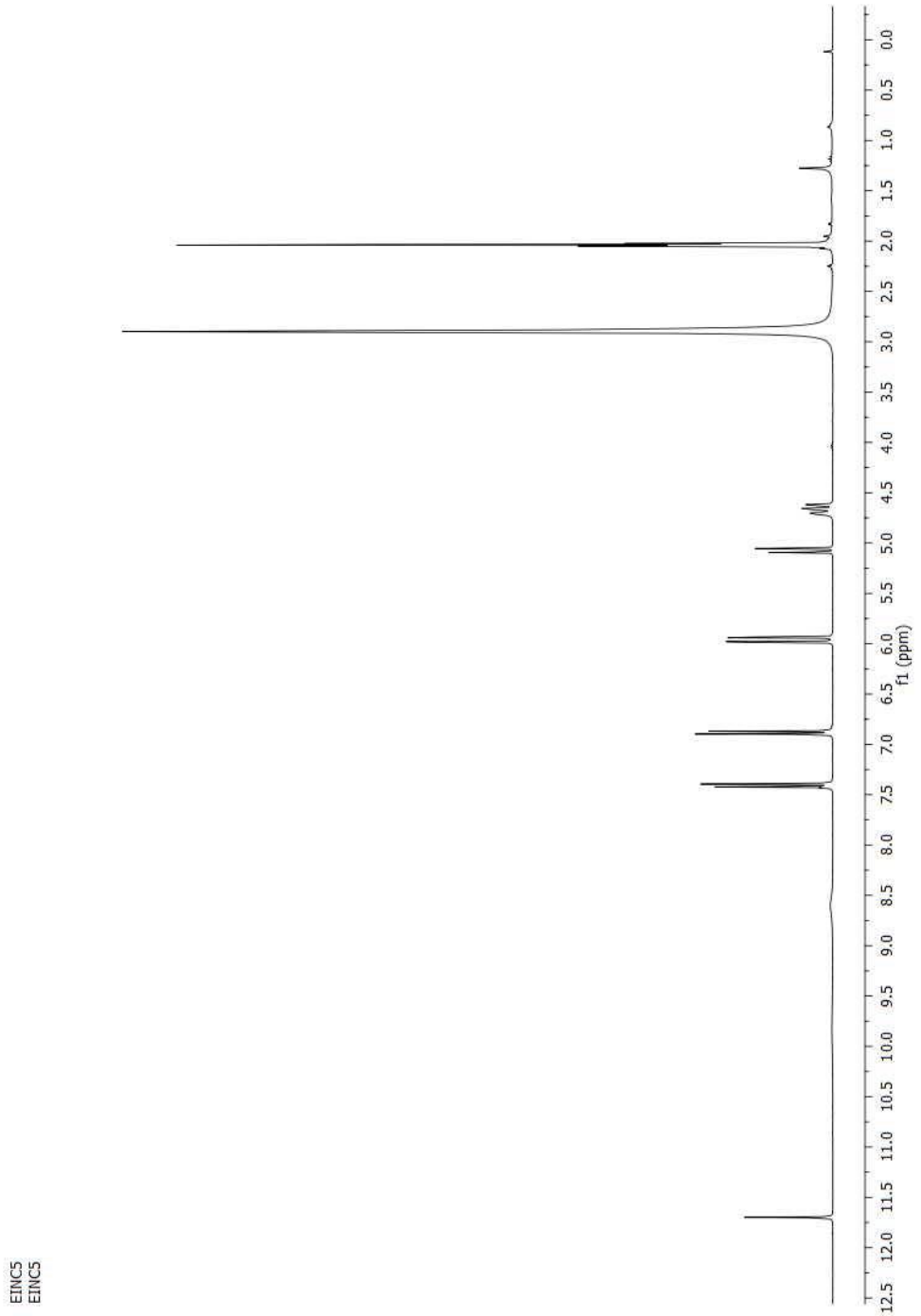

Figure 47 ^{1}H-NMR spectrum (CD_3COCD_3) of compound **II**

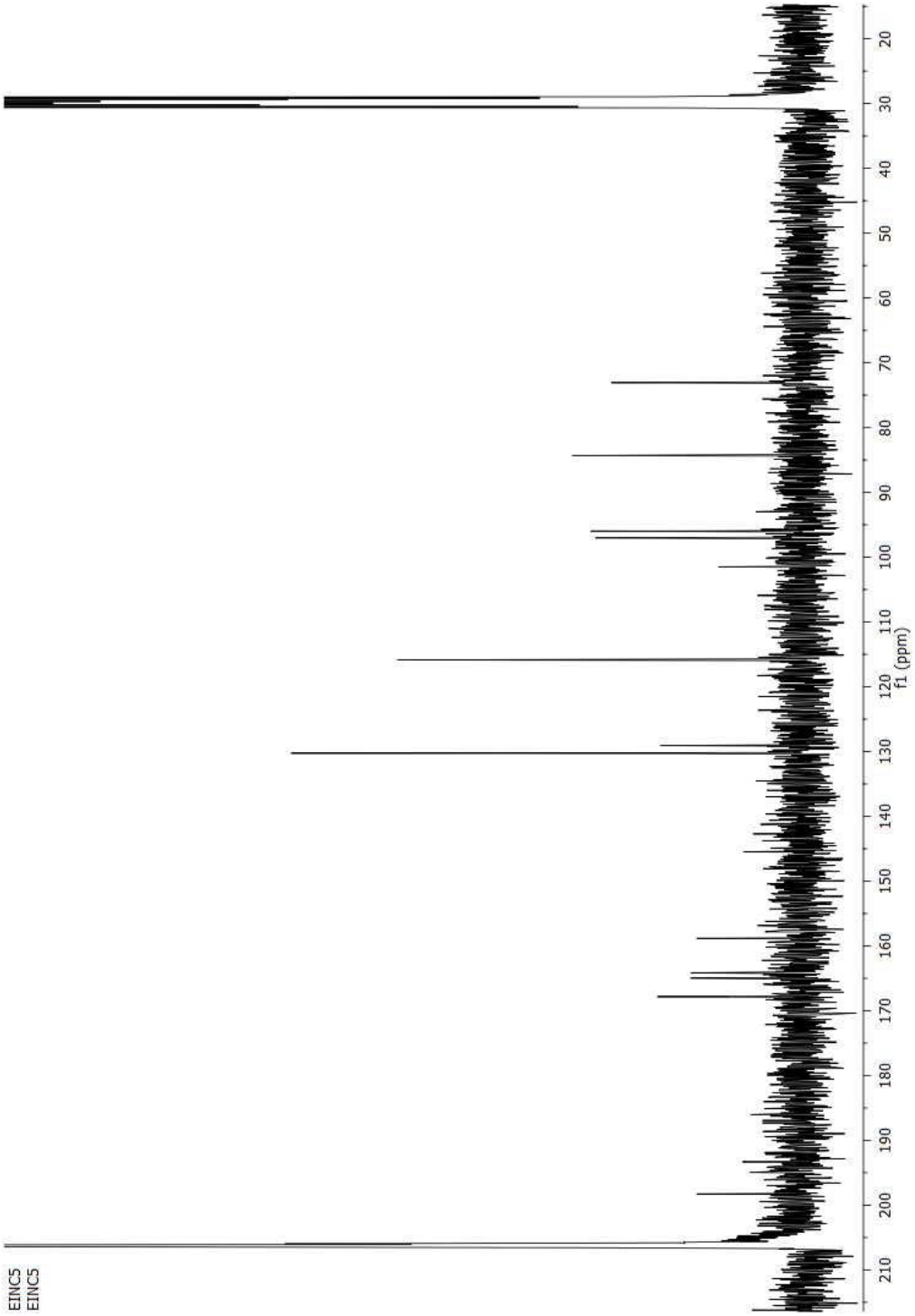

Figure 48 ^{13}C-NMR spectrum (CD_3COCD_3) of compound **II**

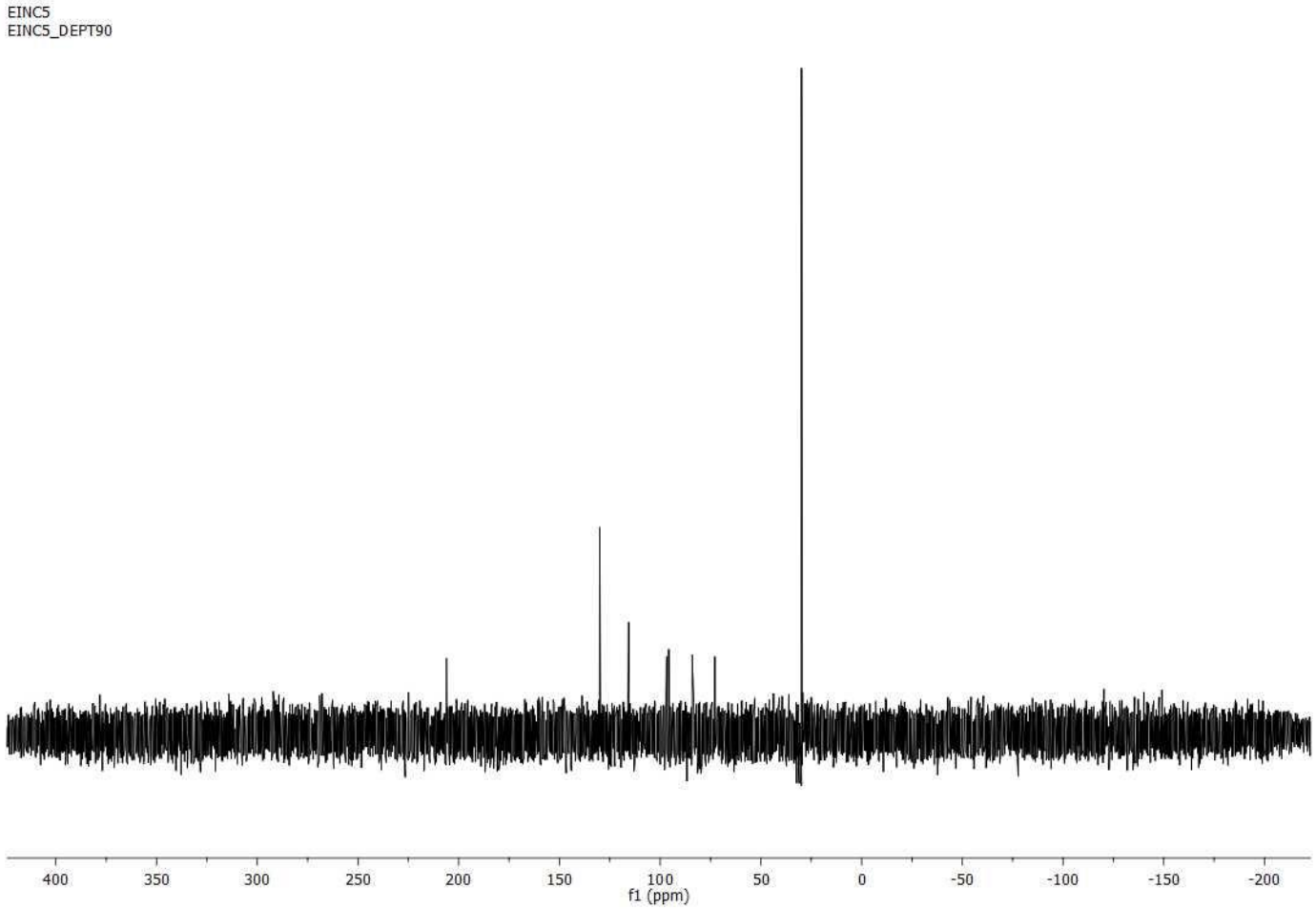

Figure 49 DEPT90 spectrum (CD_3COCD_3) of compound **II**

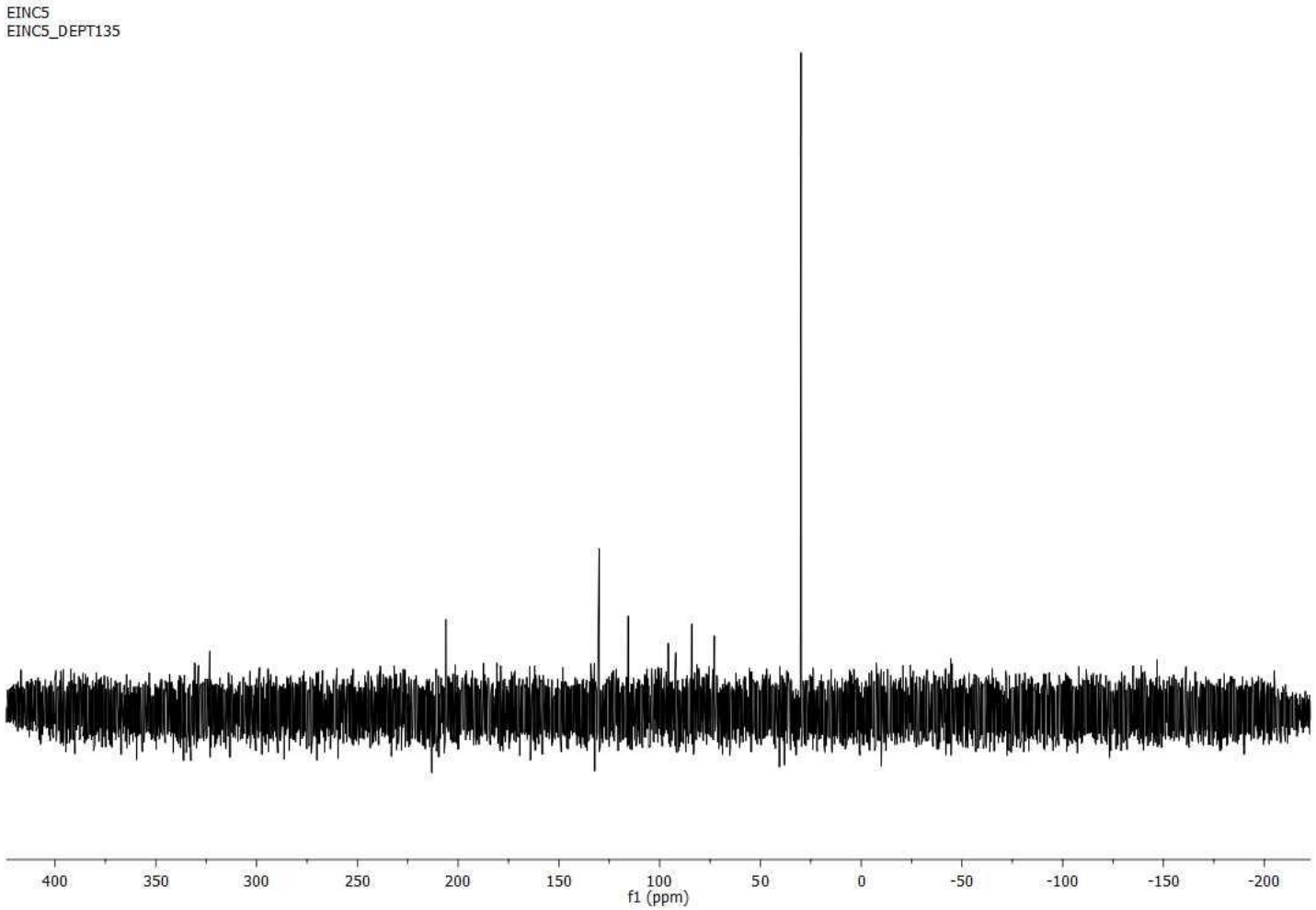

Figure 50 DEPT135 spectrum (CD_3COCD_3) of compound **II**

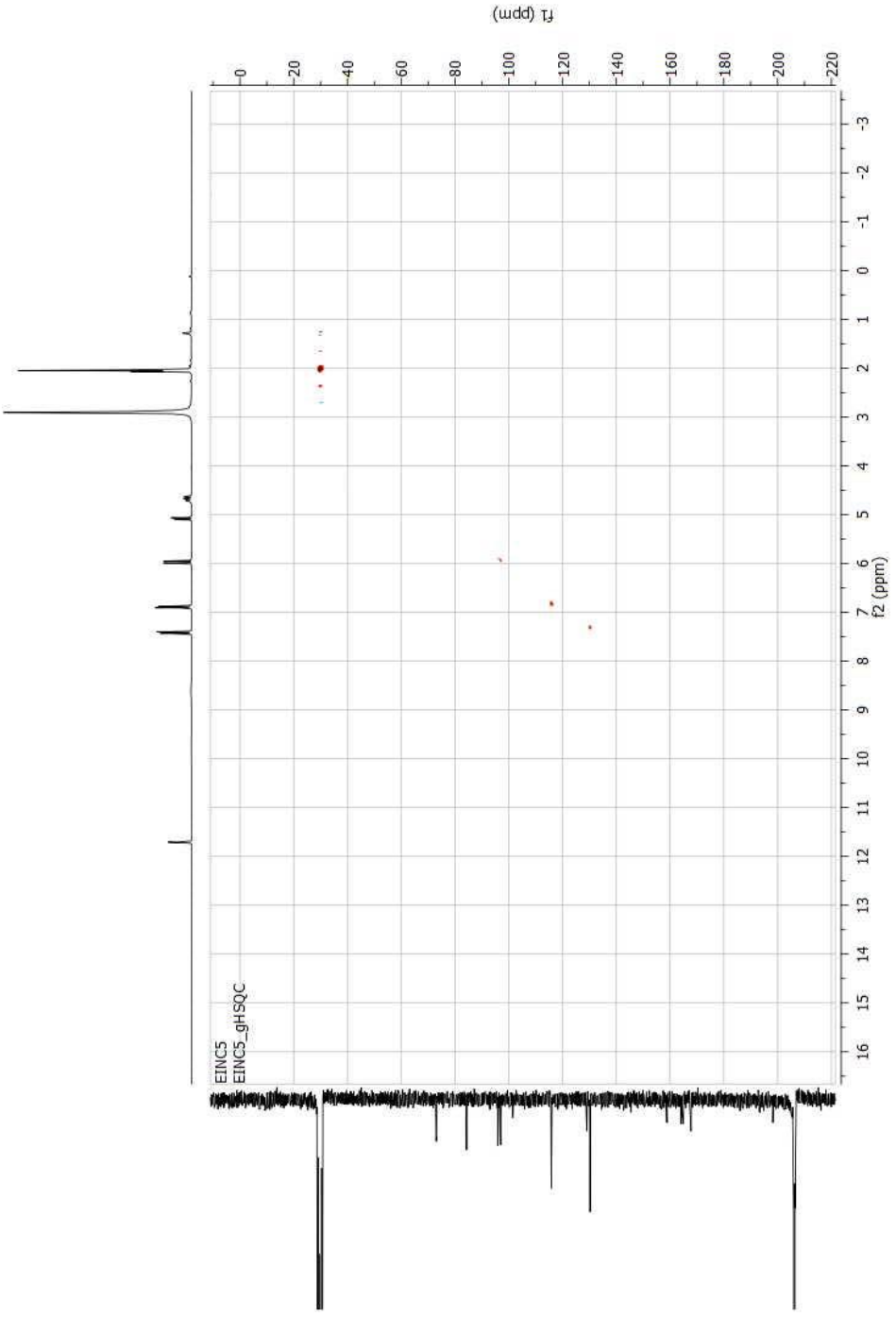

Figure 51 HSQC spectrum (CD_3COCD_3) of compound **II**

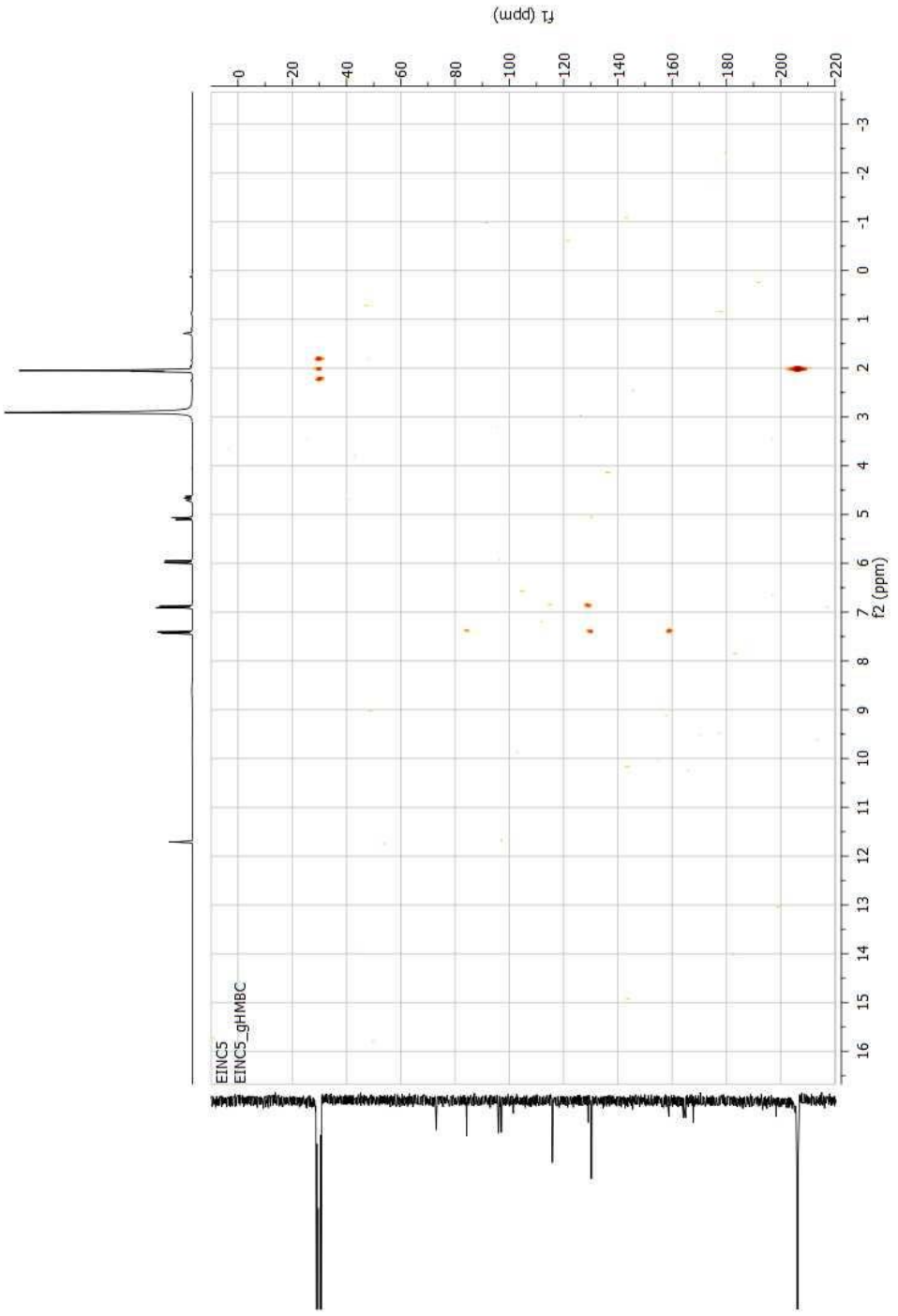

Figure 52 HMBC spectrum (CD_3COCD_3) of compound **II**

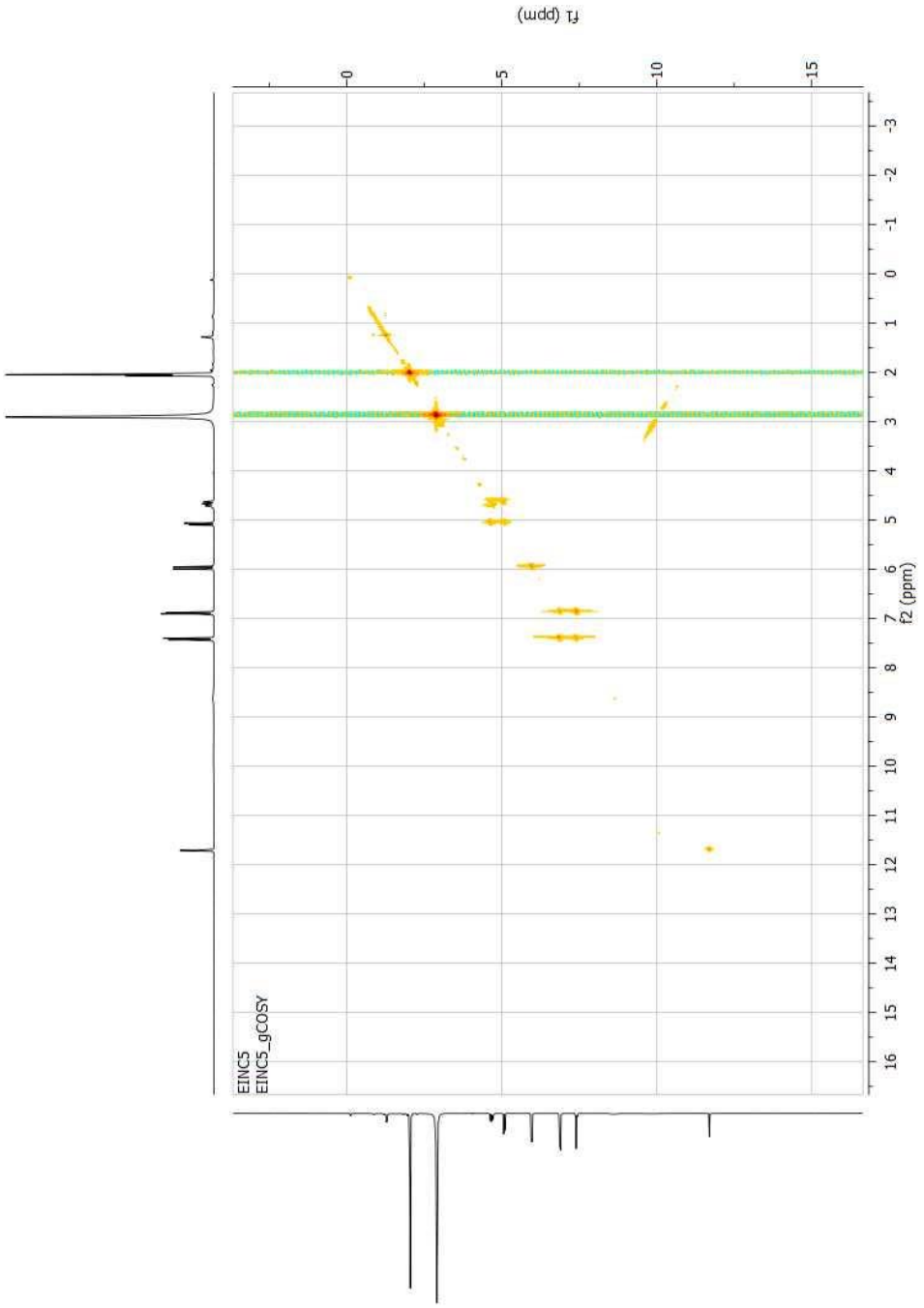

Figure 53 COSY spectrum (CD_3COCD_3) of compound **II**

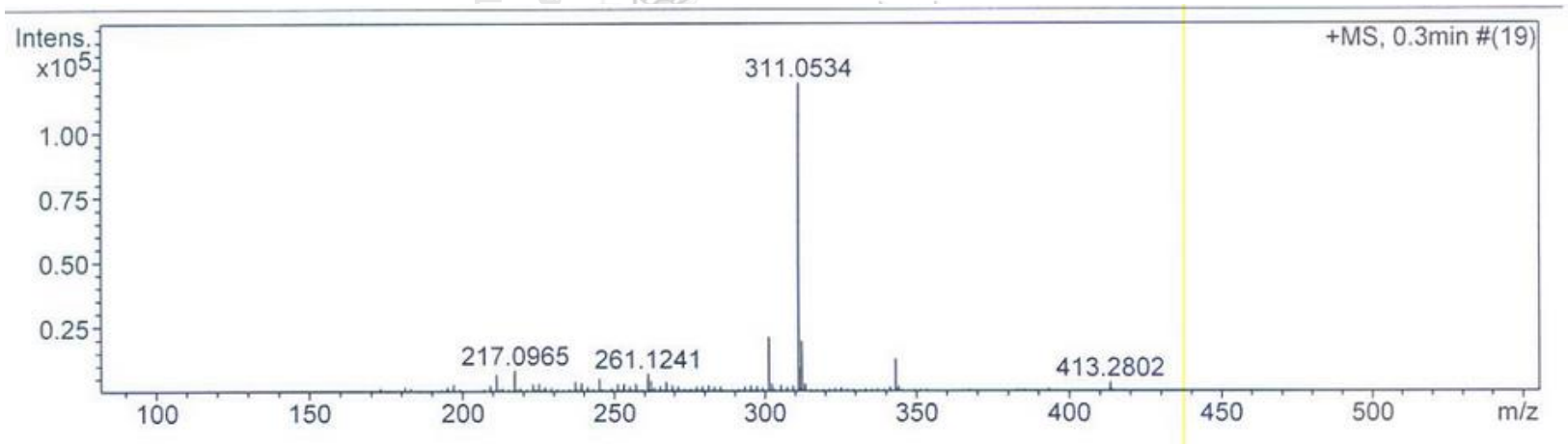

Figure 54 HR-ESI-MS spectrum of compound **II**

VITA

Ms. Sirinada Srisupap was born on December 21st, 1991 in Nongkhai, Thailand. She graduated high school from Pathumthepwittayakarn School, Nongkhai province in 2009. She received her Bachelor's degree of Science in Biotechnology from King Mongkut's Institute of Technology Ladkrabang in 2014. After that, she was admitted Master's degree of Program in Biotechnology, Faculty of Science, Chulalongkorn University in 2014.

Ms. Sirinada Srisupap attended the 6th Burapha University International Conference 2017 scheduled on August 3-4, 2017 at Pattaya, Thailand for poster presentation. She is going to attend the 13th International Symposium in Science and Technology at Cheng Shiu University 2018 schedule on August 9-11, 2018 at Kaohsiung, Taiwan for oral presentation. Moreover, she submitted a manuscript to Pharmacognosy magazine in the title "Total phenolic and flavonoid contents, antioxidant and antityrosinase activities of Manilkara kauki (L.) Dubard".